# THE EFFICIENCY OF ACTIVATING THE MASR/ANG 1-7 PATHWAY TO REDUCE MUSCLE ATROPHY AND FUNCTIONAL LOSS FOLLOWING DENERVATION

uOttawa

By

**HIND ALBADRANI**

A thesis submitted in partial fulfillment of the requirements for the Doctorate in Philosophy degree in Cellular and Molecular Medicine

Department of Cellular and Molecular Medicine
Faculty of Medicine
University of Ottawa

# ABSTRACT

Denervation leads to skeletal muscle atrophy, which is a decrease in muscle mass and force; the latter exceeding expectation from mass loss. In some cases, nerve regeneration following an injury takes several months. During this time, muscle mass and force loss become severe as fibers are replaced by connective and fat tissue, which can further prolongs normal muscle function recovery once reinnervation occurs. The objectives of this study were 1) document the angiotensin 1-7 (Ang 1-7) hypertrophic effect in innervated mouse skeletal muscle; 2) test the hypothesis that Ang 1-7 prevents muscle atrophy and maintain force following short 2 and 4 week denervation; 3) as well as following long 16 week denervation. Innervated and denervated mice were treated with Ang 1-7 or diminazene aceturate (DIZE), an ACE2 activator, to increase plasma Ang 1-7 level. In normal innervated extensor digitorum longus (EDL) and soleus muscle, Ang 1-7 increased muscle weight, cross sectional area (CSA) and tetanic force, which represents the muscle maximum force. During the short denervation period (2-4 weeks), Ang 1-7 did not prevent muscle mass and CSA loss, but fully abolished the loss of normalized tetanic force to CSA while accentuating twitch force. Normalized tetanic force was maintained as Ang 1-7 partially reduced the extent of membrane depolarization which normally observed with denervation, and it fully prevented the loss of membrane excitability. The protective effect of Ang 1-7 on maximum tetanic force was also observed after 16 weeks of denervation, but only in EDL not in soleus. About 35-40% of denervated EDL and soleus muscle fibers became reinnervated over the 16 week period and Ang 1-7 enhanced the recovery of muscle mass and tetanic force in both EDL and soleus. All Ang 1-7 effects on twitch and tetanic force were

completely blocked by A779, a Mas receptor (MasR) antagonist, and were not observed in MasR deficient ($MasR^{-/-}$) muscles. Ang 1-7 did not affect how denervation modulates changes in the protein content MuRF-1 atrogin-1, two atrophic proteins, total and phosphorylated Akt, S6K and 4EPB, three hypertrophic proteins. So, the Ang 1-7 effect involves an activation of its MasR, but it is not clear which intracellular pathway it then affects. This is the first study providing evidence that Ang 1-7 maintains normal muscle function in terms of tetanic force and membrane excitability during 2, 4 and 16 week denervation periods.

# ACKNOWLEDGEMENTS

First and foremost, I would like to express my gratitude to my supervisor, **Dr. Jean-Marc** Renaud. It has been an honour for me to work with him. He has taught me how to expand my vision and my way of thinking in science and life. I appreciate all the effort he invested in me, the time he dedicated to me, his guidance and unlimited support during my PhD journey. The joy and enthusiasm he has for his research were contagious and motivational for me, as well as for each lab member working with him. I would like to extend my thanks and appreciation to thesis advisory committee members Dr. **Jeffrey Dilworth,** Dr. **Jocelyn Côté** and Dr. **Nadine Wiper-Bergeron** for their constructive criticisms, insightful advice and continued interest. I would like to thank past and present members of Dr. Renaud's lab, Tarek, Wei, Mohammad and Callum, for their help and support.

I gratefully acknowledge the funding source (Majmaah University in Majmaah, Kingdom of Saudi Arabia: represented by the Saudi Cultural Bureau, Canada) for allowing me to pursue my passion for research. I was honoured to receive a full scholarship to finish my graduate studies.

Special thanks to my family for all their love and encouragement. Thanks to my parents who raised me with love and supported me throughout my pursuits. Thank you to my adorable sisters Aljazi, Haifa and Munirah for your endless support, love, and generosity. Thanks to my brother and friends who has helped me along the way. At last but not least, deep thanks and appreciation to my husband Sanad for his financial and emotional support, encouragement and unconditional love. Thank you for standing at my back during all challenges and difficult times that I have been

through. My baby Alia and you are the sources of happiness and strength; I am grateful for having you in my life.

Finally, I wish to dedicate this thesis to my mother Nora, who sacrificed her life for me to achieve my goals and took care of my baby while I was working in the lab. Without you, none of this would be possible.

# TABLE OF CONTENTS

# LIST OF TABLES

# LIST OF FIGURES

# ABBREVIATIONS

| | |
|---|---|
| **4E-BP** | Eukaryotic Translation Initiation Factor 4E-Binding Protein 1 |
| **ACE** | Angiotensin Converted Enzyme |
| **AChR** | Acetylcholine Receptor |
| **ActRIIB** | Activin Type IIB Receptor |
| **AIF** | Apoptosis Inducing Factor |
| **Akt** | Activated Protein Kinase B |
| **Ang II** | Angiotensin II |
| **Ang1-7** | Angiotensin 1-7 |
| **AP** | Action Potential |
| **ATG7** | Autophagy Related 7 |
| **ATP** | Adenosine Triphosphate |
| **BMP** | Bone Morphogenic Protein |
| **$Ca^{2+}$** | Calcium |
| **CAD** | Caspase-Activated DNase |
| **$Ca_V1.1$, L-type $Ca^{2+}$** | Calcium Channel |
| **$Cl^-$** | Chloride Ions |
| **CLC** | Chloride Channels |
| **CSA** | Cross Sectional Area |
| **DHPR** | Dihydropyridine Receptor |
| **DIZE** | Diminazene Aceturate |
| **EDL** | Extensor Digitorum Longus |
| **EGTA** | Ethylene Glycol Tetraacetic Acid |
| **elF3F** | Eukaryotic Translation Initiation Factor 3F |
| **Endo G** | Endonuclease G |
| **FDB** | Flexor Digitorum Brevis |

| | |
|---|---|
| **FoxO** | Forkhead Box |
| **GLUT4** | Glucose Transport 4 |
| **HDAC** | Histone Deacetylase |
| **IGF-1** | Insulin Like Growth Factor-1 |
| **IL6** | Interleukin 6 |
| **IRS** | Insulin Receptor Substrate |
| **$K^+$** | Potassium Ions |
| **Kir.2.1** | Potassium Inward Rectifier Channels |
| **KV** | Potassium Channels |
| **LC 3II** | Light Chain 3 Protein |
| **LPS** | Lipopolysaccharide-Endotoxin |
| **Mdx** | Dystrophic Mice Model |
| **mTOR** | Mammalian Target of Rapamycin |
| **MuRF1** | Muscle RING-Finger Protein-1 |
| **mV** | Mille Volte |
| **Myog** | Myogenin |
| **$Na^+$** | Sodium Ions |
| **$Na^+$ $K^+$ ATPase pump** | sodium–potassium adenosine triphosphatase pump |
| **Nav.1.4, Nav1.5** | Voltage Gated Sodium Channels |
| **NEP** | Neprilysin Enzyme |
| **NMJ** | Neuromuscular Junction |
| **NOX** | NADPH Oxidase |
| **p38 MAPK** | Mitogen Activated Protein Kinase |
| **P70s6K** | Ribosomal Protein S6 Kinase-1 |
| **PCl** | Chloride permeability |
| **PI3K** | Phosphatidylinositol-3-Kinase |
| **PK** | Potassium permeability |
| **$P_{Na}$** | Sodium Permeability |

| | |
|---|---|
| **RAS** | Renin-Angiotensin System |
| **ROS** | Reactive Oxygen Species |
| **RyR1** | Ryanodine Receptor |
| **SCI** | Spinal Cord Injury |
| **SERCA** | $Ca^{2+}$ ATPase Pump |
| **SK** | Amall-Conductance $Ca^{2+}$-Sensitive $K^{+}$ |
| **SR** | Sarcoplasmic Reticulum |
| **SUC** | Sucrose |
| **TA** | Tibialis Anterior |
| **TGF-β** | Transforming Growth Factor Beta |
| **TNFα** | Tumor Necrosis Factor Alpha |
| **TORC1, TORC2** | Mammalian Target of Rapamycin Complex |
| **TRAF6** | TNF Receptor Associated Factors 6 |
| **t-tubules** | Transverse Tubules |
| **UPP** | Ubiquitin-Proteasome System |

# CHAPTER 1

# INTRODUCTION

Muscle atrophy is defined as a decrease in muscle mass and size, which can eventually lead to partial or complete muscle wasting. Muscle atrophy occurs as a consequence of aging; chronic diseases including heart failure, kidney disease, cancer and diabetes; or due to loss of muscle activity for such reasons as limb immobilization, spinal cord injury (SCI), peripheral nerve injury and space travel (Martinez et al., 2010; Wang and Mitch, 2014; Gosker et al., 2000). A consequence of muscle atrophy is a decrease in the force generated by the muscle, which is in fact greater than the expected loss from the reduction in muscle mass. The decrease in force associated with atrophy restricts patients' movement and ability to perform the activities of normal life such as walking or moving objects. It also increases the risk of accidents while performing tasks, thereby reducing quality of life. Another consequence of atrophy is a significant impact on metabolism, such as glucose homeostasis, because of lower glucose uptake by atrophied muscles. Therefore, preventing muscle atrophy associated with chronic diseases can improve quality of life.

Serious complications also occur following major peripheral nerve injury when nerve regeneration requires a long time to complete (Galvin and Eichinger, 2016; Berry and Bril, 1982; Blom and Dahlbäck, 1970). For example, nerve repair following a level II injury or axonotmesis takes 3 to 6 months, while for a level III injury or neurotmesis, the repair can be as long as 6-12 months (Galvin and Eichinger, 2016; Berry and Bril, 1982; Blom and Dahlbäck, 1970; Menorca et al., 2013). However, connective tissue and fat start to replace muscle fibers within two months of denervation. When innervation is achieved, more time is needed to restore muscle fiber morphology and functionality. Therefore, finding a mechanism to prevent muscle atrophy and functional loss until reinnervation is completed will improve final function recovery.

Recent studies have provided evidence that activation of the Mas Receptor (MasR)/Angiotensin 1-7 (Ang1-7) signaling pathway reverses muscle atrophy induced by Angiotensin II (Ang II) in chronic diseases and muscle immobilization (Martinez et al., 2010; Wang and Mitch, 2014; Gosker et al., 2000). The effectiveness of activating the MasR /Ang1-7 signaling pathway to prevent muscle atrophy and functional loss associated with denervation remains to be determined. Accordingly, the overall objective of this PhD project is to test the effectiveness of Ang 1-7 at preventing muscle atrophy and function loss during short (2-4 weeks) and prolonged denervation (16 weeks) periods, and to understand the mechanisms of action of Ang 1-7.

## 1.1 THE CYCLE OF MUSCLE CONTRACTION

Muscle contraction is initiated when the motor neuron releases acetylcholine at the synaptic cleft of the neuromuscular junction (NMJ). Acetylcholine binds to ligand nicotinic receptors, causing a membrane depolarization that eventually triggers an action potential (AP) which propagates along the sarcolemma and down the t-tubules, where it activates the $Ca^{2+}$ release from sarcoplasmic reticulum (SR) (Fig. 1.1). Once $Ca^{2+}$ diffuses to the sarcomere, where force is developed, it binds to troponin C, a protein located on the thin filament (actin) of the sarcomere. Then, the troponin allosterically moves tropomyosin, another protein on the thin filament, freeing the myosin binding site on actin. Myosin has along fibrous tail and globular head, which binds to actin. After myosin binds to actin, it pulls the actin filaments toward the centre of the sarcomere to generate force or do work, while using ATP to convert chemical energy to mechanical energy. Relaxation occurs when there is no more action potential on the cell membrane, allowing $Ca^{2+}$ to be pumped back into the SR by the active $Ca^{2+}$ ATPase transport mechanism (Macintosh et al., 2012).

# FIGURE 1.1

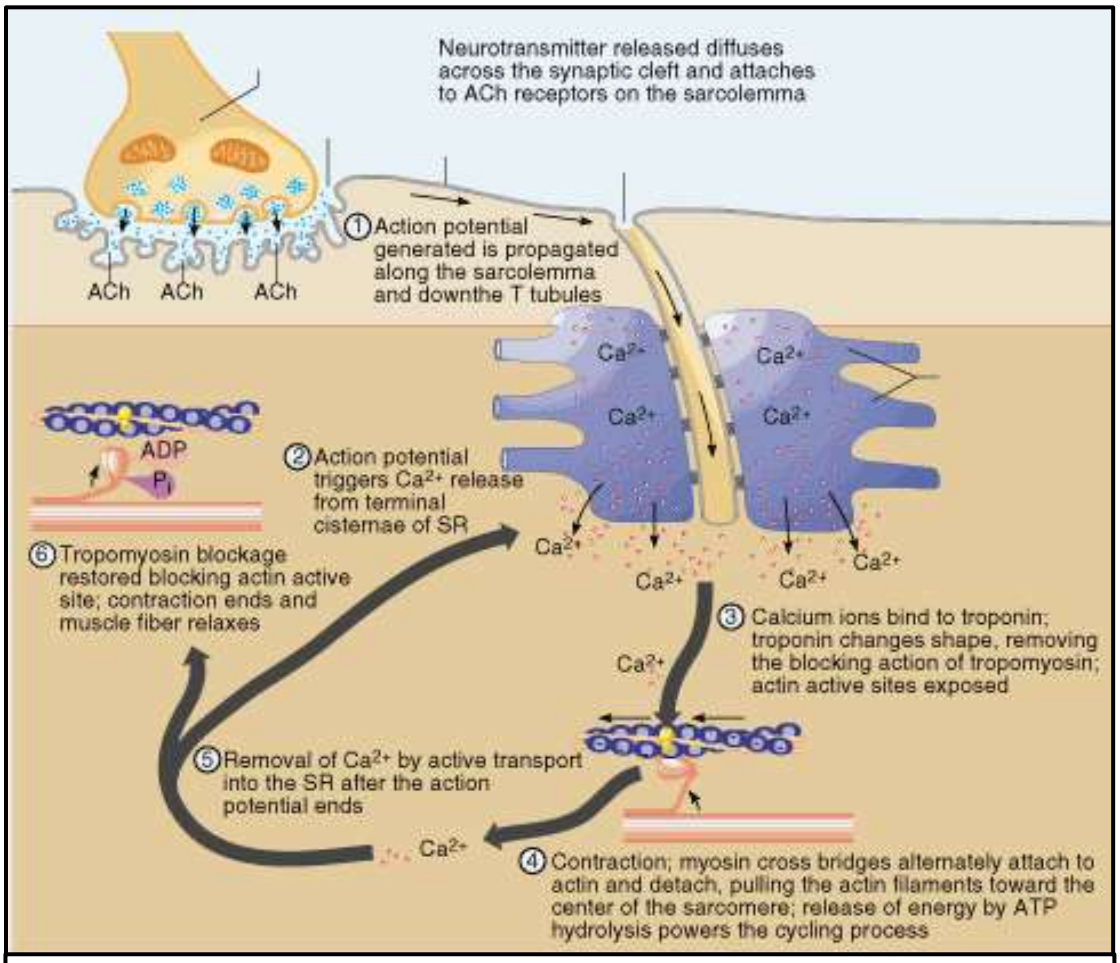


**Figure 1.1: Skeletal muscle contractzion cycle** (Macintosh et al., 2012)**.**

Skeletal muscle expresses various fiber types, each with specific contractile and biochemical characteristics to meet the functional demand. Based on the myosin isoform expression, skeletal muscle fibers are first divided into slow twitch (type I) and fast twitch (type II) fibers. Type II is further categorized into type IIA, IIB and IIX fibers. In general, type I and IIA fibers have high oxidative capacity, which allows them to be very efficient at using oxygen to generate ATP, and can be active for long periods of time before they fatigue. Type IIB fibers have the highest glycolytic capacity, as they fatigue much more quickly than oxidative fibers. Finally, type IIX fibers have intermediate properties between IIA and IIB (Schiaffino and Reggiani, 2011).

## 1.2 KEY CHANGES DURING MUSCLE ATROPHY

Skeletal muscle atrophy occurs in a variety of conditions, including starvation; aging; systematic diseases such as diabetes, heart or renal failure; cancer; and muscle disuse such as immobilization and spinal cord or motor neuron injury, the latter resulting in denervation (Martinez et al., 2010; Wang and Mitch, 2014; Gosker et al., 2000). Muscle atrophy caused by fasting and diabetes involves reduction in insulin level and elevated glucocorticoid level. Cancer and cachexia are associated with increased TNFα. Renal failure involves metabolic acidosis. Despite the different pathological stimuli for muscle atrophy, there are similarities and differences in atrophied muscle characteristics and the severity of muscle damage, which will be discussed next by comparing changes that occur during fasting, diabetes, muscle immobilization and following denervation.

MUSCLE MASS AND FIBER CSA

Muscle mass is the first important indicator of atrophy under pathological conditions. Loss of muscle mass can occur very quickly in a very short period. Fasting induces a rapid muscle mass loss, reaching 14% for the gastrocnemius muscle after just two days (Lecker et al., 2004). Three to seven days denervation and immobilization result in 6 to 33% muscle weight loss (Krawiec et al., 2005; Singh and Hood, 2011a). Loss of muscle mass becomes more pronounced under chronic conditions, and varies depending on the length of the disuse period. Muscle disuse following nerve injury and/or hindlimb suspension induce significant muscle mass loss, which reaches 45-40 % at 2 weeks, 67-60% at 4 weeks and 70–80 % after 4-8 months (Gutmann and Zelená, 1962; Hník, 1962; Higashino et al., 2013; J et al., 2007; Xu and Gu, 1999; H et al., 2001). In chronic diseases such as diabetes, muscle mass loss reaches 20-33% in the gastrocnemius and 23% in the soleus muscle 2 weeks after injected mice with streptozotocin to induce type I diabetes (Ono et al., 2015).

As muscle mass decreases, the cross sectional area (CSA) also diminishes by 45% in the diabetic gastrocnemius muscle (Ono et al., 2015). Following 2-4 week denervation, the mean CSA of the tibialis anterior (TA) and extensor digitorum longus (EDL) muscles decrease by 38% and 33%, respectively (Sartori et al., 2013a). Over a 2-month period following spinal cord injury, the CSA of human quadriceps muscle type I, IIA and IIX fibers decrease by 40%, 51% and 49%, respectively (Scelsi, 2001). In general, type II fibers atrophied sooner than type I fiber (Borisov et al., 2001c; Lu et al., 1997; Karpati and Engel, 1968; Davis and Kiernan, 1980). For example, in rat EDL, the CSA for type I, IIA and IIB fibers decrease by 9%, 32% and 39% following 4 weeks denervation, while after 10 weeks, the decrease are 26%, 50% and 60%, respectively (Niederle and Mayr, 1978). Eventually, denervated muscle weight and CSA stabilize at 10-20%

of the normal innervated muscle weight and CSA (Jg and Yd, 1999; Ma et al., 2007a; Wang et al., 2001).

MUSCLE FIBER INTEGRITY

As atrophy progresses following denervation, muscle passes through several dramatic changes involving muscle integrity loss, fiber degeneration, sarcomere disorganization and replacement of muscle mass by fibrotic connective tissue and fat. At the sarcomere level, atrophic muscle shows progressive disorganization of the sarcomere pattern. Z lines lose their parallel arrangement, while SR proliferates between myofibrils and junctions with t-tubules after just one week denervation in some fibers (Lu et al., 1997; Schmalbruch et al., 1991). In regard to the actin/thin and myosin/thick filaments (where force is generated), there is a 40% loss in myosin protein content within 14 days of denervation (Jakubiec-Puka, 1992).

The excitation contraction coupling mechanism is also affected, as t-tubule networks become disorganized within 3 weeks of denervation, however, this disorganization similar to those observed in immature fibers (Takekura et al., 1996; Salvotri et al., 1988). As a result of excitation contraction mechanism dysfunction, muscle fibers stop contracting. For example, only 3-8% of fibers in rat soleus and TA muscles contract after 13-44 weeks denervation (Squecco et al., 2009).

Denervation also decreases the number of myonuclei per fiber in some but not all muscles. A 20-60% reduction in the number of nuclei has been reported in rat limb muscles following a 2- to 16-week denervation period, while no change occurred in 10-day to 16-week denervated rat diaphragms and plantaris muscles (Hikida et al., 1997; Wada et al., 2002; Zhong et al., 2005; Viguie et al., 1997; Aravamudan et al., 2006). The importance of any changes in

myonuclei numbers is therefore unclear due to this variation in the myonuclei range between studies. Denervation also activates satellite cells within days. Their numbers increase by 3-fold in the first 2 months of denervation in mice and rats (Viguie et al., 1997). A noticeable result of activating satellite cells is the generation of new fibers among the original atrophied ones (Chen et al., 2010; Carraro et al., 2005; Rossini et al., 2002).

In the advanced stage, the amount of connective tissue increases, and is followed by a progressive fiber necrosis and replacement of muscle mass by fat and fibrous connective tissue (Borisov and Carlson, 2000b; Borisov et al., 2001a). The duration of atrophy progression is different between species. For example, necrotic fibers can be detectable as early as 2 months after denervation in rats (Borisov and Carlson, 2000a; Borisov et al., 2001b), whereas denervated rabbit muscle exhibits atrophy, but not necrosis, after one year (Ashley et al., 2006). In contrast to laboratory animals like rats/mice, the rate of atrophy progression in humans is much slower, taking years to reach similar stages. For example, a biopsy of denervated human quadriceps muscle shows a 40% reduction in CSA after 1-2 years, while severe reduction in fibers diameter, replacement of muscle fibers by adipocytes and connective tissue, and pronounced fiber necrosis become detectable 4 years after denervation (Mödlin et al., 2005).

Finally, capillary loss is one feature of denervated muscle, as the capillary/muscle ratio decreases by up to 90% after 18 months in fast twitch rat muscle (Borisov et al., 2000). The extent of capillary loss is larger around type II fibers than type I fibers, implying that type II fibers atrophied sooner than type I fibers.

FORCE

A major physiological consequence of atrophy is a loss of force generating capacity. Tetanic force, which represents the maximum force a muscle can generate, decreases by 14-16 %

in mice gastrocnemius muscles during a 24-28 hour fasting period (Milan et al., 2015a; Sartori et al., 2013b). More importantly, when tetanic force is normalized to the CSA, the force loss is 8%; i.e., the decrease in force exceeds the decrease expected from muscle mass and CSA loss (Milan et al., 2015a; Sartori et al., 2013b). So, from this point on, all the decrease in force will be that of the normalized force to emphasize this aspect of muscle atrophy.

Muscle disused, following immobilization or hindlimb suspension, results in a 35% reduction in tetanic force in mice TA muscles over a period of 14 days (Morales et al., 2016). In contrast, a 14-day denervation period reduces tetanic force of rat EDL muscle by 63%, a loss that continues as denervation is prolonged, reaching 85-95% after 4-8 weeks and more than 98% after 4-12 months (Spector, 1985; Dow et al., 2004; Carlson et al., 1996; al-Amood et al., 1991; Kalliainen et al., 2002). Finally, denervation also modifies the kinetics of force development. Twitch force, which occurs following a single action potential, becomes slower, as both the time to reach peak force and the time to relax are prolonged in denervated muscles (Baumann et al., 2016a). As twitch contraction is slower, the force-frequency curve is shifted toward lower stimulation frequencies because summation of twitch contractions as the frequency is increased starts at lower frequencies in denervated muscle compared to innervated one (Baumann et al., 2016a).

The tetanic force loss and changes in contractile kinetics are most likely due to changes occurring in the excitation-contraction coupling mechanism, and loss of sarcomere proteins as mentioned above (Pellegrino and Franzini, 1963) as well as to loss in membrane excitability, which will be discussed in the next section.

MEMBRANE EXCITABILITY

Resting membrane potential depends primarily on the CLC-1 chloride channels and Kir.2.1 potassium inward rectifier channels (Pedersen et al., 2009b; a; Leech and Stanfield, 1981). At rest, ions move across the cell membrane to reach their equilibrium, and their net flux depend on the difference between the membrane potential and their electrochemical equilibrium. For $K^+$ ion, the equilibrium potential is -95 mV (Ramahi and Ruff, 2014). As the membrane resting potential (resting $E_M$) varies between -65 and -85 mV (Ammar et al., 2015b), $K^+$ diffuses more outward than inward, i.e., has a net efflux that forces the resting $E_M$ toward the $K^+$ equilibrium, making the resting $E_M$ more negative. On the other hand, $Cl^-$ ions constantly efflux at resting to bring membranes potential to its equilibrium potential, being -66 mV, and that efflux reverses to influx when resting $E_M$ depolarized during action potential to repolarized the membrane (Dulhunty, 1978). Therefore, the net balance between $K^+$ and $Cl^-$ ions movement bring the resting membranes potential ranging from -70 to -75 mV.

At rest, the voltage gated sodium channels (Nav.1.4), which are responsible for the action potential depolarization phase, and the voltage gated potassium channels ($K_V$), which are responsible for the action potential repolarization phase, are closed. When the membrane is depolarized to about -60 mV following the binding of acetylcholine to its receptor or by an electrical simulation, the $Na^+$ membrane conductance increases as $Na_V1.4$ channels open. As the $Na^+$ equilibrium potential is about +67 mV, a net $Na^+$ influx occurs, leading to a depolarization of the sarcolemma from a mean resting $E_M$ of -75 mV to an overshoot of +30 mV, which constitutes the AP depolarization phase. Eventually, $Na_V1.4$ channels become inactivated, while $K_V$ channels open, allowing a net $K^+$ efflux; both events are important for the repolarization phase back to -70 mV.(McGraw, 1999).

In denervated muscle, resting membrane potential depolarizes from a normal -70/-75 mV to -60/-55 mV within 4 days (Bray et al., 1976; Vyskočil et al., 1973; Albuquerque et al., 1971a; Albuquerque and Thesleff, 1968b; Kotsias and Venosa, 1987a). The depolarization is due to changes in $Na^+$ permeability ($P_{Na}$), $K^+$ permeability ($P_K$) and $Cl^-$ permeability ($P_{Cl}$). The $P_{Na}$ increases via an unknown mechanism that does not involve Nav 1.5 $Na^+$ channels (Seabrooke et al., 1988). As $P_{Na}$ increases, more $Na^+$ enters muscle fibers rendering resting $E_M$ less negative. Denervation reduces $P_K$ as the expression of the Kir2.1 $K^+$ channel decreases (Bray et al., 1976; Vyskočil et al., 1973; Albuquerque et al., 1971a; Albuquerque and Thesleff, 1968b). Lower $P_K$ then reduces the $K^+$ efflux and its capacity to maintain a normal resting $E_M$. ClC-1 $Cl^-$ channels account for 80% of membrane conductance. Denervation causes decrease in the mRNA level of ClC-1 channels by 20% in the gastrocnemius and TA muscles after 2-14 days denervation (Klocke et al., 1994). As there are fewer ClC-1 channels, the $Cl^-$ current significantly decreases by 50% within one week of denervation (Chen and Jockusch, 1999). Thus, concomitant higher $P_{Na}$ and lower $P_K$ and $P_{Cl}$ result in a depolarized resting $E_M$, the $K^+$ efflux and $Cl^-$ influx are less efficient at opposing the $Na^+$ depolarization.

The $Na^+$ $K^+$ ATPase pump is a primary active pump that transports three $Na^+$ out and two $K^+$ in the sarcoplasm per cycle. As it transports one extra positive charge outside, it also contributes up to 15-20 mV to the negativity of resting $E_M$ (Ammar et al., 2015a; Chibalin et al., 2012). Immobilization and denervation decrease the Na-K ATPase pump protein content by 13-25% within 2 weeks in different muscles (Clausen et al., 2011a; Zemková et al., 1990; Leivseth et al., 1992; Tyapkina et al., 2009). It is important to know that electrogenic $Na^+$ $K^+$ ATPase pump activity contributes to 10% of membrane depolarization (Tyapkina et al., 2009). After 7 day immobilization, the membrane depolarized by 10% in both EDL and soleus muscles, and

blocking $Na^+$ $K^+$ ATPase pump with ouabain brought about similar depolarization (Tyapkina et al., 2009).

A major consequence of membrane depolarization is an inactivation of $Na^+$ channels. $Na^+$ channels have three gates: i) the activation gate that starts to open at -60 mV to generate an AP, ii) a fast inactivation gate that closes during the AP to allow for the repolarization phase and iii) a slow inactivation gate that closes over sec to minutes when resting $E_M$ is depolarized (Hayward et al., 1997). Slow inactivation gates are all opened when $E_M$ is more negative than -80 mV, and reach 50% of inactivation at -62 mV (Hayward et al., 1997). All inactivation gates are closed when $E_M$ less negative than -50 mV (Chahine et al., 1996). As $Na^+$ channels are inactivated, the capacity to generate normal action potential decreases; i.e., a small degree of inactivation lowers action potential amplitude. The decrease in AP amplitude is further exaggerated by the higher $P_{Na}$ and the lower $Na^+$ $K^+$ ATPase pump activity, because they allow for increases in intracellular $Na^+$ concentration that reduce the $Na^+$ current during the depolarization phase, ultimately contributing to the decrease in AP amplitude. Eventually, no AP can be generated once all channels are inactivated; at this point, the fiber is unexcitable and can no longer contract. In fact, studies have shown that tetanic force is well maintained up to a resting $E_M$ of -65 mV, and drops drastically to zero between -60 and -55 mV (Cairns et al., 1995; Ammar et al., 2015a). Thus most of the decrease in force occurs in the range for which slow inactivation gates go from 50% to 100% (Kotsias and Venosa, 2001, 1987b).

As action potential amplitude decreases even as small as 5 mV, less $Ca^{2+}$ is released from the sarcoplasmic reticulum (SR) (Zhu et al., 2014). If the amount of $Ca^{2+}$ released results in sub-maximal sarcomere activation, then less force is generated in addition to the force loss of unexcitable fibers. Although denervation and hindlimb unloading increase the concentration of

resting intracellular $Ca^{2+}$ by 36-42% (Hines and Knowlton, 1933; Ingalls et al., 1999), $Ca^{2+}$ release upon stimulation decreases in mouse FDB maintained for 7 and 14 days in culture (Albadrani and Renaud unpublished, 2014); a condition for which adult muscle fibers behave like denervated fibers in situ in regard to physiological and morphological properties such as CSA, fiber degeneration, membrane depolarization and AChR supersensitivity (Morel et al., 2010; Bekoff and Betz, 1977). While lower AP amplitude is one mechanism responsible for the lower $Ca^{2+}$ release, a potential second mechanism may involve the $Ca^{2+}$ release mechanisms per se. The release of $Ca^{2+}$ from SR involves two $Ca^{2+}$ channels: i) the dihydropyridine receptor (DHPR), which is the $Ca^{2+}$ channel ($Ca_V1.1$, also known as L-type $Ca^{2+}$ channel), is located on the transverse tubule, and acts as a voltage sensor that detects action potential, and ii) the ryanodine receptor (RyR1), located on the SR, and responsible for $Ca^{2+}$ release. In skeletal muscle, the DHPR physically interacts with the RyR, the latter being directly activated by the former during an action potential to release $Ca^{2+}$. Contrary to the skeletal muscle isoform, the cardiac isoform does not interact with the RyR (Protasi, 2002). Long term denervation (25 to 50 days) increases the expression of DHPR α1 cardiac isoform mRNA level in rat EDL, while in the soleus muscle the skeletal isoform mRNA level increases more than control, but it remains to be determined if such changes contribute to lower $Ca^{2+}$ release (Péréon et al., 1997). So far, the expression of skeletal muscle RyR appears unaffected by denervation in rat EDL, whereas in the soleus it increases significantly, and this cannot be the reason for the lower $Ca^{2+}$ release (Péréon et al., 1997).

In summary, force loss following denervation depends on three major factors: 1) losing muscle mass; 2) changes in isoforms and/or content of the "functional proteins" that regulate resting $E_M$, action potential generation (i.e., membrane excitability, $Ca^{2+}$ release and force

generation); and 3) losing fiber integrity including t-tubule, SR and sarcomere degradation and/or disorganization. The latter two factors are responsible for the lower normalized force or greater decrease in force than the decrease expected from mass loss.

MUSCLE FIBRILLATION

Another consequence of denervation or SCI is muscle contracture or fibrillation, which occurs due to spontaneous generation of action potentials by muscle fibers themselves (Robinson et al., 1991; Purves and Sakmann, 1974). As a result of that, there is a loss of extensibility in soft tissues and spanning joints, leading to limb deformation such as a downward or upward angle of the foot or hands (Neelands et al., 2001a). This phenomenon occurs due to changes in membrane conductance, leading to a depolarized membrane potential to a potential close to the action potential threshold (Purves and Sakmann, 1974). The time course to develop fibrillation varies between muscles and species, being detectable within 1-3 weeks in human and 3-7 days in rats (Sekiguchi et al., 2012a; Heaton and Kobler, 2005; Arancio et al., 1989; Salafsky et al., 1968; Burns et al., 2007). In addition, the incidence of fibrillation can be very large, occurring in 62% of all guinea pig fibers in the soleus and 44% in the EDL (Robinson et al., 1991).

## 1.3 OTHER CHANGES IN PROTEINS INVOLVED IN THE EXCITATION AND CONTRACTION MECHANISMS

As mentioned above, the expression of several proteins that are involved in excitation, $Ca^{2+}$ release and reuptake, sarcomere activation and force development decreases during atrophy. Denervation modifies the expression of other proteins that also involved in excitability and contraction. One major denervation effect is a remodulation of the NMJ. Normally, the nAChRs are specifically expressed at the NMJ. After denervation, nAChRs are expressed all along the

muscle fiber (Adams et al., 1995a) as their mRNA level increase 100-fold within 3 day of denervation (Merlie et al., 1984). The mRNA level reaches its peak within 7-9 days of denervation, then returns back to base level after 1-4 months (Adams et al., 1995a; Ma et al., 2007a; Apel et al., 2009). Furthermore, the embryonic isoform is composed of two α, one β, one δ and one γ subunits; in the adult stage, the embryonic γ subunit replaces by the ε subunit (Ma et al., 2007b; Adams et al., 1995a). Following denervation, the adult ε subunit nAChR is replaced by the embryonic isoform γ subunit within 3 days, and reaches a peak within 1-2 weeks before returning back to normal level in 2- 4 weeks (Adams et al., 1995a; Ma et al., 2007a; Apel et al., 2009). Despite the presence of nerves, immobilization also increases embryonic nAChR isoform expression in skeletal muscle (Lee et al., 2014). This suggests that the nAChR remodelling associated with denervation/immobilization requires active motor neurons for the maintenance of normal nAChR isoforms.

During development, muscle fibers express the Nav1.5 $Na^+$ channel, which is also expressed in adult cardiac muscle. Following birth, the Nav1.5 isoform is replaced by the Nav1.4 isoform (Kallen et al., 1990). Following denervation, the reverse is observed, as the $Na_V1.4$ mRNA level transiently declines before returning back to base level within 5-7 days of denervation. Whereas the mRNA level of $Na_V1.5$ reaches its peak by day 3 of denervation, then declines to 30% of the peak (Morel et al., 2010; Yang et al., 1991; Awad et al., 2001). Following reinnervation or chronic stimulation, Nav1.5 channel expression subsequently declines, which suggests that muscle requires interaction with an active motor neuron to maintain normal $Na^+$ channel contents/isoforms (Morel et al., 2010; Yang et al., 1991; Awad et al., 2001). One consequence of the change in $Na^+$ channel isoform is the fibrillation associated with denervation (Sekiguchi et al., 2012b). Lidocaine, a $Na^+$ channel blocker with a higher affinity for Nav1.5 than

Nav1.4, decreases the extent of fibrillation in denervated muscle (Sekiguchi et al., 2012b). It has been suggested that the Nav1.5 channel has a faster recovery from the fast inactivation state, reducing the refractory period causing hyperexcitability (G. E. KirschM. F. Anderson, 1986).

$Ca^{2+}$-sensitive $K^+$ voltage channels are voltage and $Ca^{2+}$-sensitive channels that are activated by membrane depolarization and increases intracellular $Ca^{2+}$ concentration. These channels are also divided into three major groups according to their conductance (i.e., by which $K^+$ passes through their pores): the small-conductance (SK), the intermediate conductance (IK) and the big conductance (BK) $Ca^{2+}$ sensitive $K^+$ channels (Diness et al., 2015). The SK channel is normally expressed during embryonic development, while the BK channel is expressed in mature muscle fibers (Hartzell and Fambrough, 1972; Rogart and Regan, 1985; Gonoi and Hasegawa, 1991; Pribnow et al., 1999). Denervation results in the appearance of the SK channel (Neelands et al., 2001a; Vergara and Ramirez, 1997). For example, 6- to 9-day denervation increases the SK3 mRNA and protein levels of rat soleus muscle by 2.5-fold and 60%; respectively. Reinnervation or electrical stimulation prevents that increase (Favero et al., 2008). As discussed above, denervation causes membrane depolarization and increases resting intracellular $Ca^{+2}$ concentration, two events that activate SK channels. More importantly, there is evidence that the SK channel is a major component causing hyperexcitability and fibrillation (Neelands et al., 2001b). Apamin treatment, to selectively block SK channels, or EGTA treatment, to lower intracellular $Ca^{2+}$ concentration, both suppress the hyperexcitability and fibrillation in denervated rat muscle (Neelands et al., 2001b). The authors of the study suggested that the concomitant depolarization and increases resting intracellular $Ca^{2+}$ concentration increase the SK open probability, leading to a $Ca^{2+}$ entry and further membrane depolarization toward the action potential threshold. Once the depolarization causes $E_M$ to reach the threshold,

then action potentials are generated by the $Na_V1.5$ channels giving rise to the fibrillation (Sekiguchi et al., 2012b).

Denervation also affects the isoform and content of the $Ca^{2+}$ ATPase pump (SERCA), the pump that transports $Ca^{+2}$ back into the SR to allow muscles to relax. In skeletal muscle, two SERCA isoforms are expressed: the fast isoform SERCA1, which is mainly expressed in fast twitch muscles; and the slow isoform SERCA2, which is mainly expressed in slow twitch muscles (Hämäläinen and Pette, 2001). Over a 28-day denervation period, the mRNA and protein level of SERCA2 in the soleus muscle decrease by 45% and 24%, respectively, while SERCA1 remains unchanged. Over the same denervation period, SERCA1 mRNA and protein level in the EDL muscle decrease by 13% and 22%, respectively, while SERCA2 remains unaffected (Schulte et al., 1994). Overall, these changes in protein content result in a lower capacity to pump $Ca^{2+}$ back into the SR by 63% in the soleus and 22% in the EDL muscle (Schulte et al., 1994). Such reduced capacity to pump $Ca^{2+}$ has three effects: 1) lower SR $Ca^{2+}$ content contributing to the decrease in $Ca^{2+}$ release during contraction; 2) slowing down in the capacity of muscle to relax; and 3) an increased in resting intracellular $Ca^{2+}$ that can interfere with $Ca^{2+}$ sensitive signaling pathways, such as an activation of the calcineurin/ NFAT signalling pathway, which favour fiber type composition switch towards type I and IIA fibers (Schulz and Yutzey, 2004) as well as increases in mitochondrial ROS production (Powers et al., 2012; Brookes et al., 2004) .

Finally, denervation induces a shift in fiber type distribution—i.e., the myosin isoforms being expressed. For example, after 2 weeks denervation, type I and type IIA fibers decrease by 15% and 28%, respectively, while type IIX increases by 42% in the soleus muscle. In the EDL muscle, denervation increases type IIA fibers by 25% and decreases type I, IIX and IIB fibers

by 72%, 47% and 60%, respectively (Jakubiec-Puka, 1992). Furthermore, during a 50-day denervation, type IIB fibers decrease by 27% concomitantly with a 27% increase in type IIX fibers in EDL, while there is a 16% shift in fiber type composition from type I to type IIA fibers in soleus muscle (Patterson et al., 2006). Another study, this time on rabbit TA muscle, reported a shift from type IIX to type IIA fibers after 10 weeks of denervation—i.e., from 30 % type IIA and 66% type IIX fibers to 97% type IIA with no more type IIX fibers while the number of type I fibers remained unchanged, being 2% (Ashley et al., 2006). The same study also reported that 20% of fibers express the neonatal fiber type isoform after 10 weeks progressively increasing to 75% after 51 weeks (Ashley et al., 2006). In general, those studies suggested that denervation shifts fiber type composition toward faster type IIX fibers in the order of I>IIA>IIX in the slow soleus muscle and toward type IIA in the order of IIB>IIX>IIA in fast TA and EDL muscles.

## 1.4 REGULATION OF MUSCLE MASS

Muscle mass is regulated by two major pathways: the hypertrophic and atrophic pathways. A fine balance between those pathways leads to normal healthy muscle. The regulation of muscle mass is complex and involves cross-talk between several cellular signaling pathways, such as the Akt-mTOR signaling pathways, the bone morphogenic protein signaling pathway, the autophagic lysosomal pathway and the ubiquitin-proteasome system.

### HYPERTROPHY PATHWAYS

Hypertrophy is defined as an increase in the muscle mass and size of pre-existing fibers. Hypertrophy occurs during postnatal development or in response to either strength training

and/or anabolic hormone stimulation (such as testosterone and catecholamines). During hypertrophy, the rate of protein synthesis exceeds the rate of protein degradation.

Several intracellular signaling pathways have been identified for hypertrophy, including the IGF-1 activated protein kinase B (Akt) / mammalian target of rapamycin (mTOR) pathway, Bone morphogenic protein (BMP)/ Smad pathway and Wnt7a pathway (Schiaffino et al., 2013). In relation to this project, the Akt/mTOR pathway is the most important for four reasons. First, the Akt/mTOR signaling pathway is recognized as a master regulatory protein synthesis signaling pathway that increases protein synthesis (Glass, 2005; Vandenburgh et al., 1990; Bonaldo and Sandri, 2013). Second, activation of the Akt/mTOR pathway is crucial in preventing protein degradation or atrophic pathway, as it inhibits the atrophic related gene expression (Fig. 1.2). Third, this pathway is transiently activated following denervation (MacDonald et al., 2014a). Fourth, it is a major pathway that is activated by Ang 1-7, the protein of interest in this project, as discussed in a later section.

IGF-1 is a 7.6 kD protein that has 50% similarity with insulin (Boulware et al., 1994). It is a major growth factor synthesized by several tissues including skeletal muscle (Werner et al., 2008). The IGF-1 receptor is a tyrosine kinase receptor composed of two α subunits, the extracellular subunits that act as the IGF-1 binding site, and two β subunits, the intracellular subunits that contain the tyrosine kinase domains (Werner et al., 2008) . Each β subunit is linked to α-subunit by disulfide bonds on the extracellular side. Upon binding of IGF-1 to its receptor, the intrinsic tyrosine kinase (β subunits) is activated and autophosphorylates itself, which then phosphorylates the insulin receptor substrate (IRS). Phosphorylated IRS then acts as a docking site to recruit and activate phosphatidylinositol-3-kinase (PI3K) to eventually lead to the phosphorylation of Akt and mTOR (Fig. 1.2) (Schiaffino and Mammucari, 2011). There are two mTOR proteins: mTORC1 and the mTORC2 (Bhaskar and Hay, 2007). When mTORC1 is phosphorylated, it promotes protein synthesis via the phosphorylation of Eukaryotic Translation Initiation Factor 4E (elF4E)-binding protein 1 (4E-BP) and S6 kinase (S6K) proteins (Bodine et al., 2001a; Rommel et al., 2001). Phosphorylation of 4E-BP1 causes its release from eIF4E, allowing the binding of elF4E to eIF4G, which promotes mRNA translation initiation (Bodine et al., 2001a). S6K phosphorylation, on the other hand, leads to the phosphorylation of S6 ribosomal protein

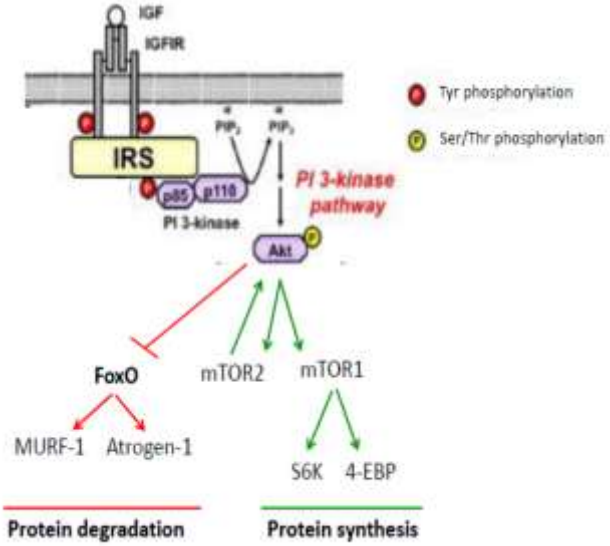


**Figure 1.2: The IGF-1 activating Akt/mTOR signalling pathway** (Hakuno and Takahashi, 2018).

involved in mRNA translation (Jefferies et al., 1997). The mTORC2 activation, on the other hand, induces a feedback phosphorylation of Akt that amplifies the Akt/mTOR signal axis, as well as allowing the phosphorylation of FoxO, a major atrophic family of transcriptional factors, to inhibit atrophic genes expression (Guertin et al., 2006). The Akt/mTOR signaling pathway is also activated by different upstream triggers to induce hypertrophy, including β-adrenergic and Ang 1-7 receptors, which will be discussed later.

Several studies have demonstrated the importance of the Akt/mTOR pathway in hypertrophy. A 3-week exposure of the gastrocnemius muscle to tamoxifen, an estrogen receptor agonist acting via Akt /mTOR, increases mean fiber CSA by 50% (Blaauw et al., 2010). Another study reported that mean gastrocnemius muscle fiber CSA from 2-week-old transgenic mice overexpressing an active Akt is 2-time greater than that of wild type mice (Izumiya et al., 2008). Physical activity, such as 14-day muscle loading of the plantaris muscle (obtained when cutting the gastrocnemius and soleus tendons) increases total Akt (T-Akt) protein content and its phosphorylation (P-Akt) level by 4- and 9-fold, respectively, concomitantly with a 45% increases in plantaris muscle weight compared to control muscles (Bodine et al., 2001b). Conversely, pathological conditions that induce muscle atrophy downregulate the Akt/mTOR signaling pathway activity. For example, 2 to 3 weeks immobilization causes a 50% decrease in the Akt phosphorylation level in TA muscle (Morales et al., 2016; MacDonald et al., 2014b). Interestingly, some pathological conditions transiently upregulate the Akt/mTOR signaling pathway such as following denervation (Castets et al., 2019; MacDonald et al., 2014b). The Akt/mTOR signaling pathway is upregulated starting from day one after denervation (Castets et al., 2019). Even after 3 weeks denervation, total Akt and P-Akt protein content in the TA muscle is 5–7 fold greater than in normal muscle (MacDonald et al., 2014a) ,despite the fact that a major

atrophy process is occurring. The authors of the study actually suggested that the increase in Akt and P-Akt acts as a compensatory mechanism to prevent further atrophy. This is an interesting fact, considering that denervation leads to muscle atrophy.

Bone morphogenic protein (BMP)/ Smad signaling pathway is another positive muscle mass regulatory pathway. BMP ligands are transforming growth factors for which 15 isoforms have been identified (Wang et al., 2014). BMP binds to a cell surface receptor that is comprised of two dimers of type I and type II serine/threonine kinase receptors forming a heterotetrameric complex (Wang et al., 2014). Upon complex formation, the constitutively active type II receptor transphosphorylates the type I receptor. As the latter becomes active, it phosphorylates downstream substrate proteins such as Smad 1/5/8, which are transcription factors (Wang et al., 2014). Phosphorylated Smad 1/5/8 forms a complex with another transcription factor, Smad 4, and the complex translocates to the nucleus to downregulate expression of several genes, such as the Fbox gene, one of the atrophic genes that encode for ubiquitin ligase (Sartori et al., 2013b).

Injecting mice muscle with either the vector encoding BMP7 to increase its expression or a constitutively active type I receptor induces hypertrophy in normal muscle. Four to seven weeks after the injection, the TA and EDL muscle mass increase by 25-35% and 20%, respectively (Sartori et al., 2013b; Winbanks et al., 2013). Following 7 weeks of active type I receptor overexpression, the TA CSA significantly increases by 50%, while the maximum tetanic force increases by 20% (Sartori et al., 2013b). The increased muscle mass is associated with a significant increase in Smad 1/5 phosphorylation level, as well as the phosphorylation levels of Akt, mTOR, 4EBP and S6K (Winbanks et al., 2013).

Overexpression of the active type I receptor reduces muscle mass loss associated with denervation (Sartori et al., 2013b; Winbanks et al., 2013). For example, overexpression of active

type I receptor in the TA muscle reduces the extent of muscle weight and CSA loss during 2-week denervation to the point that weight and CSA are no longer significantly different from that of normal innervated muscle (Sartori et al., 2013b; Winbanks et al., 2013). Also, verexpression of active type I receptor increases the phosphorylation level of Smad 1/5, whereas Smad 6, a endogenic inhibitor of phosphorylated Smad 1/5, expression decreases after 3- to 14-days of denervation (Sartori et al., 2013b; Winbanks et al., 2013).

## ATROPHY PATHWAYS

Atrophy is the result of greater protein degradation rate exceeding protein synthesis rate (Bonaldo and Sandri, 2013). There are two major protein degradation systems that are activated during muscle atrophy: i) the autophagic lysosomal pathway and ii) the ubiquitin-proteasome system (UPP) (Milan et al., 2015a; Wang and Mitch, 2014). In healthy muscle, a balanced activation of protein synthesis and protein degradation systems is crucial to maintain normal homeostasis in skeletal muscle. Autophagy is a mechanism that allows for the degradation and recycling of cellular components (Milan et al., 2015a; Wang and Mitch, 2014). During this process, targeted cytoplasmic components are isolated from the rest of the cell within a double-membrane vesicle known as an autophagosome. After the fusion of an autophagosome with a lysosome, which contains several protease enzymes, components are degraded into their smaller units, such as amino acids, fatty acids, nucleic acids and carbohydrates (Milan et al., 2015a; Wang and Mitch, 2014). A major factor upregulating autophagy is the transcription factor Forkheah box O (FoxO) family, which are transcriptional activators that regulate several atrophic gene expressions under stress conditions such as starvation, oxidative stress, ageing and disused atrophy (Baehr et al., 2007; Milan et al., 2015b; Greer and Brunet, 2008). For example, 24-hour fasting significantly increases autophagy vesicle formation in wild type TA muscle, but not in

FoxO 1, 2, 3 knockout muscle (FoxO123$^{-/-}$). The mRNA level of cathepsin L, a lysosomal protease, also increases by 3-fold in wild type muscle but not in FoxO123$^{-/-}$ muscle (Milan et al., 2015a). Compared to fasting, knockout FoxO123$^{-/-}$ partially prevents the increase in the cathepsin mRNA level in denervated muscle (Milan et al., 2015b). Furthermore, 7-day denervation significantly increases the level of several autophagy proteins by 2 to3 fold, these proteins are involved in forming autophagosomes such as LC 3II, a substrate for protease; Beclin 1, a regulator protein for autophagy; P62, an autophagy receptor; and ATG7, a ubiquitin like modifier activating enzyme (O'Leary et al., 2012).

Autophagy gene expression is also regulated by histone deacetylase (HDAC). HDAC is an enzyme that removes the acetyl group on lysine from the histone N-terminal, which then allows histone to fold tightly around DNA, making it less accessible to transcription factors (Ceccacci and Minucci, 2016). A study found that HDAC 1/2 regulates muscle autophagy by increasing the expression of autophagy genes LC3 and P62 (Moresi et al., 2012). For example, in the TA muscle, the mRNA level of LC3II and P62 increases by 5- to 6-fold after 24-hour fasting in wild type mice, and that increase is abolished in HDAC1/2 knockout mice (Moresi et al., 2012).

The ubiquitin–proteasome system is responsible for removing sarcomeric proteins. It involves three ubiquitination enzymes: E1 ubiquitin activation proteins, E2 ubiquitin conjugation enzymes, and E3 ubiquitin ligation proteins (Fig.1.3). Ubiquitin is a highly conserved protein that contains 76 amino acid residues and acts as a tag for degradation of targeted proteins. E1 activates ubiquitin by forming a thio ester bond at its C-terminal; this reaction requires ATP (Scheffner et al., 1995). Then, E1 passes the active ubiquitin protein unit to E2, and the E2-UB

complex binds to E3 ligase. Finally, the E3 ligase catalyzes the attachment of ubiquitin unit to the target protein via peptide bond.

This cycle repeats itself until the target protein has a chain of ubiquitin units, which provides a signal for the protein degradation by the proteasome 26S complex (Milan et al., 2015a; Wang and Mitch, 2014). The rate-limiting step of the ubiquitination process is with the E3 enzyme. A large number of E3 enzymes have been identified over the years, but two of them have been extensively studied in skeletal muscle: i) the atrophy F-box (atrogin-1/MAFbx) and ii) muscle RING finger 1 (MuRF1) (Milan et al., 2015a; Wang and Mitch, 2014). Both atrogin-1 and MuRF1 are highly expressed during atrophy. For example, the mRNA level of atrogin-1 and MuRF1 significantly increases by 6- to 15-fold after 3 days of fasting or denervation (Baehr et al., 2011; Milan et al., 2015b). Denervation also increases the protein level of MuRF1 by 70% compering to contralateral innervated muscle after 7 days, which then returns back to base level after 14 days (Baumann et al., 2016b). Mice lacking atrogin-1 and MuRF1 are resistant to muscle atrophy induced by denervation (Bodine et al., 2001a). Furthermore, knockout atrogin-1 prevents muscle

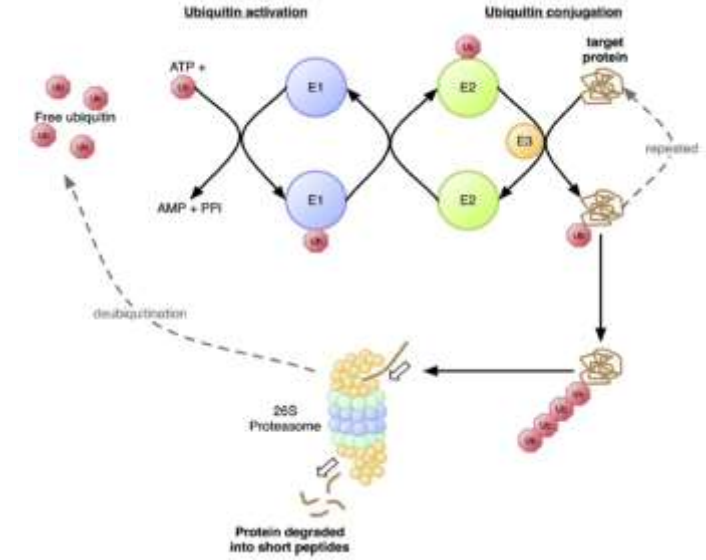


**Figure 1.3: The steps of Ubiquitin-Proteasome Pathway.** Three enzymes are required to tag proteins that need to be degraded with chains of ubiquitin unit; i) E1 (ubiquitin-activating enzyme) which activates ubiquitin units; ii) E2 (ubiquitin-conjugating enzyme) which prepares ubiquitin units for conjugation; and iii) E3 (ubiquitin ligase) which catalyzes transfer ubiquitin units to the target protein. Next, tagged protein degrades by proteasome and releases ubiquitin units (Murton et al., 2008) .

mass loss associated with fasting (Cong et al., 2011). Also, MuRF1 knockout mice are resistant to dexamethasone-induced muscle atrophy (Baehr et al., 2011). Those studies clearly establish an important role for those two ligases in muscle atrophy.

So far, few muscle specific proteins have been identified as substrate for atrogin-1 and MuRF1 E3 ligase. For example, atrogen-1 promotes degradation of eukaryotic translation initiation factor 3F (elF3F), an important translation enhancer that activates protein synthesis by acting as scaffold protein which interconnects with mTOR1 to positively regulate mTORC downstream pathway (A et al., 2010). MuRF-1 physically interacts and degrades the muscle functional proteins such as myosin heavy chain (Fielitz et al., 2007; Clarke et al., 2007), myosin binding protein C and myosin light chain (Cohen et al., 2009). The loss of these proteins is not observed in MuRF-$1^{-/-}$ muscle.

The expression of atrogin-1 and MuRF1 is regulated by specific transcription factors such as FoxO and myogenin, both are being essential for the regulation of muscle development and maximal induction of the E3 genes during atrophy (Moresi et al., 2010a; Schiaffino and Mammucari, 2011). The transcriptional activity of FoxO is also inhibited by the activation of Akt/mTOR signaling pathway. In the presence of any growth factor such as IGF-1, the PAkt directly phosphorylates FoxO to become inactive, which leads to excluding FoxO from the nucleus to suppress its transcriptional activity. The inhibition of Akt/mTOR signaling pathway allows FoxO to remain dephosphorylated (active form), so it translocates to the nucleus to promote the expression of atrogin-1and MuRF1 (Milan et al., 2015a; Wang and Mitch, 2014). For example, the mRNA level of atrogin-1 and MuRF1 increase by 12-14 fold after 24 hours in fasting mouse TA muscle, an increase that is completely abolished in knockout FoxO134 mice (Milan et al., 2015b). Moreover, following 3-day denervation, atrogin-1 and MuRF1 mRNA

levels are, respectively, 6- and 11-fold less in knockout FoxO134 than in wild type TA muscle (Milan et al., 2015b).

Myogenin is another transcriptional factor that plays important role in controlling Murf-1 and atrogin-1 expression during atrophy especially in denervated muscle (Moresi et al., 2010a). It is also essential for muscle fibroblast differentiation as it facilitates cell cycle exit (Liu et al., 2008; Brunetti and Goldfine, 1990; Walsh and Perlman, 1997). In regard to muscle atrophy, the expression of myogenin is upregulated by muscle inactivity such as denervation (Eftimie et al., 1991). For example, myogenin expression increases by 25-fold in the gastrocnemius and TA muscles during 7 day denervation (Moresi et al., 2010a). As consequence of that increase, more myogenins are translocated to the nucleus and bind to the promoter regions of Murf-1 and Atrogin-1 genes to activate their transcription (Moresi et al., 2010b). Deleting myogenin ($Myog^{-/-}$) in adult mice reduces muscle atrophy following denervation (Moresi et al., 2010a). For example, 14 days denervation induces 40% weight loss in wild type mouse TA muscle compared to only 20% loss in $Myog^{-/-}$ TA muscle (Moresi et al., 2010a). The mRNA levels of Murf-1 and atrogin-1 are also significantly reduced from 15- and 7-fold, respectively, to 5-fold in $Myog^{-/-}$ mice after 7 days denervation (Moresi et al., 2010a).

*Mitochondria in atrophy*

Mitochondria play additional roles in atrophy. Normally, mitochondria constantly goes through fusion, which is the merging of two mitochondria, and fission, which is the splitting of one mitochondria into two (Romanello and Sandri, 2016). Fused mitochondria optimize their function, and this increases the bioenergetic capacity of muscle to produce ATP (Romanello and Sandri, 2016). Fission, on the other hand, occurs to segregate dysfunctional or damaged mitochondria, allowing their removal via mitophagy, an autophagy process that selectively

degraded damaged mitochondria (Romanello and Sandri, 2016). Therefore, any fusion and fission cycle imbalance can dramatically change mitochondria content and function (Chen and Chan, 2005). Denervation and immobilization decrease mitochondria density by 50% in several muscles after 2 weeks, and a further 25% after 3-10 weeks (Kang and Ji, 2016; Kang et al., 2015; Wessig et al., 2004; Singh and Hood, 2011a). The later change leads to reduced oxygen consumption by 16 -45% (Singh and Hood, 2011b) and ATP production capacity by 50% (Kang et al., 2015). Furthermore, the reactive oxygen species (ROS) increases by 5-7 fold, which eventually activates pro-apoptotic factors (Zammit et al., 2006; Powers et al., 2010).

In fact, mitochondria play a major role in apoptosis during atrophy (Siu and Alway, 2005; Adhihetty et al., 2007). Mitochondria contain pro-apoptotic factors that can be released through a mitochondrial permeability transition pore (mtPTP) upon stress stimulation (Crompton, 1999). For example, denervation increases the maximal rate of mitochondrial pores opening in the TA muscle up to 25-35% after 21 days (Adhihetty et al., 2007), allowing for the release of pro-apoptotic factors such as cytochrome C, apoptosis inducing factor (AIF) and endonuclease G (Endo G) to cytoplasm, where they cleave and stimulate apoptotic pathway (Adhihetty et al., 2007, 2008; Dejean et al., 2006; Siu and Alway, 2005). For example, the cytochrome C protein content measured from mitochondria-free cytoplasm increases by 40% after 14-day denervation (Siu and Alway, 2005). As consequence of cytochrome C release, it triggers the activation of caspase-9, followed by engagement of caspase-3, which performs protein breakdown and DNA fragmentation via caspase-activated DNase (CAD) (Plant et al., 2009; Siu and Alway, 2005). The release of AIF and Endo G directly cause 100 fold increases in DNA fragmentation within 14 days denervation (Marzetti et al., 2010; O'Leary and Hood, 2008; Siu and Alway, 2005).

## 1.5 THE IMPORTANCE OF PREVENTING ATROPHY FOLLOWING DENERVATION

Loss of muscle mass, integrity, and functionality have major clinical implications, especially following level II and III nerve injury. Level II nerve injury or axonotmesis involves damage to axons and myelin sheaths, with intact connective tissue; in such cases, nerve repair takes 3-6 months. Level III nerve injury or neurotmesis occurs when a nerve is fully transected, and repair takes 6-12 months as the nerve grows slowly at a rate of one inch per month (Galvin and Eichinger, 2016; Berry and Bril, 1982; Blom and Dahlbäck, 1970; Menorca et al., 2013). The repaired nerve thus ends up reinnervating a deteriorated and atrophied muscle, especially in neurotmesis cases. It has been shown that muscle recovery following reinnervation depends on how long nerve repair are delayed. For example, after 6 months from surgical reinnervated gastrocnemius muscle that had denervated for 3 months, muscle weight recovers to only 20% of its original weight (Kobayashi et al., 1997).

Although the atrophy process is much faster in mice/rats (i.e., weeks/months) than in humans (i.e., years), recovery studies following reinnervation in mice/rats can highlight the difficulties facing human skeletal muscle upon reinnervation following a prolonged denervation period. For example, reinnervation after a 21-week denervation partially restores original fiber type distribution, in which the proportion of type I fiber remains greater than control in rat gastrocnemius and TA muscle (Wang et al., 2002). Among several studies that reported force measurement following denervation, only a few show full recovery when the nerve is repaired immediately after denervation, otherwise, the force recovery is partial (Cederna et al., 2000; Aydin et al., 2004). The maximum force of rat gastrocnemius muscle that has been denervated for 1-3 months, recovers only 48-50% compared to innervated muscle

after 6 months of reinnervation surgery (Aydin et al., 2004). Another study reported that reinnervation following 7-month denervation of mouse soleus allows for a recovery of maximum force by 72% after 5-6 months, and by 87% after 10 months (Irintchev et al., 1990). Resting membrane potential returns to normal values in rat EDL and soleus muscles after 22 days of nerve crushing, whereas AP properties such as overshoot does not return to normal value even after 60 days (McArdle et al., 1980). In general, muscle recovery is not a problem with short denervation period lasting less than 4 weeks, whereas recovery is very poor if the denervation period exceeds 3 months (Bain et al., 2001; Aydin et al., 2004; Brown et al., 2002). Therefore, the development of an efficient treatment to prevent atrophy associated with denervation to preserve muscle mass and function is extremely important.

One strategy to speed up reinnervation is a classical nerve repair surgery. This surgery involves nerve grafting, replacing the damaged nerve segment by a healthy nerve from another part of body. After the surgery, reinnervation is facilitated as the nerve fibers start to grow from the repair site toward the muscle. However, this approach is successful only if the distance that requires axonal regeneration is short (Mu et al., 2017). Chronic muscle stimulation is another approach used in the field of rehabilitation to prevent or slow down muscle atrophy in denervated muscles (al-Amood et al., 1991; Ashley et al., 2007a). However, chronic stimulation partially prevents muscle atrophy and fails to fully improve force recovery (Ashley et al., 2007b). During a 10-week denervation period, the CSA and force of rabbit TA muscle respectively decrease to 39% and 27% to that of innervated TA (Ashley et al., 2007b). When electrical stimulation is applied for 10 weeks after the 10-week denervation period, CSA and force partially recover to only 66%, while excitability, contractile speed, and fatigue resistance do not return to normal levels (Ashley et al., 2007b). Notably, electrical stimulation prevents

changes in some functional protein isoforms such as NMJ remodelling, Nav 1.5 and embryonic nAChR gene expression γ-subunit (Bezakova et al., 2001; Adams et al., 1995b). Finally, another issue with electrical stimulation is that while it is feasible in small animals such as rats and mice, it is a lot more difficult to use with large muscle mass as in the case for human patients.

Several pharmaceutical approaches have been tested in attempts to counteract atrophy by targeting mechanisms that controlling muscle mass. For example, activating the Akt/mTOR signaling pathway using IGF-1 analogs or β-adrenergic agonists partially prevents CSA and force loss, and decreases expression of the atrophic genes atrogin-1 and MuRF-1 in different atrophy models (Hinkle et al., 2002; Zeman et al., 1987; Mounier et al., 2007; Vandenburgh et al., 1991; Schiaffino and Mammucari, 2011; Neff et al., 1993). Inhibiting the myostatin pathway with ActRIIB, a type IIB receptor antagonist, prevents muscle mass loss as well as MURF-1 and atrogin-1 induction under conditions such as immobilization and aging, but not in denervated muscle (Tando et al., 2016; Sartori et al., 2009; Mendias et al., 2006; Baumann et al., 2003; MacDonald et al., 2014b). Targeting the ubiquitin proteasome system by using MG132 or PS341, two proteasome inhibitors, fully prevents muscle mass and CSA loss. It also inhibits induction of atrophic genes MURF-1 and atrogin-1 in different atrophy models, including immobilization and hindlimb unloading, while reducing the atrophy in denervation model (Supinski et al., 2009; Caron et al., 2011; Jamart et al., 2011; Beehler et al., 2006). However, the ubiquitin proteasome system is necessary to maintain a normal biological system, chronic inhibition of this system causes several complications such as acute cardiac failure (Hacihanefioglu et al.). Another issue is that most of these trials have focused on the

hypertrophic and atrophic pathways, and only a few have reported the effects on force generation, for which the loss is often not fully reversed for an unknown reason.

Recent studies have provided evidence that the activation of the Ang1-7/MasR signaling pathway fully inhibits skeletal muscle atrophy induced by Ang II in heart failure, chronic pulmonary disease and renal failure (Martinez et al., 2010; Wang and Mitch, 2014; Gosker et al., 2000). A similar effect has been shown in immobilization (Morales et al., 2016). Ang 1-7 is therefore a potential therapeutic approach to prevent muscle atrophy in denervated muscles.

## 1.6 THE POTENTIAL OF ANGIOTENSIN 1-7 AT PREVENTING MUSCLE ATROPHY

Renin-angiotensin system (RAS) is a hormonal system that regulates blood pressure involving central and peripheral mechanisms. Angiotensinogen is released by the liver, and is cleaved to angiotensin I (Ang I) by renin, an enzyme secreted by the kidney under the condition of hypotension (Fig. 1.4). Ang I is further cleaved by the angiotensin converted enzyme (ACE) to form angiotensin II (Ang II). Through its binding to the AT-1 receptor, Ang II causes strong vasoconstriction that increases blood pressure (Cisternas et al., 2015). Ang II also promotes water intake and sodium retention by the kidneys as further mechanisms to increase blood pressure (Hall et al., 1990).

Notably, some conditions such as heart failure, chronic pulmonary disease and renal failure cause an increased plasma level of Ang II in an attempt to maintain normal blood pressure (Martinez et al., 2010; Wang and Mitch, 2014; Gosker et al., 2000; Morales et al., 2015a). Skeletal muscles express the AT-1 receptor and Ang II binding activates several atrophic mechanisms while inhibiting hypertrophic mechanisms (Fig. 1.4) (Cabello-Verrugio et al., 2015). Treating mice with Ang II (1 µg / kg per min) for 7 days decreases myosin heavy

chain protein content by 50%, significantly reduces fiber diameter and lowers maximum force by 25% in gastrocnemius muscle (Cisternas et al., 2015). Even a single day of Ang II exposure increases the expression of two atrophy genes atrogin-1 and MuRF-1 by 2- and 3-fold, respectively, in mouse gastrocnemius muscle (Cisternas et al., 2015). Furthermore, Ang II increases oxidative stress, in part by enhancing NADPH oxidase (NOX) activity in skeletal muscle, resulting in increased ROS production (Semprun-Prieto et al., 2011; Zhao et al., 2006). Ang II also promotes fibrosis, cellular proliferation and inflammation in skeletal muscles (Semprun-Prieto et al., 2011; Kadoguchi et al., 2015, 2018; Morales et al., 2012). Finally, it increases nuclear apoptosis by 8-folds, caspase 8/9 protein level by 2.5- to 3-fold and caspase-3 activity by 3-fold in diaphragm muscle over a 14-day treatment (Meneses et al., 2015). All these effects are blocked by Losartan, an AT-1 receptor blocker, supporting the concept of a direct effect of Ang II via its AT-1 receptor in skeletal muscle (Siegl et al., 1995).

Non-classical renin-angiotensin system (non-RAS) is another regulatory axis of RAS. Angiotensin 1-7 (Ang 1-7) is the main peptide of the non-RAS and is produced from Ang II when one amino acid is cleaved by the angiotensin converting enzyme 2 (ACE2) (Fig. 1.4). ACE2 is expressed in several tissues, including the plasma membrane of skeletal muscle and capillary endothelia cells (Mori and Tokuyama, 2007; Fernandes et al., 2010). Ang 1-7 is also produced from Ang I, a reaction carried out by the neprilysin enzyme (NEP) (Ward et al., 1995; Dragović et al., 1996; Vaghy et al., 1995). Ang 1-7 acts as local vasodilator, counteracting the vasoconstriction effect of Ang II (Cabello-Verrugio et al., 2015). Similar to Ang II, the physiological effects of Ang 1-7 are not limited to a control of blood pressure. Ang 1-7 has anti-oxidant effect in diabetic hypertensive disease (Li et al., 2016) and anti-inflammatory effect in allergic asthma as well as ischemic stroke conditions (Bennion et al., 2016; El-Hashim et al.,

2012). It improves glucose uptake and insulin sensitivity in a model of type II diabetes by increasing glucose transport 4 (GLUT4) translocation to the cell membrane (Santos et al., 2014). In skeletal muscle, Ang 1-7 binds to the G-protein coupled transmembrane receptor Mas (MasR) and decreases the activity of the atrophic pathway while increases the activity of the hypertrophic pathway in different muscle atrophy models(Cabello-Verrugio et al., 2015), as discussed below.

One major impact of Ang 1-7 in skeletal muscle is a complete reversal of the Ang II-induced atrophy. For example, Ang 1-7 completely prevents the reduction in fiber diameter, myosin heavy chain protein content and force loss induced by Ang II (Cisternas et al., 2015). A major mechanism of action for Ang 1-7 involves a 3-fold increase in Akt phosphorylation as it stimulates the master hypertrophic pathway Akt/mTOR pathway (Fig. 1.4) (Cisternas et al., 2015). The Akt activation also results in the phosphorylation of FoxO, reducing its activity and resulting in a decreased expression of atrogin-1 and MuRF-1 (Morales et al., 2015b; Cisternas et al., 2015). Ang 1-7 blocks the Caspase Bax/Bcl2 axis, reducing myonuclear apoptosis of atrophic muscle associated with Ang II (Meneses et al., 2015). The chronic elevation of ROS production by Ang II is also prevented by Ang 1-7 (Morales et al., 2014). For example, pre-treating C2C12 myoblast with Ang 1-7 (10 nM) for 1 hour prior to an exposure to Ang II (500 nM) for 24 hours reduces ROS production by 2.5-fold (Morales et al., 2014).

# FIGURE 1.4

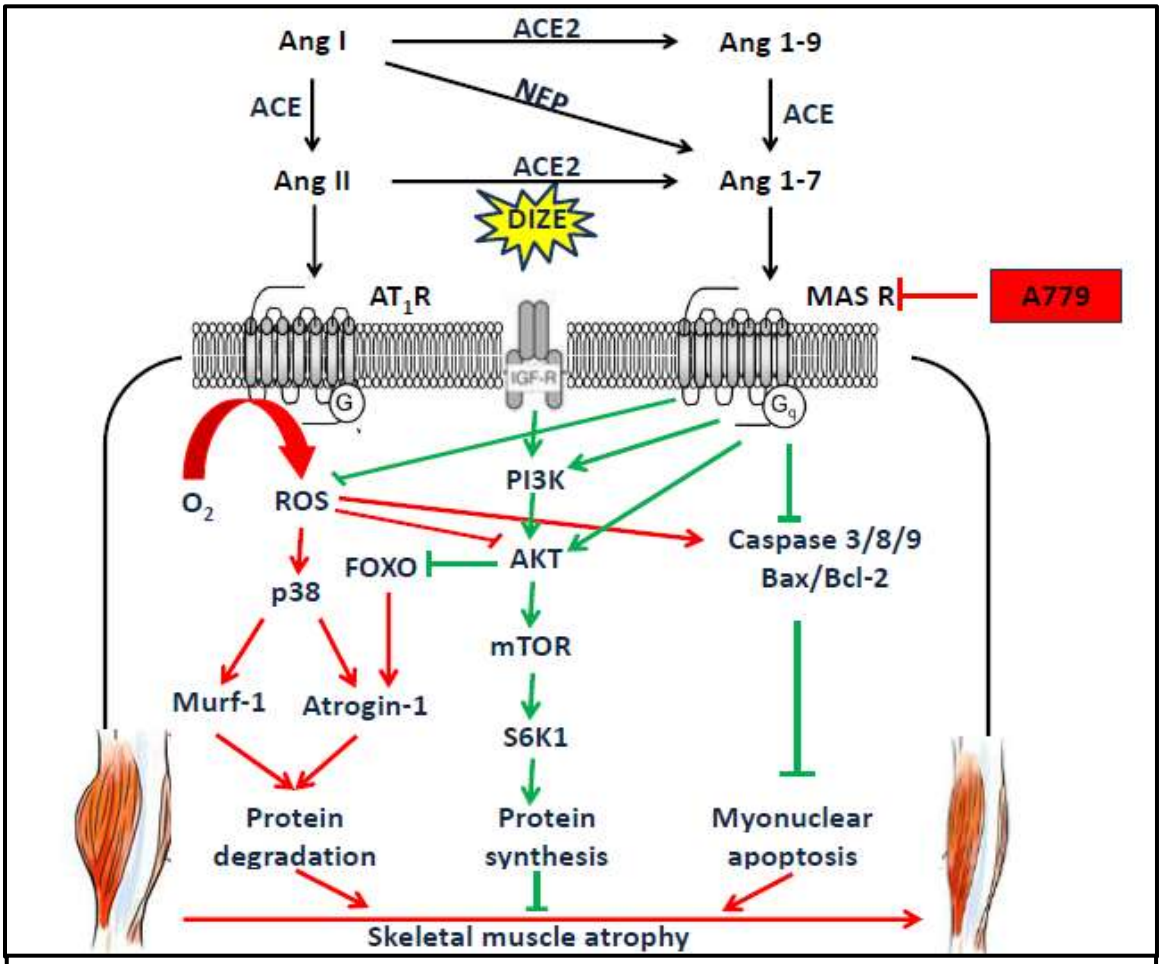


**Figure 1.4: Classical RAS and nonclassical RAS axis regulate muscle mass. "**The classical RAS pathway driven by Ang II (red arrows) is an inducer of skeletal muscle atrophy involved in the regulation of several mechanisms of muscle mass control such as protein degradation, protein synthesis and myonuclear apoptosis. Ang II induces protein degradation through ROS accumulation that modulates the expression of MuRF-1 and atrogen-1 through NF-$_k$B and P38 MAPK activation. Also, Ang II activates FoxO which also regulate the expression of MuRF-1 and atrogen-1. Moreover, Ang II increases its catabolic action by down regulating protein synthesis via Akt inhibition. In contrast to Ang II, the non-classical RAS pathway (green arrows), activated by Ang 1-7, can change the balance toward anabolic pathway by Akt activation and stimulation of protein synthesis. Ang 1-7 negative regulates protein degradation by decreasing MuRF-1 and atrogen-1 expression, as well as inhibiting pro-apoptotic pathway" reviewed in (Cabello-Verrugio et al., 2015).

In the dystrophic mice mdx model, Ang 1-7 decreases local fibrosis, restores muscle architecture, increases muscle mass and improves muscle function by inhibiting the TGF-β signaling pathway (Acuña et al., 2014). The maximum tetanic force generated by the gastrocnemius muscle of dystrophic mice is 80% less than its wild type counterpart. Tetanic force increases during a 2-month Ang 1-7 treatment, becoming only 42% less than in wild type muscle (Acuña et al., 2014). A779, a MasR antagonist, completely abolished the Ang 1-7 effects in dystrophic mice, supporting the concept that Ang 1-7 acts via its receptor MasR (Acuña et al., 2014). Furthermore, Ang 1-7 prevents muscle atrophy associated with sepsis syndrome (Pinsky, 2004; Winters et al., 2010). Treating mice with lipopolysaccharide-endotoxin (LPS, 1 mg/Kg) for 14 days to induce sepsis reduces gastrocnemius maximum force by 25% compared to control; concomitant administration of Ang 1-7 (100 ng/kg/min) prevents the force loss (Morales et al., 2015b). It also prevents the increase in MURF-1 and atrogin-1, as well as the phosphorylation of mitogen activated protein kinase (p38 MAPK) induced by LPS (Morales et al., 2015b). The authors of this study have suggested that Ang 1-7 prevents muscle atrophy associated with endotoxin through p38MAPK dependent mechanism.

Finally, Ang 1-7 prevents muscle atrophy and force loss associated with the disuse model. For example, immobilization of TA muscle for 2 weeks decreases isometric strength by 35%, but not in Ang 1-7 treated mice (Morales et al., 2016). The other immobilization effects — that are, the 38% muscle mass loss, the 2.5- to 2.7-fold increase atrogin-1 and MuRF-1 mRNA level, and the decrease Akt phosphorylation level — are also prevented by Ang 1-7 treatment (Morales et al., 2016). Notably, all Ang 1-7 effects in immobilized muscle are not observed in MasR knockout mice, again suggesting that the Ang 1-7 effects involves MasR.

Together, these studies provide evidence that Ang 1-7 acts as a potential anti-atrophic factor under different pathological conditions. It remains to be determined, however, how effective Ang 1-7 is at preventing muscle atrophy and function loss following denervation model.

# OBJECTIVES AND HYPOTHESIS

The overall objective of this Ph.D. thesis is to test the hypothesis that **"Angiotensin 1-7 (Ang 1-7) prevents muscle atrophy and force loss following denervation".**

To test this hypothesis, three aims are proposed as follows:

Aim 1: To document the hypertrophy effect of Ang 1-7 in normal mouse skeletal muscle.

Aim 2: Test the hypothesis that Ang 1-7 prevents muscle atrophy and force loss following a short 2 and 4 weeks denervation period.

Aim 3: Test the hypothesis that Ang 1-7 prevents muscle atrophy and force loss following a long 16 week denervation period.

# CHAPTER 2

# METHODS AND MATERIALS

## 2.1 ANIMALS

Wild type CD-1 mice and the Mas receptor knockout mice ($MasR^{-/-}$) generated by Walther et al., 1998 (Walther et al., 1998) were used. Mice were bred, fed *ad libitum* and housed according to the guidelines of CCAC (Canadian Council for Animal Care). The Animal Care Committee of the University of Ottawa approved all surgical and experimental procedures.

## 2.2 GENOTYPING

All $MasR^{-/-}$ mice were genotyped using NucleoSpin Tissue kit (cat# 740952.250, Macherey Nagel, Germany). Briefly, a 2-3 mm piece of ear was incubated in a proteinase digestion buffer overnight at 56°C. After adding elution buffer, digested tissues were incubated at 70°C for 10 min before being centrifuged 5 min at 11000 g. Supernatant was washed with ethanol, and the extracted DNA subjected to PCR using the following primers:

Forward: GCC GTT GCC CTC CTG GCG CCT GGG

Reverse: GGC AGC GCG GCT ATC GTG G

Bands were visualized using gel Doc imager (Bio Rad, U.S.A).

## 2.3 DENERVATION PROCEDURE – ANG 1-7, DIZE AND A779 TREATMENT

Mice received a subcutaneous injection of buprenorphine (0.05 mg/kg) before surgery. For the surgery, mice were anesthetized using 2.5-3.5% isoflurane and 1 ml of sterile 0.9% NaCl solution was injected in the neck to minimize dehydration. A small posterolateral (mid-thigh) incision was made, and 3-4 mm of the sciatic nerve was removed. For the Ang 1-7 treatment

(Sigma Life Science) with and without A779 (Tocris bioscience), a small incision was made in the subscapular area to create a pocket to insert an osmotic pump just under the skin (Alzet, Durect Co. 1002 (period of 2 weeks), 1004 (period of 4 weeks) and 2006 model (period of 6 weeks with replacements when it necessary). Both Ang 1-7 and A779 were administrated at dose of 100 ng/kg•min. A topical application of 2% bupivacaine was placed on the wound. Diminazene Aceturate (DIZE) (Santa Cruz Biotechnology), on the other hand, was administrated by oral gavage at a dosage of 15 mg/kg•day, which increases plasma Ang 1-7 levels by almost 4-fold (Zhang et al., 2015), without or with a treatment with A779 by osmotic pump as described above. One group of denervated mice received sucrose at 1 g/kg•day also by oral gavage as a control for the DIZE treatment.

## 2.4 FORCE MEASUREMENT

Prior to muscle excision, mice were anaesthetized with a single intraperitoneal injection of 65 mg ketamine/13 mg xylazine/2 mg acepromazine per kg body weight, and sacrificed by cervical dislocation. EDL and soleus were then dissected out for *in vitro* experiments. Muscles were positioned horizontally in a Plexiglas chamber. One end of the muscle was fixed to a stationary hook, while the other end was attached to a force transducer (Model # 400A, Aurora Scientific Canada). The transducer was connected to a KCPI3104 data acquisition system (Keithley, USA) and data were recorded at 5 kHz.

Muscle length was adjusted to give maximal tetanic force while muscles were stimulated every 100 sec. The force-frequency relationship was measured after a 30 min equilibrium period. Frequency 50 represented the stimulation frequency at which muscles generated 50% of maximum force (i.e., tetanic force). Force-frequency relationship of each muscle was fitted by

non-linear regression analysis to a sigmoidal curve (Sigma, U.S.A., Version 13) from which frequency 50 was calculated as follows:

$$FF50 = \frac{FORmax}{1 + e^{\left(\frac{-(\text{Freq}-\text{FF50})}{C}\right)}}$$

Where,

FF50: Frequency 50

FORmax: Maximum tetanic force

Freq: Stimulation frequency

C: Constant

Twitch and tetanic force, defined as the force developed following a single stimulation pulse or a train of pulses respectively, was calculated as the difference between the maximum force during a contraction and the force measured 5 msec before the contraction was elicited. Forces are presented in N and $N/cm^2$ (i.e., normalized to CSA). At the end of each experiment, muscle weight (free of tendons) was measured and converted to a volume using a density of 1.06 $g/cm^3$ and CSA was calculated by dividing muscle volume by the length measured in the bath. Time to peak was defined as the time interval between the first stimulation and the time force reached its maximum during a contraction. Half-relaxation time for a twitch contraction was defined as the time interval between the time at which force reached a peak and the time force had decayed by 50% during the relaxation phase while for a tetanic contraction it was the time interval between the time of the last stimulation was applied and the time when force had decayed by 50% during the relaxation phase.

Stimulation

Electrical stimulations were applied across two platinum wires (4 mm apart) located on opposite sides of the muscles. They were connected to a Grass S88X stimulator and a Grass

stimulation isolation unit (Grass Technologies/Astro-Med Inc., U.S.A.). Twitch contractions were elicited with a 0.3 ms, 10 V (supramaximal voltage) single pulse while tetanic contractions were elicited with 400 ms trains of the same pulses at frequencies varying between 10 and 200 Hz.

Physiological Solutions

Physiological saline solution contained (in mM): 118.5 NaCl, 4.7 KCl, 2.4 $CaCl_2$, 3.1 $MgCl_2$, 25 $NaHCO_3$, 2 $NaH_2PO_4$, and 5.5 D-glucose. Solutions were continuously bubbled with 95% $O_2$–5% $CO_2$ to maintain a pH of 7.4. Experimental temperature was 37°C. Total flow of solutions in the muscle chamber was 15 ml/min being split just above and below the muscle in order to prevent any buildup of reactive oxygen species, which is quite large at 37°C and deleterious in terms of force generation (Edwards et al., 2007).

## 2.5 RESTING EM AND ACTION POTENTIAL MEASUREMENTS

Resting membrane potential (resting $E_M$) and action potential were measured using glass microelectrodes. Microelectrodes tip resistances were 7-10 MΩ and that of the reference electrode ~1 MΩ. All electrodes were filled with 3 M KCl. A recording was rejected when the change in potential upon penetration was not a sharp drop or when the microelectrode potential did not return to zero upon withdrawal from the fiber. Stimulating electrodes for force measurements were disconnected. Instead, single action potentials were elicited using fine platinum wires 2 mm apart placed as close as possible to the surface fibers and move laterally to stimulate fibers in the region where the microelectrode was positioned. This approach was used to reduce the extent of contracting fibers and prevent the breaking or dislodging of microelectrodes. To further reduce the number of contracting fibers, action potentials were triggered using a single 2-10 V, 0.3 ms square stimulating pulse; usually a low voltage was

enough to trigger an action potential in innervated muscle fibers while higher voltages were often necessary with denervated fibers. When an action potential was not triggered, voltage was always increased to 10 V to properly verify that the fiber was unexcitable. Data were digitized using a KCP13104 data acquisition system (Keithley, USA) at 400 kHz.

The number of excitable fibers, resting $E_M$, action potential overshoot and maximum rate of depolarization were determined in 5-15 fibers in each muscle. Overshoot was taken from the action potential peak while maximum rate of depolarization was first calculated by linear regression analysis of every 10 data points and taken from the peak value. Individual values for each muscle were averaged, and the final mean was calculated from the muscle average values. For these parameters, the numbers of samples are reported as the number of muscles with the total number of tested fibers in parentheses.

## 2.6 FIBRE TYPING AND CROSS SECTIONAL AREA (CSA)

EDL and soleus muscles were embedded in Tissue-Tek, frozen in isopentane precooled in liquid nitrogen and stored at −80°C. Ten $\mu$m sections were cut at −20°C using a cryostat (Leica CM 1850), placed on positive charged glass slides and stored at −80°C. Sections were stained using a Mouse on Mouse fluorescein kit (cat# FMK-2201, MJS Biolynx, Canada) for type I, IIA and IIB fibers. Briefly, section was incubated 1 hour in M.O.M mouse Ig blocking reagent and washed with PBS. Cross-section were incubated 5 min in a M.O.M diluent protein concentrated solution before being exposed 1 hour to either mouse monoclonal anti-myosin type I (A4.840), anti-myosin IIA ( SC-71) and anti-myosin heavy chain type IIB (BF-F3; Developmental Studies Hybridoma Bank, USA). After 3 washout with PBS, cross-sections were exposed 10 min to biotinylated anti mouse IgG reagent solution. Finally, cross-sections were incubated 15 min in a fluorescein avidin (1:500) followed by 3 washout in PBS. Laminin

staining was done by incubating cross-sections with anti-laminin antibody (1:1000, Sigma, cat# L9393, rabbit polyclonal) for 30 min followed by Alexa 594 (1: 500, Invitrogen, cat# A-11012). After 3 washout with PBS, slides were mounted using wet mounting media and covered it with coverslip. Images were captured on a Zeiss Axiolmager.M2 microscope (Canada) using a digital camera (AxioCam mRm CCD). Pictures were taken from overlapping regions of each muscle and then collaged together. Fiber type and CSA (from the laminin boundaries) were determined for all fibers of each muscle using Imaris software (Bitplane an Oxford Instruments company). Unless specify otherwise, fiber type and CSA was determined for each muscle and the mean was calculated from the individual muscles; the number of samples are reported as the number of muscles with the total number of tested fibers in parentheses.

## 2.7 WESTERN BLOT ANALYSIS

EDL and soleus muscles were freeze-clamped in liquid nitrogen and kept at -80°C until used. Muscles were homogenized in Tris lysis buffer containing 20 mM Hepes, 10 mM NaCl, 1.5 mM MgCl, 1 mM dithiothreitol, 20% glycerol, 0.1% Triton X-100, cocktail of protease inhibitors (cat# 04693124001, Millipore Sigma, Oakville, ON, Canada) and phosphatase inhibitors (cat# 04693124001, Millipore Sigma, Oakville, ON, Canada). Homogenates were centrifuged 10 min at 12000 g and 4°C. Proteins concentrations in the supernatants were determined using the BCA assay method (Thermo Scientific, U.S.A.). The final protein concentrations were adjusted using Laemmli buffer (45 SDS, 20% glycerol, 10% beta mercaptoethanol, 0.004% bromophenol blue, 0.125M tris HCl PH6.8) to 25 µg/ml and heated 5 min at 95°C. Proteins (25 µg) were subjected to 8% SDS/PAGE, transferred on to nitrocellulose membrane (Bio-Rad Laboratories Inc. Miniprotean III apparatus) and probed with the primary antibodies listed in Table 2.1.

| ANTIBODY NAME | DILUTION | SOURCE | CATALOG NUMBER |
|---|---|---|---|
| rabbit anti-total-AKT | 1:1000 | Cell Signaling Technology, USA | 4691 |
| rabbit anti-phospho-AKT | 1:2000 | Cell Signaling Technology, USA | 4060 |
| rabbit anti-total-4EBP | 1:1000 | Cell Signaling Technology, USA | 9452 |
| rabbit anti-phospho-4EBP | 1:1000 | Cell Signaling Technology, USA | 9459 |
| rabbit anti-total-S6K | 1:1000 | Abcame, USA | Ab32529 |
| mouse anti-phospho-S6K | 1:1000 | Millipore Sigma, USA | MABS82 |
| rabbit anti-MURF-1 | 1:1000 | Cedarlane, USA | 554561AP |
| rabbit anti-Atrogin-1 | 1:1000 | ECM Bioscience, USA | AP2041 |
| rabbit anti-αActin | 1:1000 | Cedarlane, USA | CSB-PA00750E0RB |
| mouse anti-total-myosin heavy chain | 1:1000 | Cedarlane, USA | MAB4470 |
| rabbit anti- Na-K pumpα1 | 1:1000 | Cell Signaling Technology, USA | 3010S |
| rabbit anti- Na-K pumpα2 | 1:1000 | Millipore Sigma, USA | 07674 |

**Table 2.1. List of primary antibodies used for Western blots.**

To visualize the band, blots were subjected to either horseradish peroxidase conjugated goat anti-rabbit antibody (1:5000 dilution, cat#7074, Cell Signaling Technology, USA) or goat anti-mouse antibody (1:5000 dilution, cat#G21040, Thermo Fisher Scientific, USA) as secondary antibody. Immunoreactions were visualized and quantified by chemiluminescence ECL (PerkinElmer, Inc. MA, USA) using the LICOR imaging system (model# 2800, USA).

## 2.8 EXPERIMENTAL PROTOCOL

Three aims were proposed in the Introduction. For each aim, the wild type CD-1 mice were used to test the effects of Ang 1-7 per se and DIZE, an ACE2 agonist to increase plasma Ang 1-7 levels. To determine that the Ang 1-7 is via its Mas receptor, two approaches were used: i) Ang 1-7 or DIZE treated mice were concomitantly treated with A779, a MasR antagonist, and ii) a $MasR^{-/-}$ mouse model. For force, membrane potential, fiber types and CSA measurements,

the treatment durations were either 2, 4 and 16 weeks while a 3 day treatment period was added for the Western blots analyses of the hypertrophic and atrophic pathways. The details of all the experimental conditions are also listed in Table 2.2.

| AIMS | MICE | TREATMENT CONDITIONS | TIME PERIOD |
|---|---|---|---|
| 1. To document the hypertrophy effect of Ang 1-7 in normal mouse skeletal muscle | • CD-1<br>• MasR$^{-/-}$ | • Untreated (control)<br>• Ang 1-7 treated | • 4 week<br>• 16 week |
| 2. Test the hypothesis that Ang 1-7/ DIZE prevents muscle atrophy and maintain force following a short 2 and 4 weeks denervation period | • CD-1<br>• MasR$^{-/-}$ | • Innervated (control)<br>• Denervated<br>• Denervated / Ang 1-7<br>• Denervated / Ang 1-7-A779<br>• Denervated / sucrose<br>• Denervated / DIZE<br>• Denervated / DIZE -A779 | • 3 days<br>• 2 weeks<br>• 4 weeks |
| 3. Test the hypothesis that Ang 1-7/DIZE prevents muscle atrophy and maintain force following a long 16 week denervation period | • CD-1<br>• MasR$^{-/-}$ | • Innervated (control)<br>• Denervated<br>• Denervated / Ang 1-7<br>• Denervated / Ang 1-7-A779<br>• Denervated / sucrose<br>• Denervated / DIZE<br>• Denervated / DIZE-A779 | • 16 week |

**Table 2.2. Details of the various Ang 1-7/DIZE treatment and the time periods for each of the three aims listed in the Introduction.**

## 2.9 STATISTICAL ANALYSIS

Data are expressed as mean ± standard error (S.E.). One way ANOVAs was used to determine statistical differences for protein content measured by western blots, muscle weights and CSA. For force measurements, split plot ANOVAs were used to determine statistical differences. Comparisons between mouse groups involved muscles from different mice and thus the data were independent from one another. In this case, the S.E. for statistical differences was

the population S.E. (whole plot). Comparisons between force at different frequencies involved data from the same muscles, and thus data were not independent from one another. In this case, the S.E. for statistical differences was the S.E. between muscles (split plot). Calculations were made using the GLM (General Linear Model) procedures of the Statistical Analysis Software (SAS Institute Inc., Cary, NC, USA). When a main effect or an interaction was significant, the least square difference (L.S.D.) was used to locate the significant differences. The word "significant" refers only to a statistical difference ($P<0.05$).

# CHAPTER 3

# RESULTS

# AIM 1

# ANGIOTENSIN 1-7 IS A HYPERTROPHIC FACTOR IN MOUSE SKELETAL MUSCLE

This Results section contains the text from a manuscript in preparation, which will soon be submitted to the American Journal of Physiology: Cell Physiology. Text and title of this section are from the manuscript in preparation.

## BODY AND MUSCLE WEIGHT

Ang 1-7 did not significantly increase body weight over a 4 and 16 week period in wild type mice and MasR$^{-/-}$ mice (Fig. 3.1). Notably, mean body weights of MasR$^{-/-}$ mice were significantly less than wild type mice. Ang 1-7 had few significant effects on wild type muscle mass (Fig. 3.2). After 4 weeks, mean soleus and tibialis weights were greater with than without Ang 1-7, but when expressed as a ratio of body weight, there was no difference between control and Ang 1-7-treated mice (Fig. 3.2). After 16 weeks, muscle weight to body weight ratios were significantly greater in Ang 1-7 treated than in non-treated soleus and gastrocnemius. Ang 1-7 had no effect on EDL muscle mass. Mean muscle mass to body weight ratios of MasR$^{-/-}$ EDL and soleus were significantly greater than those of wild type muscles. The same was observed for control and Ang 1-7 treated MasR$^{-/-}$ gastrocnemius for the 16 week group. Ang 1-7 did not significantly affect MasR$^{-/-}$ muscle mass.

# FIGURE 3.1

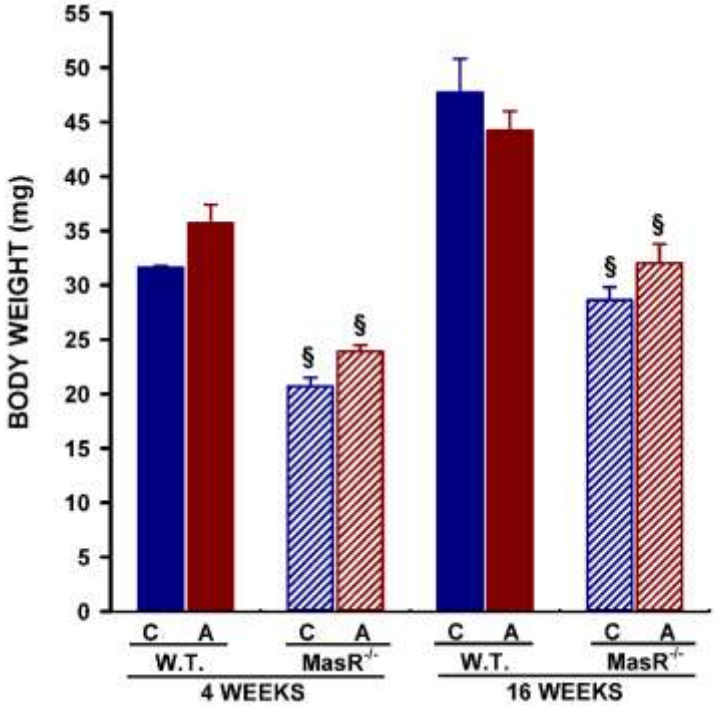


**Figure 3.1. Ang 1-7 had no effect on body weight while mean body weights of MasR$^{-/-}$ mice were significantly less than that of wild type mice.** Ang 1-7 was delivered using an osmotic pump at a rate of 100 ng/kg•min for 4 or 16 weeks. Abbreviations: C: control; A: Ang 1-7; W.T.: wild type. Vertical bars represent the S.E. of 5-11 mice. Ang 1-7 had no significant effect on body weight (ANOVA, $P > 0.05$).

§ Mean body weight of MasR$^{-/-}$ mice significantly different from that of wild type; ANOVA, and LSD, $P < 0.05$.

# FIGURE 3.2

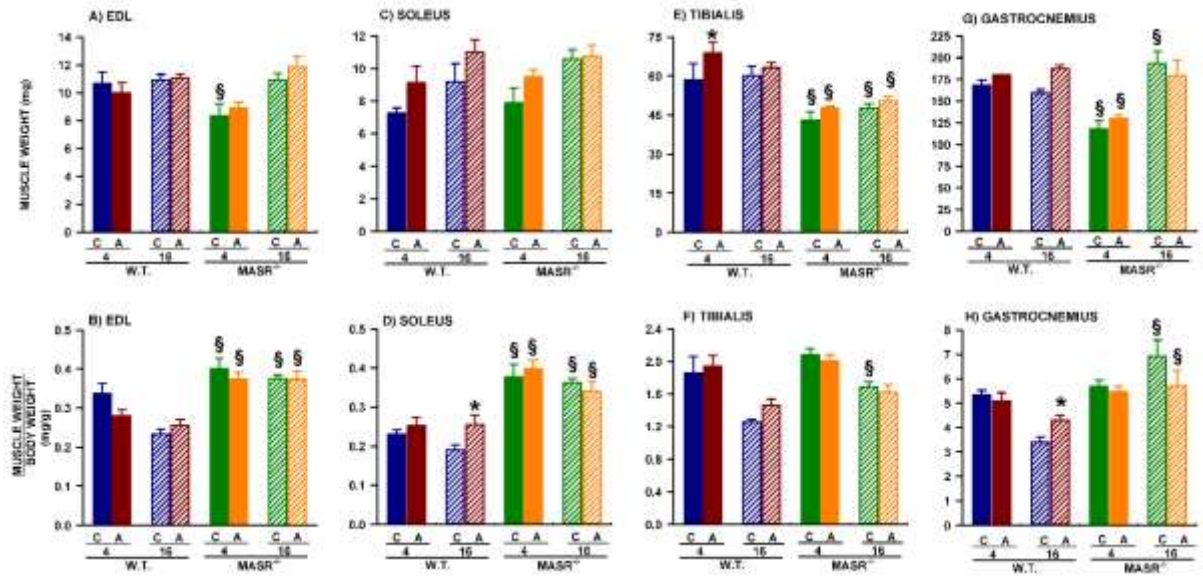


**Figure 3.2. Ang 1-7 significantly increased soleus and gastrocnemius muscle/body weight ratios after 16 weeks of treatment.** Muscle weights are expressed in mg (A, C, E, G) and as a ratio of body weight (mg/g, B, D, F, H). Abbreviations: C: control; A: Ang 1-7; W.T.: wild type. Vertical bars represent the S.E of 5-21 muscles.

***** Mean value significantly different from that of control.

**§** Mean value from $MasR^{-/-}$ muscle significantly different from that of wild type; ANOVA, and LSD, $P < 0.05$.

## TWITCH AND TETANIC FORCE

Ang 1-7 increased mean normalized twitch force after 4 and 16 week treatment in both wild type EDL and soleus muscles compared to untreated muscle (Fig. 3.3 C, D). The increased twitch force was associated with significantly longer relaxation phase but not time to peak (Fig 3.3 A, B, Table 3.1). Ang 1-7 also caused significant increases in normalized maximum tetanic force, which represents the maximum force a muscle can generate; the increases being 21-23% in EDL and 22-37% in soleus muscles (Fig. 3.3 E, F). Mean half-relaxation times following a tetanic contraction were longer in wild type EDL and soleus, but significant only for soleus and after 16 weeks (Table 3.2). Finally, Ang 1-7 caused a shift in the force-frequency relationship toward lower stimulation frequencies (Fig. 3.3G, H). The Ang 1-7 effects were significant at 4 weeks as mean frequencies at which muscle generated 50% of maximum force, named here frequency 50, decreased from 129 to 103 Hz for EDL and from 62 to 46 Hz for soleus (Fig. 3.3I, J). Although the decreases were not significant at 16 weeks, mean frequency-50 for EDL and soleus were respectively 14% and 16% less than in untreated muscles.

On an average base, $MasR^{-/-}$ EDL and soleus significantly generated greater twitch force than their wild type counterparts (Fig. 3.4 C, D). The greater twitch forces were associated with significantly longer half-relaxation time (Fig. 3.4A, B; Table 1), but not with longer time to peak, which on average were actually significantly shorter in $MasR^{-/-}$ than in wild type soleus (Table 3.1). Mean tetanic forces were not significantly different between wild type and $MasR^{-/-}$ muscles (Fig. 3.4E, F). $MasR^{-/-}$ EDL force-frequency relationship occurred at lower stimulation frequencies than in wild type EDL, with a significant difference at 4 weeks (Fig. 3.4G, I). A similar difference in force-frequency relationship between wild type and $MasR^{-/-}$ soleus was observed, but the difference was not significant (Fig. 3.4H, J). Ang 1-7 had no significant effects on any of the contractile properties of $MasR^{-/-}$ EDL and soleus (Table 3.1, 2; Fig. 3.4).

# TABLE 3.1

| PARAMETERS | MUSCLE | MOUSE | 4 WEEKS | | 16 WEEKS | |
|---|---|---|---|---|---|---|
| | | | CONTROL | Ang 1-7 | CONTROL | Ang 1-7 |
| Time to Peak (msec) | EDL | Wild type | 7.2 ± 1.1 | 8.5 ± 0.8 | | 5.8 ± 0.4 |
| | | $MasR^{-/-}$ | 8.2 ± 0.8 | 6.6 ± 0.4 | 5.1 ± 0.3 | 5.7 ± 0.7 |
| | SOLEUS | Wild type | 15.7 ± 0.6 | 15.5 ± 0.8 | | 12.9 ± 0.6* |
| | | $MasR^{-/-}$ | 13.3 ± 0.7§ | 12.8 ± 0.8§ | 11.1 ± 0.4§ | 12.9 ± 0.5* |
| ½-Relaxation Time (msec) | EDL | Wild type | 5.8 ± 0.3 | 7.4 ± 0.6* | | 7.7 ± 0.6* |
| | | $MasR^{-/-}$ | 10.2 ± 1.2§ | 8.5 ± 0.6* | 7.5 ± 0.4§ | 7.4 ± 0.7 |
| | SOLEUS | Wild type | 10.3 ± 1.1 | 14.5 ± 1.3* | | 16.3 ± 1.1* |
| | | $MasR^{-/-}$ | 16.6 ± 2.2§ | 14.6 ± 1.7 | 10.8 ± 0.8 | 12.6 ± 0.8§ |

**Table 3.1. Ang 1-7 prolonged twitch half-relaxation time but not the time to peak in wild type and not in $MasR^{-/-}$ muscles**. Ang 1-7 was delivered using an osmotic pump at a rate of 100 ng/kg•min for either 4 or 16 weeks. Data are presented as MEAN ± S.E. of 4-6 muscles.

* Mean value significantly different from that of control.

§ Mean value significantly different from that of wild type; ANOVA and L.S.D., $P < 0.05$.

# TABLE 3.2

| PARAMETERS | MUSCLE | MOUSE | 4 WEEKS | | 16 WEEKS | |
|---|---|---|---|---|---|---|
| | | | CONTROL | Ang 1-7 | CONTROL | Ang 1-7 |
| Time to Peak (msec) | EDL | Wild type | 118.8 ± 11.0 | 107.4 ± 9.3 | | 129.8 ± 11.3 |
| | | $MasR^{-/-}$ | 118.5 ± 22.2 | 102.3 ± 8.0 | 139.1 ± 31.2 | 95.4 ± 6.6 |
| | SOLEUS | Wild type | 204.6 ± 0.7 | 201.3 ± 1.3 | | 210.4 ± 1.1 |
| | | $MasR^{-/-}$ | 211.8 ± 1.2§ | 210.2 ± 0.9§ | 208 ± 12.4 | 202.1 ± 3.8§ |
| ½-Relaxation Time (msec) | EDL | Wild type | 19.0 ± 2.9 | 15.7 ± 0.7 | | 24.4 ± 0.9 |
| | | $MasR^{-/-}$ | 27.8 ± 1.4§ | 28.3 ± 1.4§ | 24.5 ± 12.2§ | 16.4 ± 1.4*§ |
| | SOLEUS | Wild type | 43.3 ± 1.7 | 48.6 ± 3.0 | | 63.0 ± 3.1* |
| | | $MasR^{-/-}$ | 52.3 ± 3.6 | 52.6 ± 3.9 | 45.7 ± 12.8 | 41.9 ± 8.1§ |

**Table 3.2. Ang 1-7 prolonged the half-relaxation time, especially in soleus, while it had no effect in $MasR^{-/-}$ EDL and soleus.** Ang 1-7 was delivered using an osmotic pump at a rate of 100 ng/kg•min for either 4 or 16 weeks. Data are presented as MEAN ± S.E. of 5-6 muscles.

***** Mean value significantly different from that of control.

**§** Mean value significantly different from that of wild type; ANOVA and L.S.D., $P < 0.05$.

# FIGURE 3.3

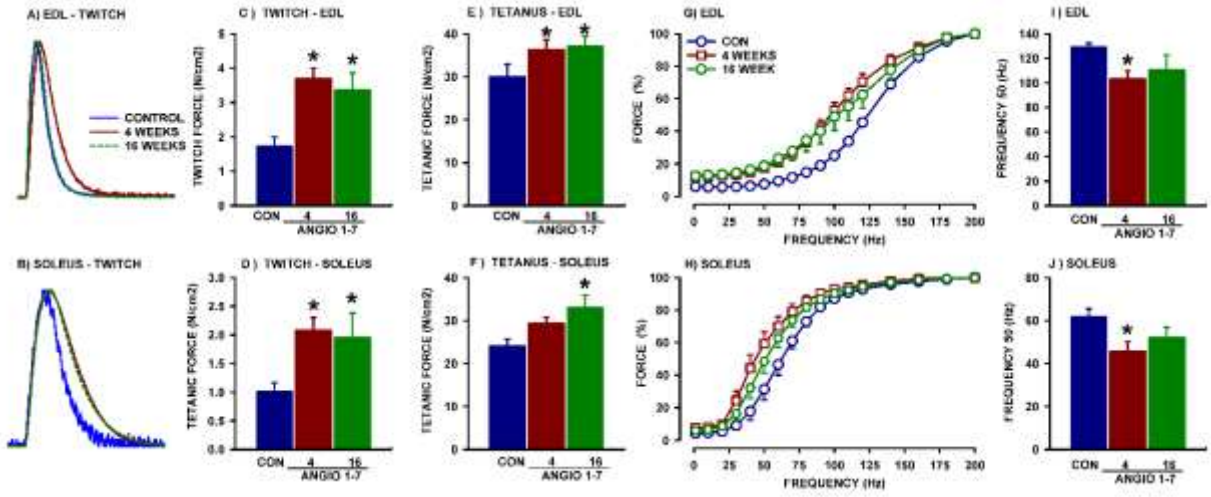


**Figure 3.3. After 4 and 16 weeks of treatments, Ang 1-7 significantly increased twitch and tetanic force as well as shifted the force-frequency curve toward lower stimulation frequencies in wild type EDL and soleus muscle.** A-B) Each twitch trace is plotted as a percent of the maximum force. C-D) Mean twitch forces ($N/cm^2$) measured from a single stimulation. E-F) Mean tetanic forces ($N/cm^2$), representing the maximum force muscles generated, was measured during a 400 msec train of pulses at 200 Hz. G-H) Force-frequency relationships with force expressed as a percent of the force measured at 200 Hz. I-J) Frequency 50 is the stimulation frequency at which 50% of maximum force is reached (see Methods for details). Vertical bars represent the S.E of 5-6 muscles.

***** Mean twitch, tetanic force or frequency 50 significantly different from that of control; ANOVA, and LSD, $P < 0.05$.

# FIGURE 3.4

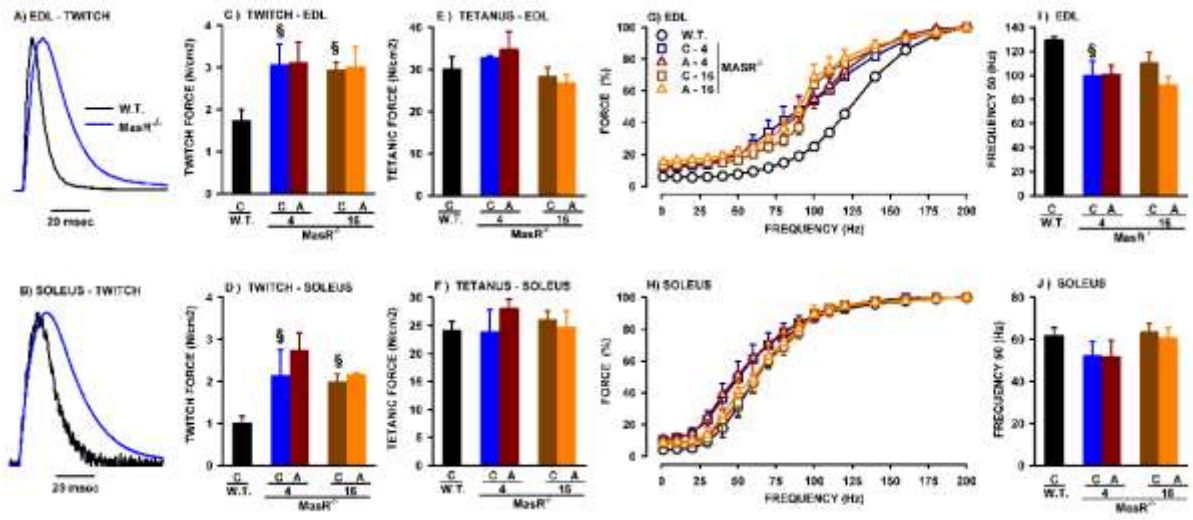


**Figure 3.4. After 4 and 16 weeks of treatments, Ang 1-7 did not increase twitch and tetanic force as well as did not cause a shift in the force-frequency relationship in MasR$^{-/-}$ EDL and soleus**. A-B) Each twitch trace is plotted as a percent of the maximum force. C-D) Mean twitch forces (N/cm$^2$) measured from a single stimulation. E-F) Mean tetanic forces (N/cm$^2$), representing the maximum force muscles generated, was measured during a 400 msec train of pulses at 200 Hz. G-H) Force-frequency relationships with force expressed as a percent of the force measured at 200 Hz. I-J) Frequency 50 is the stimulation frequency at which 50% of maximum force is reached (see Methods for details). Vertical bars represent the S.E of 5-6 muscles. For all parameters, Ang 1-7 had no significant effect on MasR$^{-/-}$ muscles (ANOVA, $P > 0.05$).

§ Mean twitch, tetanic force or frequency 50 of MasR$^{-/-}$ muscles under control conditions were significantly different when compared to that of wild type; ANOVA, and LSD, $P < 0.05$.

## CONTRACTILE COMPONENT

Myosin and α-Actin protein content

Ang 1-7 did not alter α-actin protein content in EDL muscles while in soleus a 44% and 66% increases was observed after 4 and 16 weeks of treatment, albeit the differences were not significant (Fig. 3.5A, B). Ang 1-7 had no significant effect on myosin protein content in both EDL and soleus (Fig. 3.5C, D).

# FIGURE 3.5

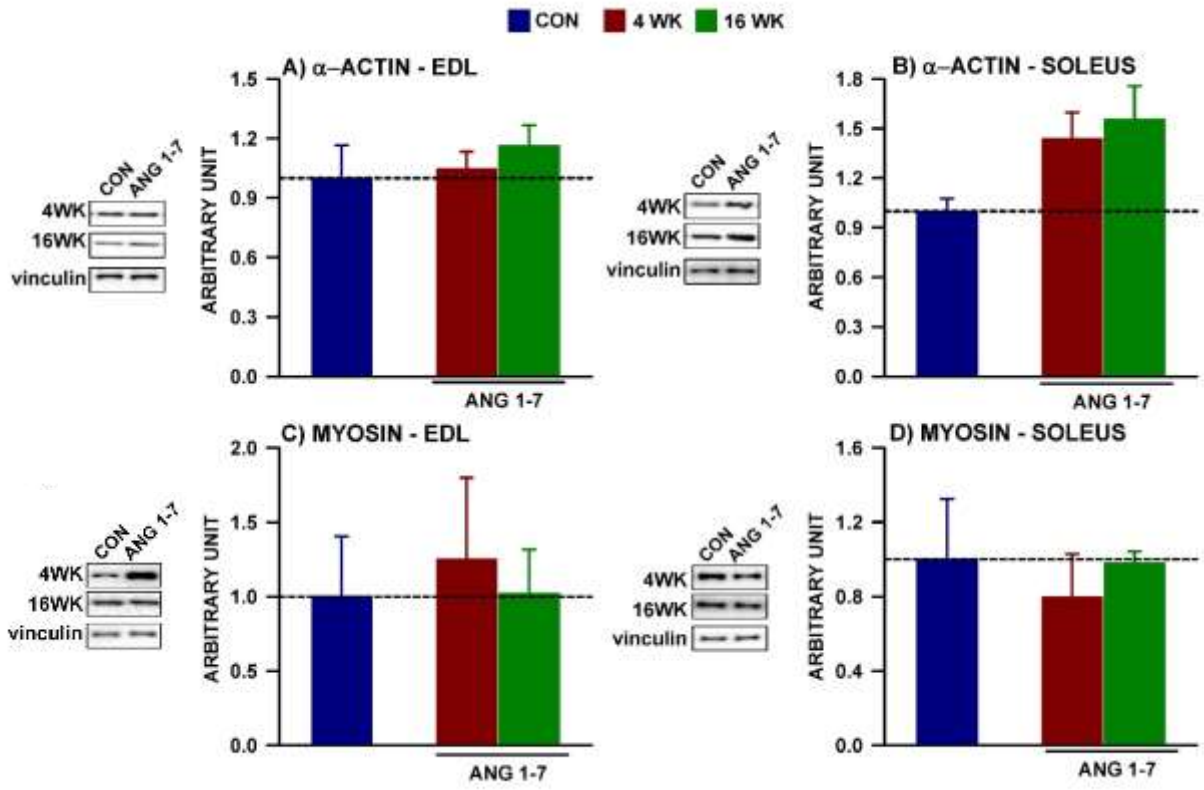


**Figure 3.5. Ang 1-7 slightly increased α-actin protein content in soleus while having no effect on myosin protein content.** For each time period, protein contents are expressed relative to the content in untreated soleus (CON) from age matched mice. Dotted lines represent a ratio of one. Vertical bars represent the S.E. of 4-5 muscles (the S.E. of CON is from the 4 week data). None of the differences were significant; ANOVA $P > 0.05$.

Fiber type composition

The number of wild type EDL fibers expressing type I, IIA and IIB myosin were respectively 2%, 15% and 60% (Fig. 3.6). Ang 1-7 did not significantly modify the EDL fiber type composition. $MasR^{-/-}$ EDL had a similar fiber type composition when compared to wild type EDL. In wild type soleus with and without Ang 1-7, the number of fibers expressing type I myosin was 62-58% while for type IIA myosin it was 54-37% type IIA, with no fibers expressing type IIB myosin (Fig. 3.7). The proportion of fibers expressing type I myosin was significantly lower in $MasR^{-/-}$ than wild type soleus while a slightly greater number of fibers expressed type IIA myosin in $MasR^{-/-}$ than in wild type soleus.

# FIGURE 3.6

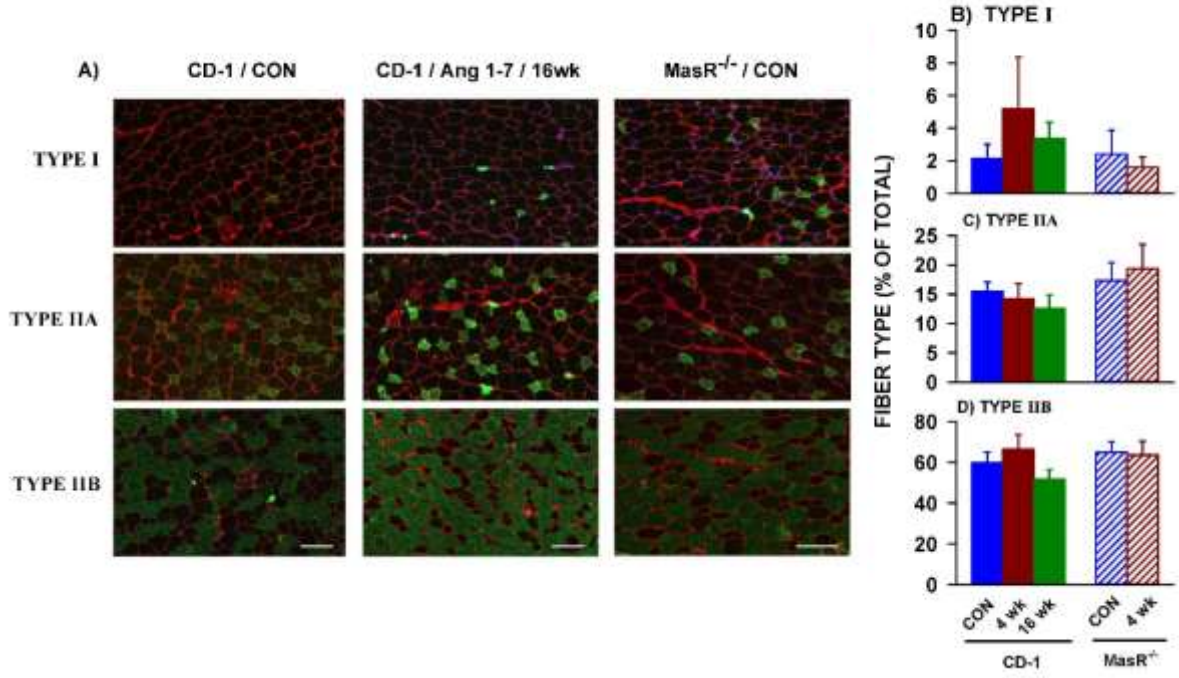


**Figure 3.6. Ang 1-7 did not significantly alter the fiber type composition of CD-1 and MasR$^{-/-}$ EDL**. A) Images of fibers expressing type I, IIA and IIB myosin in untreated (CON) or 16 week Ang 1-7 treated EDL. Color: green, myosin; red, laminin. The number of fibers expressing B) type I, C) type IIA and D) type IIB myosin is expressed as a percent of the total number of fibers. White horizontal bars: 100 µm. Vertical bars represent the S.E. of 4-5 muscles (total number of fibers: 52-105 for myosin I; 431-727 for myosin IIA; 1738-2729 for myosin IIB).

# FIGURE 3.7

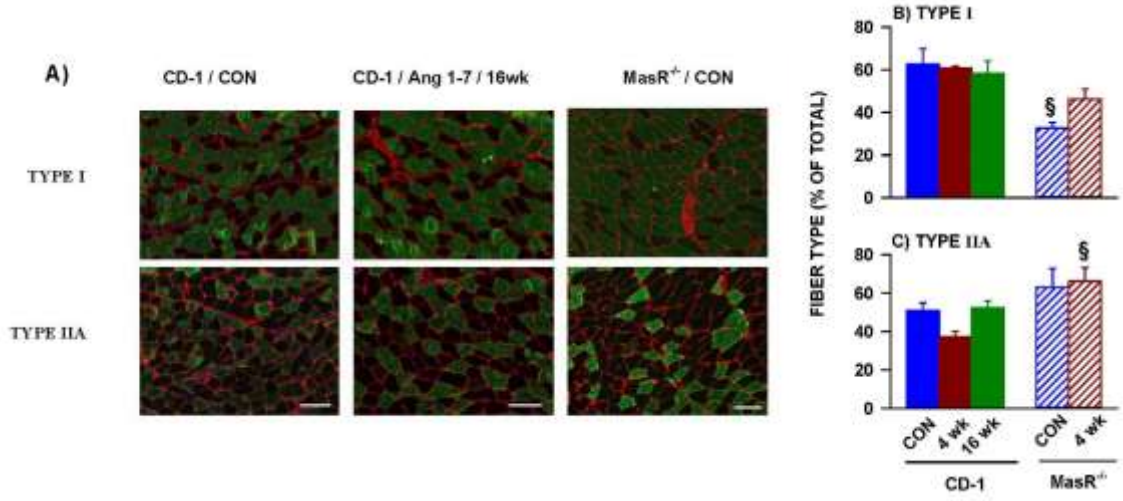


**Figure 3.7. Ang 1-7 had no significant effect on soleus fiber type composition.** A) Images of fibers expressing type I and IIA myosin in untreated (CON) or 16 week Ang 1-7 treated soleus. Color: green, myosin; red, laminin. The number of fibers expressing B) type I and C) type IIA myosin is expressed as a percent of the total number of fibers. White horizontal bars: 100 µm. Vertical bars represent the S.E. of 4-5 muscles (total number of fibers: 1,111-2,166 for myosin I; 1,256-2,600 for myosin IIA).

§ Mean value for MasR$^{-/-}$ soleus significantly different from that of control wild type soleus under similar conditions; ANOVA and L.S.D., $P < 0.05$.

Fiber type cross section area (CSA)

Ang 1-7 significantly increased mean CSA of wild type EDL type I fibers by 80% after 4 week and by 108% after 16 week (Fig. 3.8A). The CSA frequency distribution of type I fibers was also significantly shifted toward larger fibers (Fig. 3.8 B, C). All type I of control EDL had CSA ranging between 200 and 700 $\mu m^2$, this proportion fell to 57% and 44% after 4 and 16 weeks of Ang 1-7 treatment, respectively; i.e., about half of the Ang 1-7 treated EDL type I fibers had CSA becoming greater than 700 $\mu m^2$. The Ang 1-7 effects were less apparent for type IIA and IIB fibers. On average, there were slight, but non-significant, increases in mean CSA for type IIA (Fig. 3.8E) and type IIB (Fig. 3.8I) fibers. However, there was a significant shift toward greater CSA for type IIA fibers after 16 week of Ang 1-7 treatment: 60% of untreated fibers had CSA ranging from 200 to 600 $\mu m^2$, a number that significantly decreased to 38% with Ang 1-7 while for the 600-1000 $\mu m^2$ range the number of untreated fibers was 33% increasing to 56% for treated fibers (Fig. 3.8G). A smaller, but not significant, shift was also observed at 16 weeks for type IIB fibers: there was a 10% decrease in the number of Ang 1-7 treated fibers in the 1500-2200 $\mu m^2$ range and a 7% increase in the 2200-4000 $\mu m^2$ range (Fig. 3.8K).

Considering the effect of Ang 1-7 in wild type EDL, we also determined the effect of lacking of MasR on the CSA of each fiber type. On an average basis, mean CSA of control $MasR^{-/-}$ type I and IIA fibers were not significantly different from their wild type counterpart (Fig. 3.8A, E). Control $MasR^{-/-}$ type IIB fibers, on the other hand, had significantly smaller mean CSA than their wild type counterpart (Fig. 3.8I). Accordingly, the CSA distribution for control type I and IIA fibers were similar between wild type and $MasR^{-/-}$ while a significant shift toward lower CSA was observed for control $MasR^{-/-}$ type IIB fibers (Fig. 3.8D, H, L). A 4 week Ang 1-7 treatment had no effect on mean and distribution of CSA for all three fiber types in $MasR^{-/-}$ EDL.

Ang 1-7 treatment also caused significant hypertrophy in CD-1 soleus. For type I, mean CSA increased by 17% and 33% after 4 and 16 week of Ang 1-7 treatment, respectively (Fig. 3.9A). There were also clear and significant shifts in the CSA frequency distribution toward larger CSA after an Ang 1-7 treatment (Fig. 3.9B, C). For example at 16 weeks, type I fibers with CSA ranging between 1,100 and 2,000 $\mu m^2$ decreased from 54% (control) to 29% (Ang 1-7 treated) while for fibers with CSA greater than 2,300 $\mu m^2$ the proportion increased from 16% (control) to 38% (Ang 1-7). As observed for EDL, Ang 1-7 had a smaller effect on the CSA of type IIA fibers (Fig. 3.9E). Although a significant shift toward larger CSA was observed after 4 week Ang 1-7 treatment, the shift was less obvious after 16 weeks (Fig. 3.9F, G). Fiber CSA of $MasR^{-/-}$ soleus fibers were smaller than their wild type counterpart, especially type IIA, and Ang 1-7 did not cause any significant increases in CSA.

# FIGURE 3.8

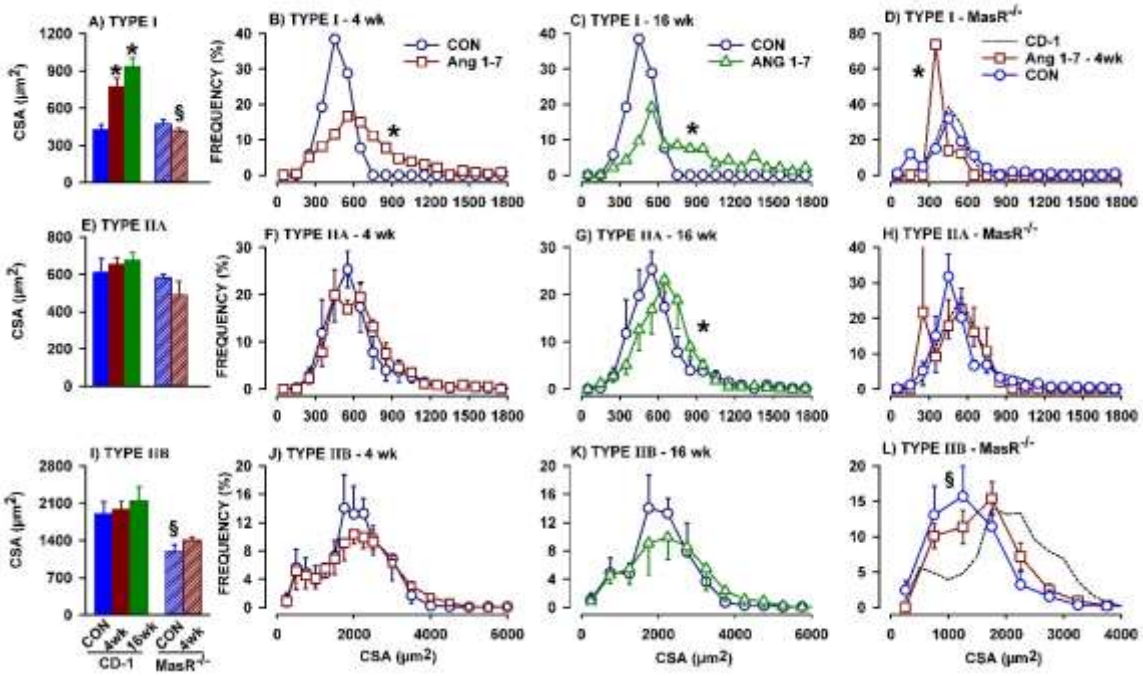


**Figure 3.8. Ang 1-7 significantly increased the CSA of wild type (CD-1) EDL type I and IIA but not of IIB fibers.** CD-1 and MasR$^{-/-}$ mice were either untreated (CON) or Ang 1-7 treated for either 4 or 16 weeks. Mean CSA for A) type I, E) IIA and I) IIB fibers; the vertical bars represent the mean from 4-5 EDL (total number of fibers: 3,309-4,233). For the CSA frequency distributions, CSA were divided in bin of 100 µm$^2$ and the numbers of fibers in each bin are given as a percent of the total number of fibers. The number of type I fibers (B-D) being very low, data from 4-5 EDL (for a total of 52-179 fibers) were combined together (so no S.E.). For type IIA and IIB fibers, a frequency distribution was calculated for each muscle and the mean and S.E. are from 4-5 muscles (total of 431-727 type IIA fibers - F-H and 1,772-2,730 type IIB fibers – J-L).

***** Mean CSA (A, E) or frequency distribution (B-D, F-H) significantly different from that of control (CON).

**§** Mean CSA or frequency distribution of MasR$^{-/-}$ EDL significantly different from that of control wild type EDL under similar conditions; ANOVA and L.S.D. for mean CSA value, Fisher test for CSA distribution; $P < 0.05$.

# FIGURE 3.9

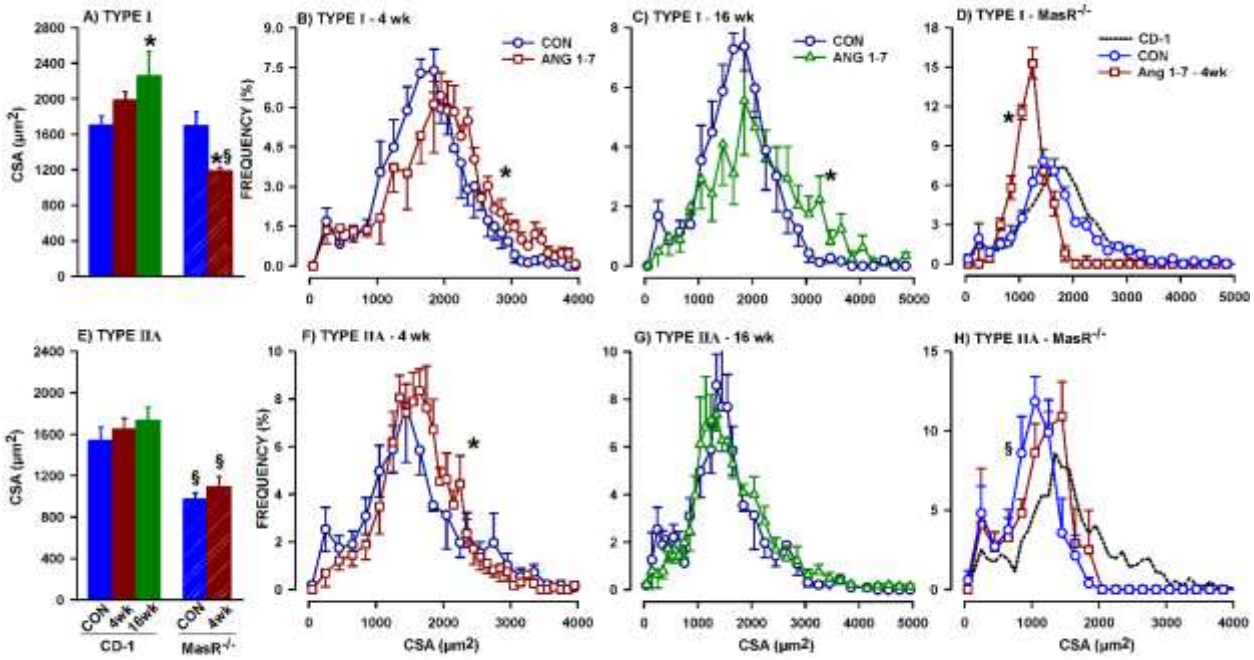


**Figure 3.9. Ang 1-7 significantly increased fiber CSA in wild type soleus.** CD-1 and MasR$^{-/-}$ mice were either untreated (CON) or Ang 1-7 treated for either 4 or 16 weeks. Mean CSA for A) type I and E) IIA; the vertical bars represent the mean from 4-5 soleus (total number of fibers: 2,392-3,542). For the CSA frequency distributions, CSA were divided in bin of 100 µm$^2$ and the number of fibers in each bin are given as a percent of the total number of fibers. A frequency distribution was calculated for each muscle and the mean and S.E. are from 4-5 muscles (total of 1,111-2,166 type I fibers – B-D and 1,258-2,512 type IIA fibers – F-H).

***** Mean CSA (A, E) or frequency distribution (B-D, F-H) significantly different from that of control (CON).

**§** Mean CSA or frequency distribution of MasR$^{-/-}$ soleus significantly from that of control wild type soleus under similar conditions; ANOVA and L.S.D. for mean CSA value, Fisher test for CSA distribution; $P < 0.05$.

## HYPERTROPIC AND ATROPHIC PROTEINS

As a MasR activation by Ang 1-7 results in an activation of the Akt pathway, we first determine how Ang 1-7 affects the total and phosphorylation levels of Akt and two mTOR downstream targets, 4-EPB and S6K. We also expected that the Ang 1-7 effects on this pathway might occur sooner than 4 and 16 weeks; so, we added two extra times: 3 days and 2 weeks. Ang 1-7 had no effect on the total content of all three proteins in EDL muscle (Fig. 3.10A). At 3 days of Ang 1-7 treatment, P-Akt protein content and the P-Akt/T-Akt ratio were respectively 41% and 56% greater than in control EDL (Fig.3.10 A, B). Such increases were not observed at 2, 4 and 16 weeks of Ang 1-7 treatment. Similarly, P-4EPB protein content and P-4EPB/T-4EPB ratio increased by 58-59% at 3 days with no changes at 2, 4 and 16 weeks (Fig. 3.10C, D). On the other hand, Ang 1-7 had no effect on P-S6K protein content (Fig. 3.10 E, F). The effects of Ang 1-7 in soleus were basically the same as those observed in EDL. The increased in P-Akt and P-4EPB, respectively, protein content at 3 days were 78% and 49% with no change thereafter as well as no effect on S6K (Fig. 3.11). As an activation of Akt pathway leads to the inhibition of the atrophic pathway, we also determined the Ang 1-7 effects on MuRF-1 and atrogin-1 protein content. There were some tendencies in lower MuRF-1 and atrogin-1 protein content, but the differences were very small (Fig. 3.12).

# FIGURE 3.10

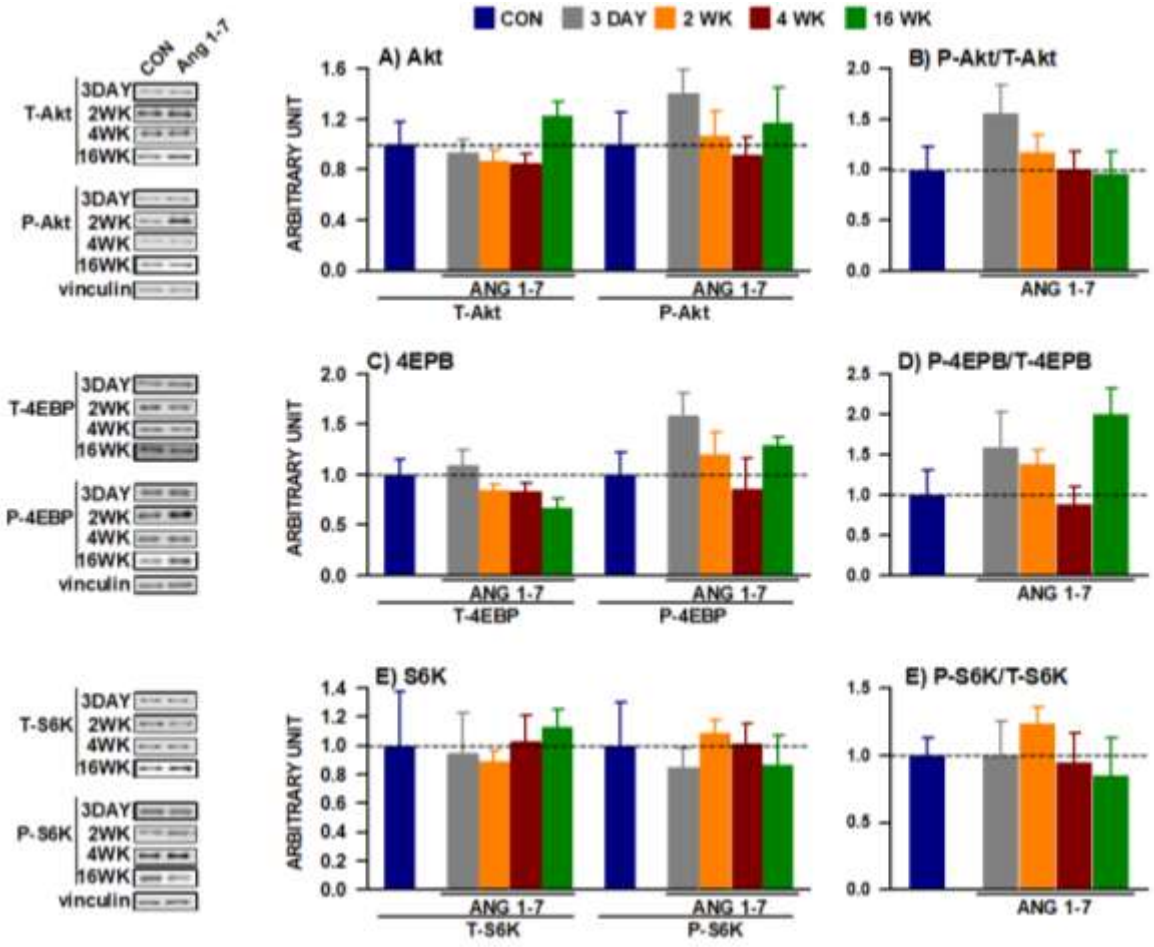


**Figure 3.10. In EDL and only after three days, Ang 1-7 slightly increased the phosphorylation of Akt (P-Akt) and 4EPB (P-4EPB), but not of S6K (P-S6), while it had no effect on the total (T) protein content at any one time periods.** For each time period, protein contents are expressed relative to the content in untreated EDL (CON) from age matched mice. Dotted lines represent a ratio of one. Vertical bars represent the S.E. of 4-5 muscles (the S.E. of CON is from the 3 day data). None of the differences were significant; ANOVA $P > 0.05$.

# FIGURE 3.11

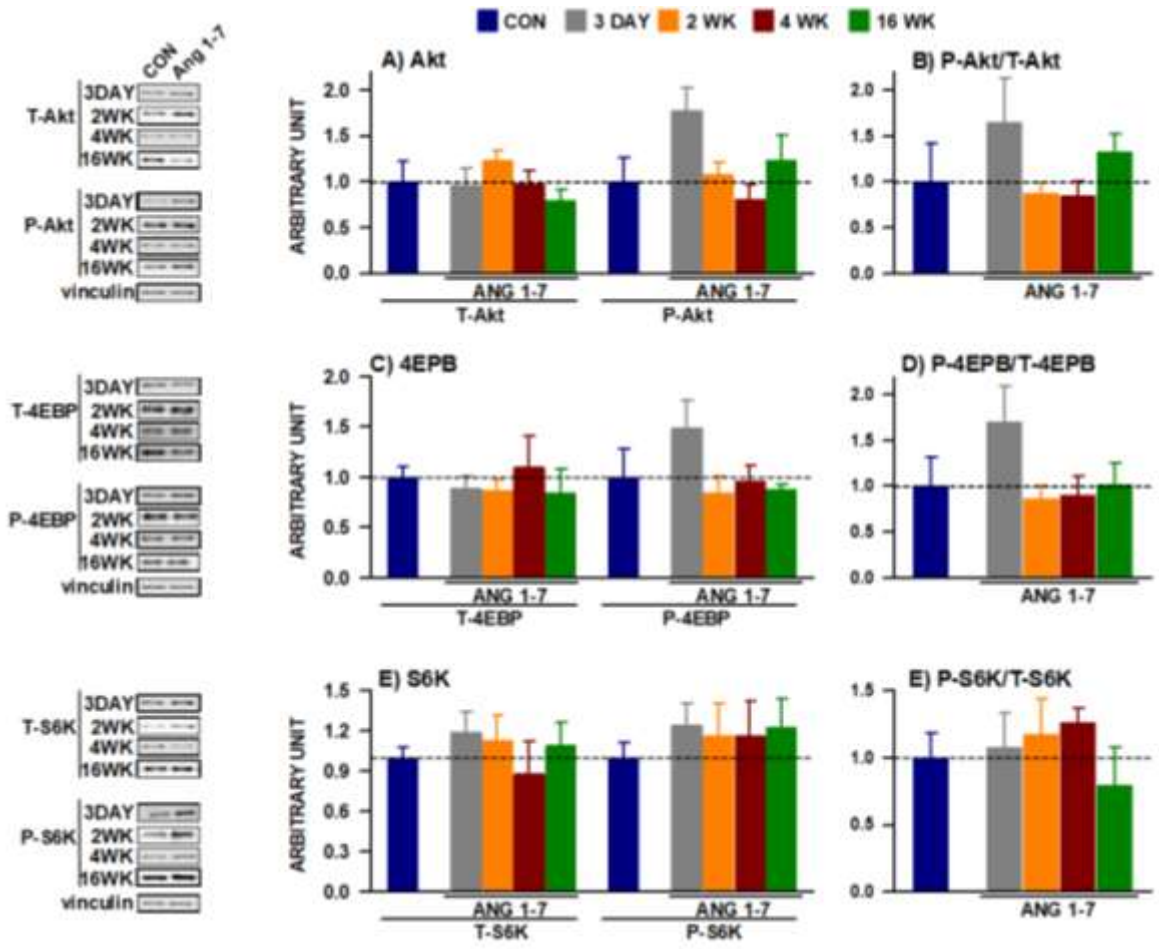


**Figure 3.11. In soleus and only after three days, Ang 1-7 slightly increased the phosphorylation of Akt (P-Akt) and 4EPB (P-4EPB), but not of S6K (P-S6), while it had no effect on the total (T) protein content at any one time periods.** For each time period, protein contents are expressed relative to the content in untreated soleus (CON) from age matched mice. Dotted lines represent a ratio of one. Vertical bars represent the S.E. of 4-5 muscles (the S.E. of CON is from the 3 day data). None of the differences were significant; ANOVA $P > 0.05$.

# FIGURE 3.12

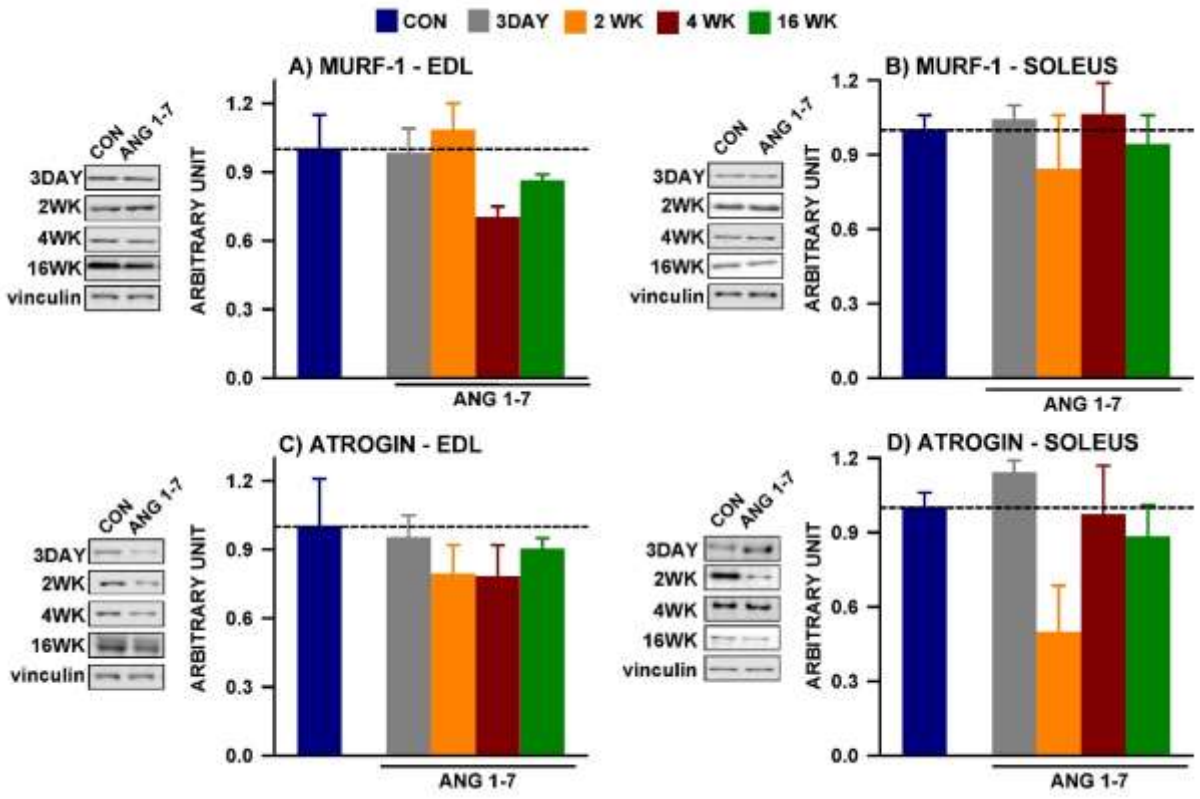


**Figure 3.12. In EDL and soleus, Ang 1-7 did not significantly affected MuRF-1 and atrogin-1 protein content** (ANOVA $P > 0.05$)**.** For each time period, protein contents are expressed relative to the content in untreated EDL or soleus (CON) from age matched mice. Dotted lines represent a ratio of one. Vertical bars represent the S.E. of 4-5 muscles (the S.E. of CON is from the 3 day data).

# CHAPTER 4

# RESULTS

# AIM 2

# "ANGIOTENSIN 1-7 COMPLETELY PREVENTS THE EXCESSIVE FORCE LOSS ASSOCIATED WITH 2-4 WEEK DENERVATION IN MOUSE EDL AND SOLEUS"

This Results section contains the text from a manuscript, which is being revised for the Journal of General Physiology. Text and title of this section are from the manuscript.

## MUSCLE WEIGHT AND CSA

EDL and soleus muscle weight per se (data not shown) or expressed as a ratio of body weight (Fig. 4.1) gave rise to similar results. EDL muscle to body weight ratio did not significantly decrease during the first three days of denervation (Fig. 4.1A) whereas a significant 17% decrease occurred for the soleus (Fig. 4.1B). Neither Ang 1-7 nor DIZE altered muscle weight loss. Muscle to body weight ratio further decreased over the 2 and 4 week denervation period; the decreases after 4 week being 38% and 48% for EDL and soleus, respectively. Treating mice with Ang 1-7 had no significant effect on the weight ratio. DIZE-treated muscles, on the other hand, had significantly higher weight ratio than denervated-sucrose treated muscles; the significant effects occurred only for the 2 week denervation period for EDL and both 2 and 4 week period for soleus; for the latter muscle A779, a MasR antagonist, inhibited the DIZE effect at 4 week. $MasR^{-/-}$ EDL and soleus muscle to body weight ratios were greater than the CD-1 muscles (Fig. 4.1 B, D). The loss of muscle weight over a 4 week denervation period was 52% and 48% for EDL and soleus, respectively. Treating $MasR^{-/-}$ with Ang 1-7 did not affect the extent of muscle weight loss.

# FIGURE 4.1

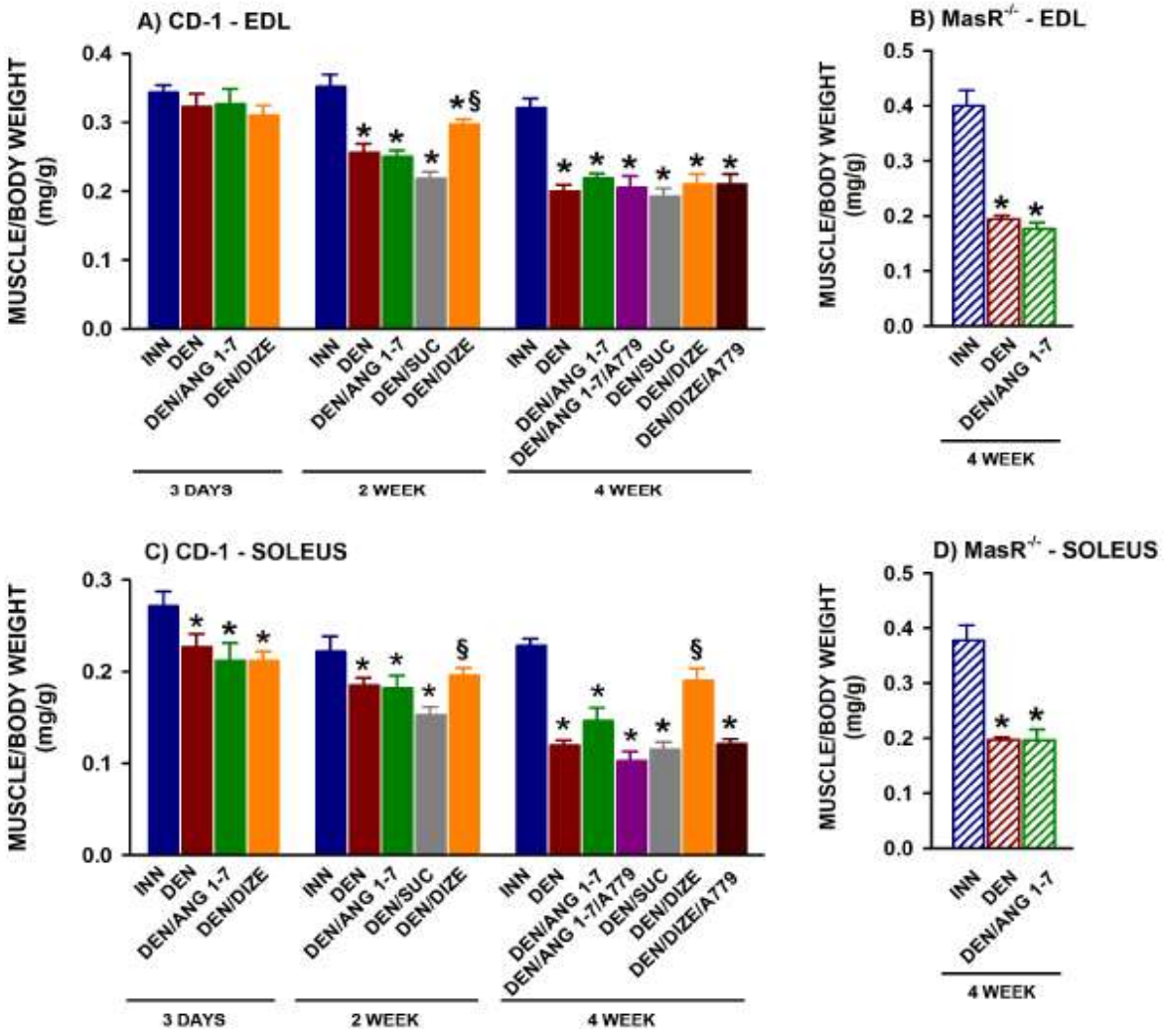


**Figure 4.1. Ang 1-7/DIZE significantly reduced muscle weight loss at 2 week denervation for EDL and at 2 and 4 week denervation for soleus; an effect not observed in the presence of A779 or in MasR$^{-/-}$ soleus.** Ang 1-7 and A779 were delivered using an osmotic pump (100 ng/kg•min) while sucrose (1 g/kg•day) and DIZE (15 mg/kg•day) were given once daily by gavage. Abbreviations**:** INN: innervated; DEN: denervated; SUC: sucrose. Vertical bars represent S.E of 5-19 muscles.

***** Mean muscle weight significantly different from that of INN muscles.

**§** Mean muscle weight significantly different from that of DEN or DEN/SUC muscles; ANOVA and L.S.D., $P < 0.05$.

To specifically determine how Ang 1-7 affects muscle fibers, we next measured fiber cross sectional area (CSA). Mean EDL fiber CSA decreased by 32% during a 4 week denervation period (DEN and DEN/SUC in Fig. 4.2A). The extent of the decreases in CSA was not altered when mice were treated with either Ang 1-7 or DIZE. Denervation significantly reduced the proportion of fibers with CSA greater than 1500 $\mu m^2$ while it significantly increased the proportion of fibers with CSA below 1200 $\mu m^2$ (Fig. 4.2B). Neither Ang 1-7/DIZE nor A779 (data not shown for the latter) affected the CSA frequency distribution. The effects of denervation, Ang 1-7 and DIZE on soleus fiber CSA (Fig. 4.3) were very similar to those of EDL with three exceptions. One, 4 week denervation reduced soleus fiber CSA by 61% compared to only 32% in EDL. Two, the shift toward lower CSA in the CSA distribution was much more pronounced in soleus. Three, A779 significantly exaggerated the CSA loss in soleus muscle, but not in EDL.

# FIGURE 4.2

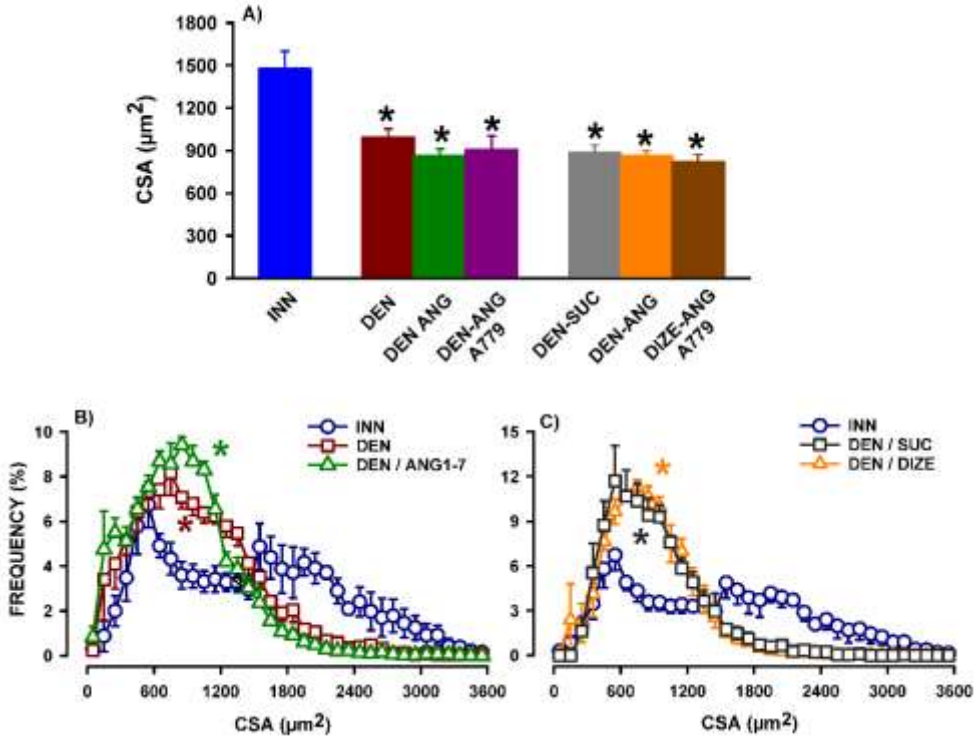


**Figure 4.2. Ang 1-7 did not prevent the decrease in fiber CSA associated with 4 week denervation in EDL.** CSA values were divided in bin of 100 µm$^2$ and the numbers of fibers in each bin are presented as a percent of the total number of fibers analyzed. For clarity, the CSA distributions of EDL from mice treated with the MasR antagonist, A779, is not shown as it was similar to that of DEN/Ang 1-7 and DEN/DIZE. Abbreviations: INN: innervated; DEN: denervated; SUC: sucrose. The CSA frequency distribution was first determined for each muscle, then mean and S.E. (vertical bars) were calculated from 4-5 muscles (with a total number of fibers ranging between 2,728 and 4,797).

***** The CSA distribution was significantly shifted toward lower CSA when compared to INN; ANOVA, and L.S.D., $P < 0.05$.

# FIGURE 4.3

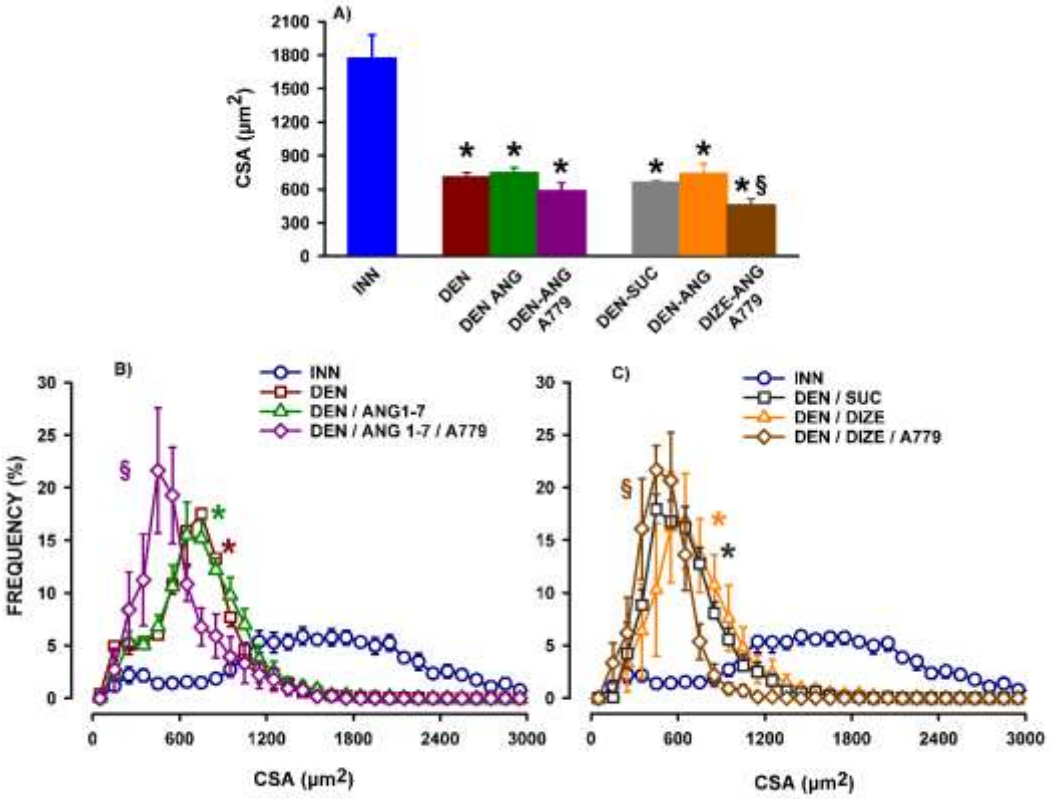


**Figure 4.3. Ang 1-7 did not prevent the decrease in fiber CSA associated with 4 week denervation but A779 significantly worsened the decrease in CSA in soleus.** CSA values were divided in bin of 100 µm$^2$ and the numbers of fibers in each bin are presented as a percent of the total number of fibers analyzed. Abbreviations**:** INN: innervated; DEN: denervated; SUC: sucrose. The CSA frequency distribution was first determined for each muscle, then mean and S.E. (vertical bars) were calculated from 4-5 muscles (with a total number of fibers ranging between 1,970 and 3,850).

***** The CSA distribution was significantly shifted toward lower CSA when compared to INN.

**§** The CSA distribution was significantly shifted toward lower CSA when compared to DEN or DEN/SUC; ANOVA AND L.S.D., $P < 0.05$.

## TETANIC AND TWITCH FORCE

As EDL became smaller over the 2 and 4 week denervation period, mean tetanic forces in Newton (N) decreased significantly when compared to their innervated counterpart (Fig. 4.4A, B). Mean tetanic forces of Ang 1-7 or DIZE treated denervated EDL were significantly greater compared to that of untreated denervated EDL, but remained significantly less than innervated EDL. However, when tetanic forces were normalized to CSA, EDL mean tetanic forces from Ang 1-7 and DIZE treated denervated EDL were no longer significantly different from that of innervated EDL while those of untreated denervated EDL were still significantly less by 36% (Fig. 4.4C, D). Thus, both Ang 1-7 and DIZE fully prevented the loss of normalized tetanic force associated with denervation; an effect completely inhibited by A779. Mean tetanic force of $MasR^{-/-}$ EDL also decreased during a 4 week denervation period, a decrease that was similar to that of CD-1 EDL (Fig. 4.4B). However, when tetanic force was normalized to CSA, mean tetanic force of denervated $MasR^{-/-}$ EDL decreased by only 17% compared to 36% in CD-1 denervated EDL (Fig. 4.4D). Ang 1-7 did not allow for an increased in normalized tetanic force during a 4 week denervation period as it did for CD-1 EDL.

Similarly, all denervated soleus mean tetanic forces in N were significantly lower than in innervated soleus (Fig. 4.4E, F), whereas the CSA normalized mean tetanic forces of Ang 1-7/DIZE treated but not of untreated denervated soleus remained similar to those of innervated soleus (Fig. 4.4G, H). Again A779 completely blocked the Ang 1-7/DIZE effect. For $MasR^{-/-}$ soleus 4 week denervation resulted in lower mean tetanic force in N (Fig. 4.4F), but notably no loss in the CSA normalized tetanic force whether or not mice were Ang 1-7 treated (Fig. 4.4G).

Two week denervated EDL generated greater mean twitch forces, either in N or $N/cm^2$, than innervated EDL (Fig. 4.5A, C); the increased in the normalized twitch force being 88% for

denervated (DEN) and 53% for sucrose-treated denervated EDL (DEN/SUC). Ang 1-7 and DIZE treated denervated EDL generated even greater twitch force than untreated denervated EDL; mean normalized twitch forces of Ang 1-7 and DIZE treated EDL were respectively 200% and 270% greater than that of innervated EDL. Similarly, 4 week denervation resulted in greater twitch force that was further increased by Ang 1-7 and DIZE; their effects being completely blocked by A779 (Fig. 4.5B, D). Innervated $MasR^{-/-}$ EDL mean normalized twitch force was 1.8-times greater than that of innervated CD-1 EDL. For $MasR^{-/-}$ EDL, mean twitch force after 4 week denervation became 2.8-times greater than in innervated $MasR^{-/-}$ EDL; an effect much greater when compared to wild type EDL for which the difference was only 1.8-fold. Ang 1-7 did not caused any further increase in twitch force of denervated $MasR^{-/-}$ EDL. Denervation, Ang 1-7, DIZE and A779 effects in soleus were similar to those described for EDL for CD-1 and $MasR^{-/-}$ soleus (Fig. 4.5 E-H).

# FIGURE 4.4

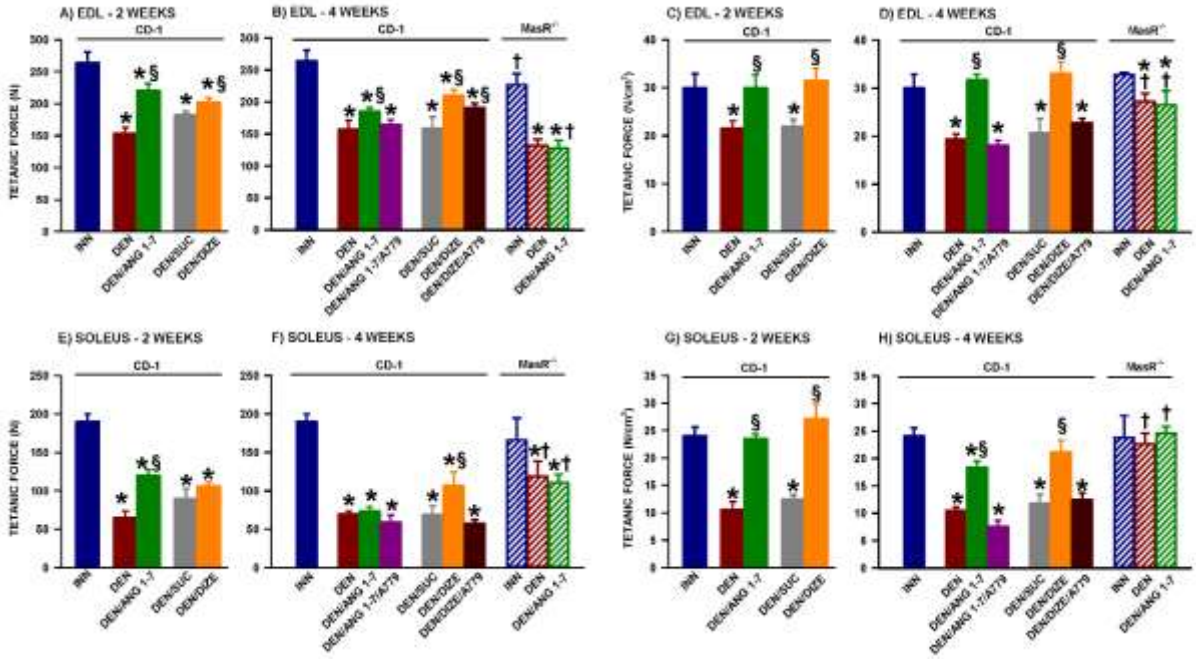


**Figure 4.4: Ang 1-7 and DIZE significantly prevented the loss of tetanic force in CD-1 EDL and soleus associated with 2 and 4 week denervation periods.** Tetanic force represents the maximum force a muscle can generate and was measured at 200 Hz. It is expressed in newton (N) (A, B, E, F) and as normalized to CSA in $N/cm^2$ (C, D, G, H). Abbreviations**:** INN: innervated; DEN: denervated; SUC: sucrose. Vertical bars represent the S.E of 5-6 muscles.

***** Mean tetanic force significantly different from that of INN muscles;

**§** Mean tetanic force significantly different from that of DEN or DEN/SUC muscles.

**†** Mean tetanic force significantly different from that of CD-1 muscles ANOVA, and L.S.D., $P < 0.05$.

# FIGURE 4.5

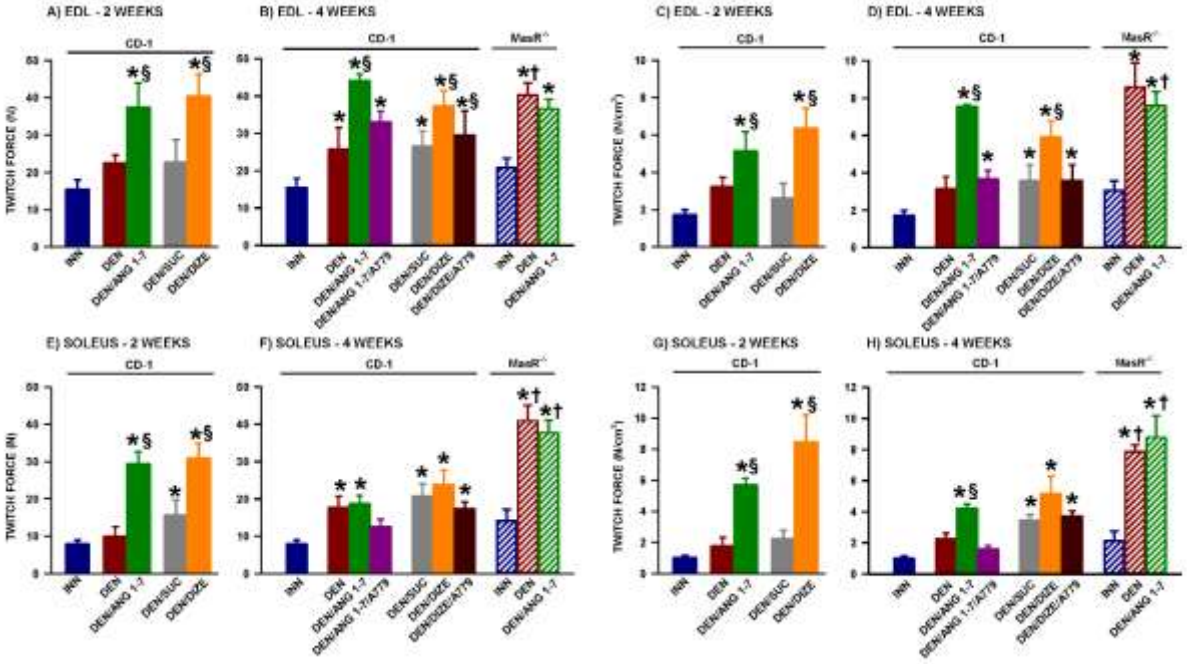


**Figure 4.5. Ang 1-7 and DIZE significantly increased twitch force of CD-1 EDL and soleus associated with 2 and 4 week denervation periods, but not in MasR$^{-/-}$ muscles.** Mean twitch force is expressed in N (A, B, E, F) and as normalized to CSA in N/cm$^2$ (C, D, G, H). Abbreviations**:** INN: innervated; DEN: denervated; SUC: sucrose. Vertical bars represent the S.E of 5 muscles.

***** Mean twitch force significantly different from that of INN muscle;

**§** Mean twitch force significantly different from that of DEN or DEN/SUC muscle.

**†** Mean twitch force significantly different from that of wild type soleus; ANOVA and L.S.D., $P < 0.05$.

Two and four week denervation was also associated with a significant shift in the CD-1 EDL force-frequency relationship toward lower stimulation frequencies; a shift that was not prevented by Ang 1-7 or DIZE (Fig. 4.6A-D). The shift occurred as twitch contractions became slower (Fig. 4.6E) with mean times to peak and half-relaxation times becoming significantly longer in denervated muscles (Table 4.1). As a consequence of prolonged twitch contractions, stimulation at 50 Hz still resulted in individual twitches in innervated EDL while there was a clear summation of twitch contractions in denervated EDL (Fig. 4.6F). Wild type EDL time to peak and half-relaxation time during tetanic contractions also became significantly prolonged following 4 week denervation (Table 4.2). Neither Ang 1-7 (Tables 4.1, 2) nor DIZE (data not shown) reversed the denervation effects on time to peak and half-relaxation time. Similar to wild type EDL, the force-frequency relationship of denervated soleus was significantly shifted toward lower stimulation frequencies (Fig. 4.7). Contrary to EDL, however, the shift was accentuated by Ang 1-7 and DIZE for both the 2 and 4 week denervation. Soleus twitch contractions also became significantly longer with prolonged time to peak and half-relaxation time; effects not reversed by Ang 1-7 (Table 4.1) or DIZE (data not shown). For tetanic contractions, time to peak was not affected while half-relaxation time were significantly longer in wild type denervated than innervated soleus (Table 4.2).

# FIGURE 4.6

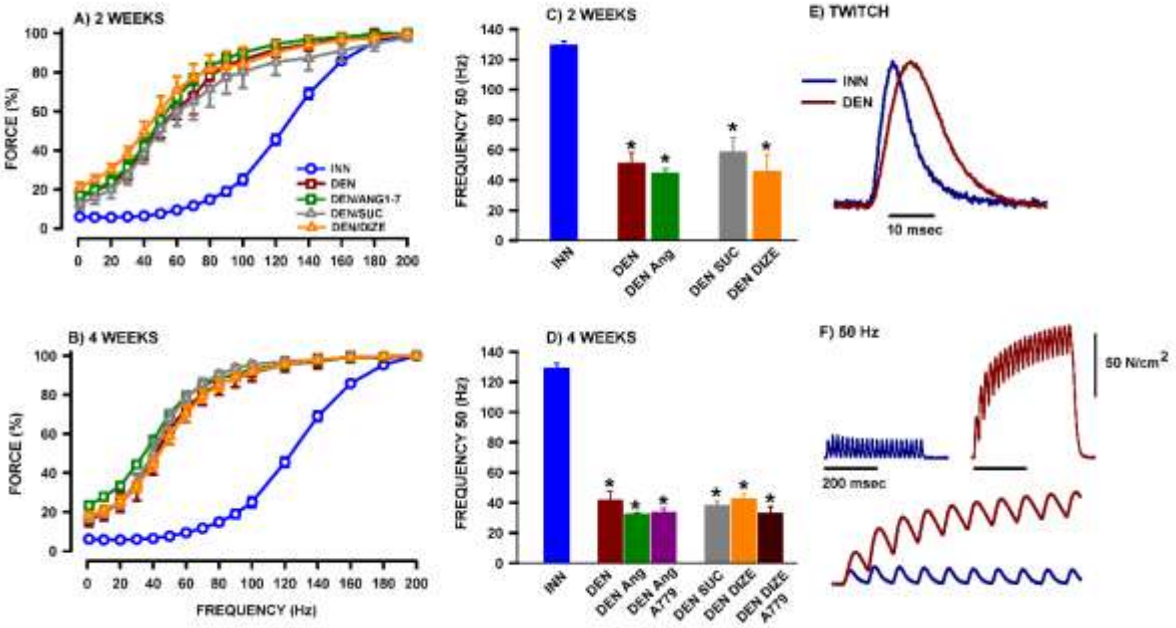


**Figure 4.6: In CD-1 EDL, Ang 1-7 did not prevent the shift in the force-frequency relationship toward lower stimulation frequencies that occurred after 2 and 4 week of denervation.** A-B) Force-frequency relationships. Force is expressed as a percent of the force measured at 200 Hz. C-D) Frequency 50 is the stimulation frequency at which force was 50% of the maximum tetanic force (see Methods for calculations). E) Examples of twitch force traces from innervated and denervated muscles. Forces are plotted as a percent of the maximum force during contraction. F) Example of force traces elicited at 50 Hz from innervated and denervated muscle. Horizontal bars show the 200 msec portions of the contractions that are expanded below. Abbreviations**:** INN: innervated; DEN: denervated; SUC: sucrose. Vertical bars (A, B) represent the S.E of 5 muscles.

***** Mean frequency 50 significantly different compared to INN muscles; ANOVA, and L.S.D., $P < 0.05$.

# FIGURE 4.7

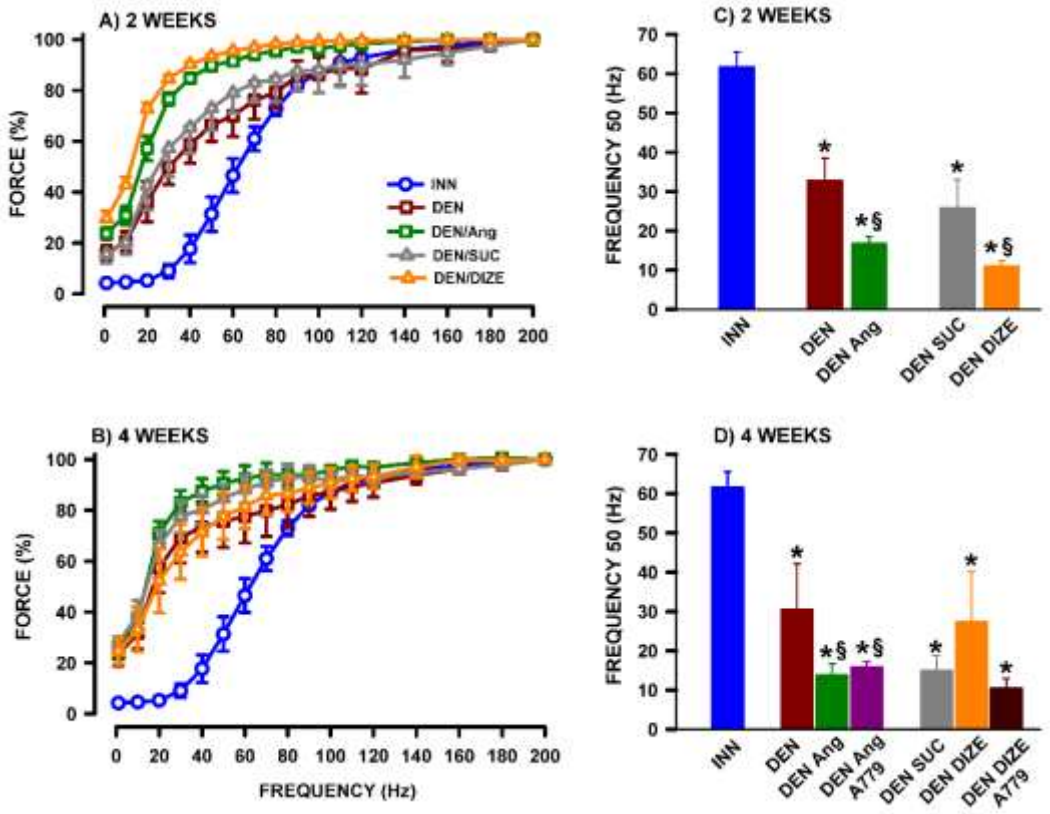


**Figure 4.7: In CD-1 soleus, Ang 1-7 did not prevent the shift of the force-frequency relationship toward lower stimulation frequencies following 2 and 4 week of denervation.** A-B) Force frequency relationships. Forces are expressed as a percent of the force at 200 Hz. C-D) Frequency 50 is the stimulation frequency at which force was 50% of the maximum tetanic force (see Methods for calculations). Abbreviations**:** INN: innervated; DEN: denervated; SUC: sucrose. Vertical bars represent S.E of 5 muscles.

***** Mean frequency 50 significantly different from that of INN.

**§** Mean frequency 50 significantly different from that of DEN or DEN/SUC soleus; ANOVA, and L.S.D., $P < 0.05$.

# TABLE 4.1

| MUSCLE | CONDITIONS | WILD TYPE | | MasR$^{-/-}$ | |
|---|---|---|---|---|---|
| | | TIME TO PEAK (msec) | HALF -RELAXATION TIME (msec) | TIME TO PEAK (msec) | HALF-RELAXATION TIME (msec) |
| EDL | INNERVATED | 7.2 ± 1.1 | 5.8 ± 0.3 | 8.2 ± 0.8 | 10.2 ± 1.2 |
| | DENERVATED | 14.8 ± 1.4***** | 9.4 ± 1.1 | 13.4 ± 0.8***** | 17.0 ± 1.5***†** |
| | DENERVATED ANG 1-7 | 13.0 ± 1.1***** | 11.9 ± 0.7***** | 17.3 ± 4.2***†** | 20.5 ± 5.3***†** |
| SOLEUS | INNERVATED | 15.7 ± 0. 6 | 10.3 ± 1.1 | 13.3 ± 0.7 | 16.6 ± 2.24 |
| | DENERVATED | 33.7 ± 1.0***** | 38.5 ± 4.9***** | 28.9 ± 1.7***** | 43.9 ± 4.5***** |
| | DENERVATED ANG 1-7 | 34.7 ± 1.1***** | 37.2 ± 2.7***** | 25.3 ± 3.5***†** | 35.6 ± 9.1***** |

**Table 4.1. Ang 1-7 did not reverse the significant prolongation of twitch contraction associated with 4 week denervation for wild type and MasR$^{-/-}$ EDL and soleus.** Ang 1-7 was delivered using an osmotic pump at a rate of 15 mg/kg/day. Data are presented as MEAN ± S.E. of 5-6 muscles.

***** Mean value significantly different from that of innervated muscles.

**†** Mean value significantly different from CD-1 muscles; ANOVA and L.S.D., $P < 0.05$.

# TABLE 4.2

| MUSCLE | CONDITIONS | WILD TYPE | | $MasR^{-/-}$ | |
|---|---|---|---|---|---|
| | | TIME TO PEAK (msec) | HALF - RELAXATION TIME (msec) | TIME TO PEAK (msec) | HALF -RELAXATION TIME (msec) |
| EDL | INNERVATED | 118.8 ± 11.0 | 19.0 ± 2.9 | 118.5 ± 22.2 | 27.8 ± 1.4 |
| | DENERVATED | 196.9 ± 3.8* | 44.8 ± 2.7* | 178.4 ± 18.7* | 53.4 ± 3.0* |
| | DENERVATED ANG 1-7 | 197.4 ± 2.7* | 45.2 ± 2.5* | 191.7 ± 8.4* | 63.8 ± 13.1*† |
| SOLEUS | INNERVATED | 204.6 ± 0.7 | 43.3 ± 1.7 | 211.8 ± 1.2 | 52.3 ± 3.6 |
| | DENERVATED | 208.0 ± 6.0 | 95.3 ± 5.9* | 213.4 ± 1.4 | 103.8 ± 10.2* |
| | DENERVATED ANG 1-7 | 210.0 ± 5.3 | 97.6 ± 11.7* | 212.0 ± 5.0 | 85.2 ± 11.3* |

**Table 4.2. Ang 1-7 did not reverse the prolongation of the tetanic time to peak in EDL and half-relaxation time of EDL and soleus associated with 4 week denervation in wild type and $MasR^{-/-}$ mice**. Ang 1-7 was delivered using an osmotic pump at a rate of 15 mg/kg/day. Tetanic contractions for EDL and soleus were respectively elicited at 200 and 140 Hz. Data are presented as MEAN ± S.E. of 5-6 muscles.

* Mean value significantly different from that of innervated muscles.

† Mean value significantly different from CD-1 muscles; ANOVA and L.S.D., $P < 0.05$.

Although 4 week denervation had small effects on tetanic force loss in $MasR^{-/-}$ than in wild type EDL and soleus, significant shift of the force-frequency relationship toward lower stimulation frequencies were observed in denervated compared to innervated $MasR^{-/-}$ muscles (Fig. 4.8). However, contrary to wild type muscles, Ang 1-7 did not accentuate the shift in $MasR^{-/-}$ soleus. Again, the shift in the force-frequency relationship was linked to prolonged twitch contractions as both time to peak and half-relaxation time were significantly longer in denervated than innervated EDL and soleus (Table 4.1). Notably, mean half-relaxation time of denervated $MasR^{-/-}$ EDL and soleus were significantly longer than those of denervated wild type EDL and soleus. Longer tetanic contraction times to peak and half-relaxation times were also observed in denervated than in innervated $MasR^{-/-}$ EDL, whereas only half-relaxation times were significantly longer in denervated $MasR^{-/-}$ soleus (Table 4.2).

# FIGURE 4.8

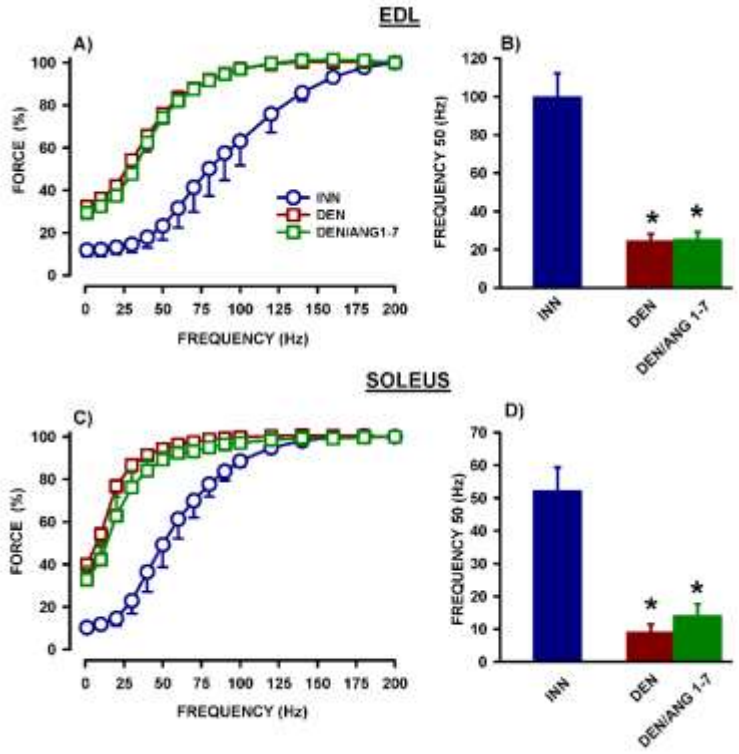


**Figure 4.8. Force-frequency relationships of MasR$^{-/-}$ EDL and soleus were significantly shifted toward lower stimulation frequencies after a 4 week denervation period**. Mean forces of A) EDL and C) soleus are expressed as a percent of the force at 200 Hz. Mean frequency 50 is the stimulation frequency at which force was 50% of the maximum tetanic force (see Methods for calculations). Abbreviations**:** INN: innervated; DEN: denervated. Vertical bars represent S.E of 5 muscles.

***** Mean frequency 50 significantly different compared to innervated muscles; ANOVA, and L.S.D., $P < 0.05$.

## MEMBRANE EXCITABILITY, RESTING $E_M$ AND ACTION POTENTIAL

It is well established that the sarcolemma of denervated muscle fibers are depolarized (Albuquerque and Thesleff, 1968b; Albuquerque et al., 1971b; Wareham, 1978; CLAUSEN et al., 1981). Thus, we next tested whether Ang 1-7 improves resting $E_M$ as one potential physiological mechanism that prevents the loss of normalized tetanic force following denervation. Fiber excitability was 100% in innervated EDL as all fibers generated an action potential upon a single stimulation (Fig. 4.9A). After a 4 week denervation period, fiber excitability fell to 42-49% (DEN and DEN-SUC). The Ang 1-7 treatment completely prevented the loss of fiber excitability while excitability was 85% in DIZE treated denervated EDL. As previously reported, denervated fibers were significantly depolarized compared to innervated fibers; mean resting $E_M$ being -62 mV for denervated fibers vs. -73 mV for innervated fibers (Fig. 4.9B). Both Ang 1-7 and DIZE significantly, but not completely, reduced the extent of depolarization in denervated EDL fibers; resting $E_M$ being -69 mV. Mean overshoots were significantly less in denervated than innervated fibers, an effect completely prevented by Ang 1-7 and DIZE (Fig. 4.9C). Mean maximum rate of depolarization of denervated fibers were 2.2-2.7 fold less than in innervated fibers; however, for this parameter neither Ang 1-7 nor DIZE significantly abolished the denervation effect (Fig. 4.9D). The effects of denervation, Ang 1-7 and DIZE in soleus were basically similar to those of wild type and $MasR^{-/-}$ EDL (Fig. 4.9E-H).

Considering that the normalized mean tetanic forces of $MasR^{-/-}$ EDL and soleus were less affected by denervation than their CD-1 counterpart and that Ang 1-7 fully prevented the loss of membrane excitability and normalized tetanic force, we also determined the effect of denervation on fiber excitability of $MasR^{-/-}$ EDL and soleus. Although mean fiber excitability and resting $E_M$ significantly decreased during the 4 week denervation compared to innervated muscles, the extent of the decreases was less in $MasR^{-/-}$ than in CD-1 muscles. Contrary to CD-1, mean action

potential overshoot was completely abolished in denervated MasR$^{-/-}$ EDL and soleus as the mean action potential peak were respectively -8 and -4 mV.

Fiber excitability is suppressed when resting $E_M$ becomes less than about -60 mV (Cairns et al., 1995; Ammar et al., 2015b). So, to better understand how the reduced resting $E_M$ depolarization with Ang 1-7/DIZE affected membrane excitability, we determined the frequency distribution of resting $E_M$. For innervated EDL, resting $E_M$ ranged from -90 to -60 mV (Fig. 4.10A); i.e., none of the fibers was in the unexcitable range. The resting $E_M$ distribution of denervated fibers was significantly shifted toward less negative $E_M$, and up to 35% of the fibers had resting $E_M$ less negative than -60 mV. Ang 1-7 significantly shifted the resting $E_M$ distribution toward more negative $E_M$, reducing the number of fibers with resting $E_M$ less negative than -60 mV to zero. A similar situation was observed with DIZE, except that the number of fibers with resting $E_M$ below -60 mV was 11% (Fig. 4.10B) in agreement with the decrease in fiber excitability (Fig. 4.9A). The effects of denervation, Ang 1-7 and DIZE in soleus were basically similar to those of EDL (Fig. 4.10C, D).

# FIGURE 4.9

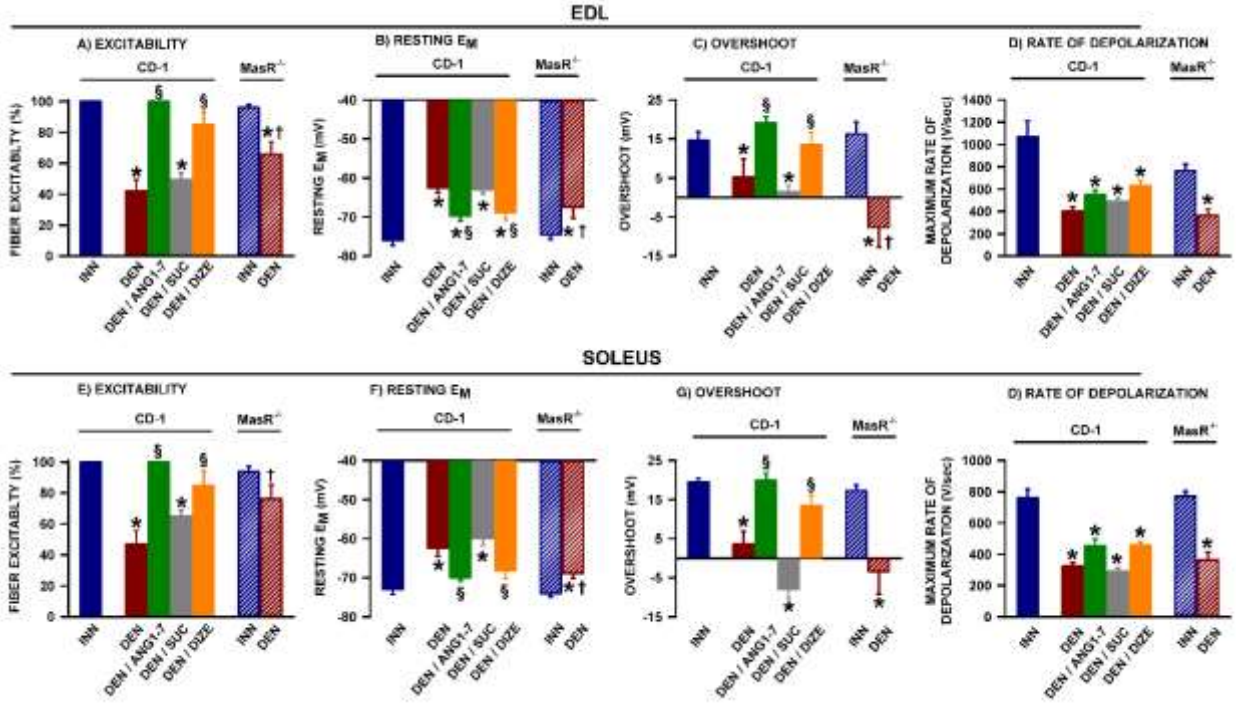


**Figure 4.9. Ang 1-7 significantly improved membrane excitability in 4 week denervated EDL and soleus.** Action potentials were triggered with a single stimulation. Excitability is defined as the number of fibers that generated an action potential upon stimulation and is expressed as a percent of all tested fibers. Abbreviations**:** INN: innervated; DEN: denervated. Mean values from individual fibers were first averaged for each muscle, and mean and S.E. (vertical bars) were calculated from 5-6 muscles with a total number of tested fibers ranging between 70 and 123.

***** Mean value significantly different from that of INN muscle;

**§** Mean value significantly different from that of DEN or DEN/SUC muscle;

**†** Mean value for DEN $MasR^{-/-}$ muscles significantly different from mean value of DEN CD-1 muscles; ANOVA and L.S.D., $P < 0.05$.

# FIGURE 4.10

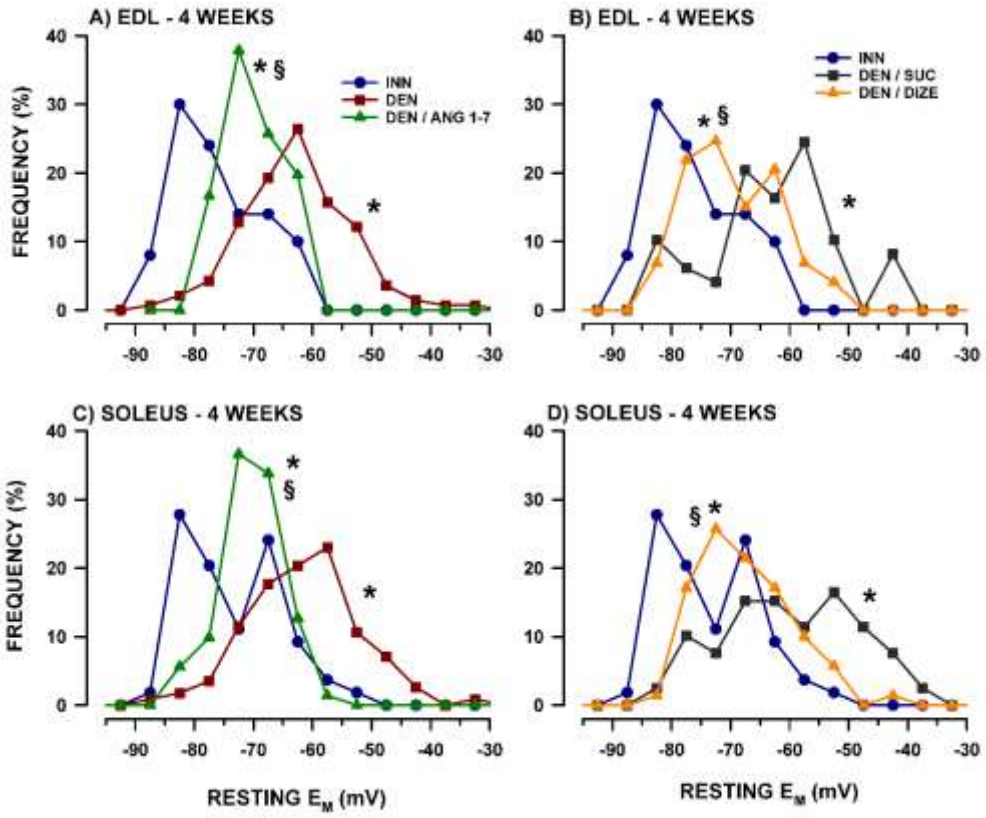


**Figure 4.10. Ang 1-7 partially shifted the resting $E_M$ distribution of 4 week denervated CD-1 EDL and soleus toward that of innervated muscles.** Resting $E_M$ were divided in bin of 5 mV; the number of fibers from all muscles was counted for each bin and is expressed as a percent of the total number of fibers tested. Abbreviations**:** INN: innervated; DEN: denervated. Total number of samples used for the distribution was 70-123 fibers from 5-6 muscles.

***** Resting $E_M$ distribution significantly shifted compared to that of INN muscle;

**§** Resting $E_M$ distribution significantly shifted compared to that of DEN or DEN/SUC muscle; Fisher test, $P < 0.05$.

The membrane depolarization associated with denervation is due to an increased $Na^+$ permeability and decreased $K^+$ permeability (Kotsias and Venosa, 1987b). The $Na^+$ $K^+$ pump content, which contributes up to -15 mV to the resting $E_M$ in innervated muscles (Chibalin et al., 2012; Ammar et al., 2015b), also decreases during denervation (Clausen et al., 1982; CLAUSEN et al., 1981; Wareham, 1978). So, we measured the Ang 1-7 effects on the pump α1 and α2 subunit protein content over a 4 week denervation period. Denervated EDL had significantly greater α1 and α2 protein content than innervated EDL, the differences being 1.8- and 1.5-fold, respectively (Fig. 4.11A-B). The increase in α1 reached 2.9- and 2.3-fold for Ang 1-7 and DIZE treated, respectively. Ang 1-7 also increased the α2 protein content by 2.0-fold when compared to innervated EDL. Contrary to the situation in EDL, 4 week denervation resulted in significant decreases in both α1 and α2 content by 40-50% while neither Ang 1-7 nor DIZE had any effect.

## CONTRACTILE COMPONENTS

Denervation also leads to decreases in sarcomere contents, especially near the cell membrane within 2 week (Yang et al., 2020). We therefore determined the total α-actin and myosin content to document whether Ang 1-7 reduces the loss of contractile proteins during 4 week denervation period. The α-actin protein content was reduced by 23% in denervated EDL, by 10% in Ang 1-7 treated and by 19% in DIZE treated EDL (Fig. 4.11C). Denervation caused greater decreases in α-actin in soleus as the content was reduced by 52%. Although no decrease in α-actin was detected with Ang 1-7, the difference with denervated soleus was not significant while DIZE had no effect. Ang 1-7 and DIZE caused decreases in total myosin content even when denervation alone had small effect (Fig. 4.11D).

# FIGURE 4.11

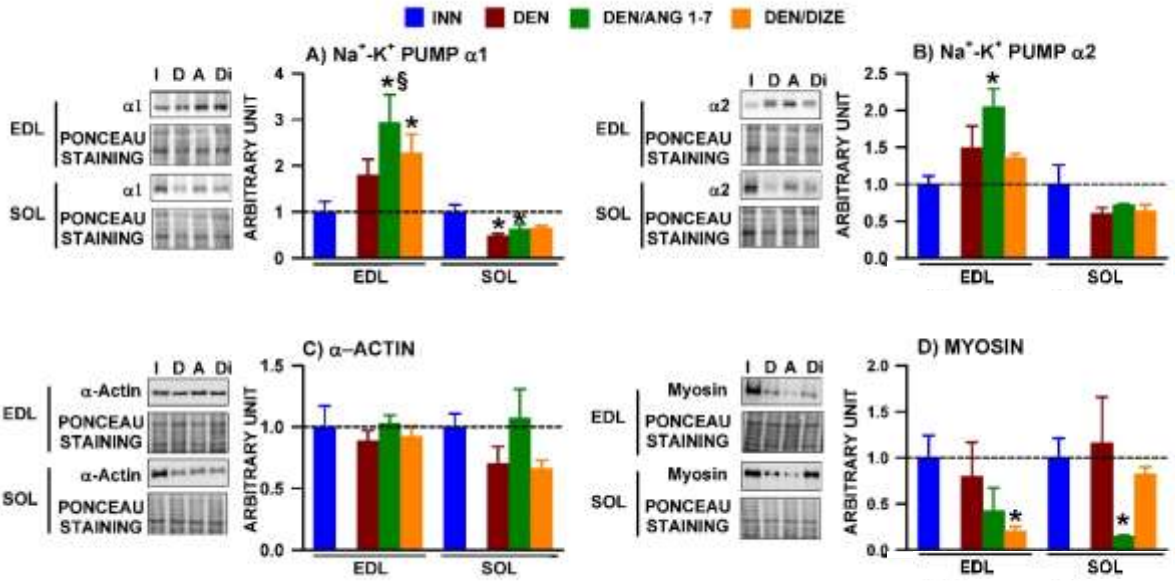


**Figure 4.11. Ang 1-7 significantly increased the $Na^+$ $K^+$ pump protein content in CD-1 EDL but not the α-actin and myosin content after 4 weeks denervation period.** Ponceau staining is from the 4 weeks Western Blots to provide an example for total proteins. Abbreviations: I, innervated, D, denervated; A, denervated-Ang 1-7 treated; Di, denervated-DIZE treated. Vertical bars represent the S.E of 6-8 muscles.

***** Mean value significantly different from that of INN muscle;

§ Mean value significantly different from that of DEN muscle; ANOVA and L.S.D., $P < 0.05$.

Fiber type composition

Normal innervated EDL muscle contained 60% type IIB, 15% type IIA and 2% type I fibers (Fig. 4.12A, B, D, F). After 4 week denervation, the proportion of fibers expressing type I and IIA myosin significantly increased in EDL muscle to 7% and 96%, respectively, while the number of fibers expressing type IIB myosin did not change. However, as shown in Fig. 4.12A, while a large number of denervated fibers still expressed type IIB myosin, the intensity of the staining is much less in denervated than innervated fibers. Ang 1-7 partially reduced the increase in the number of fibers to 4% for the expression of type I myosin and to 54% for type IIA myosin. Contrary to EDL, innervated soleus muscle contain 62% type I fibers and 44% type IIA fibers (Fig. 4.13). Neither denervation nor Ang 1-7 significantly affected the fiber type composition in soleus.

# FIGURE 4.12

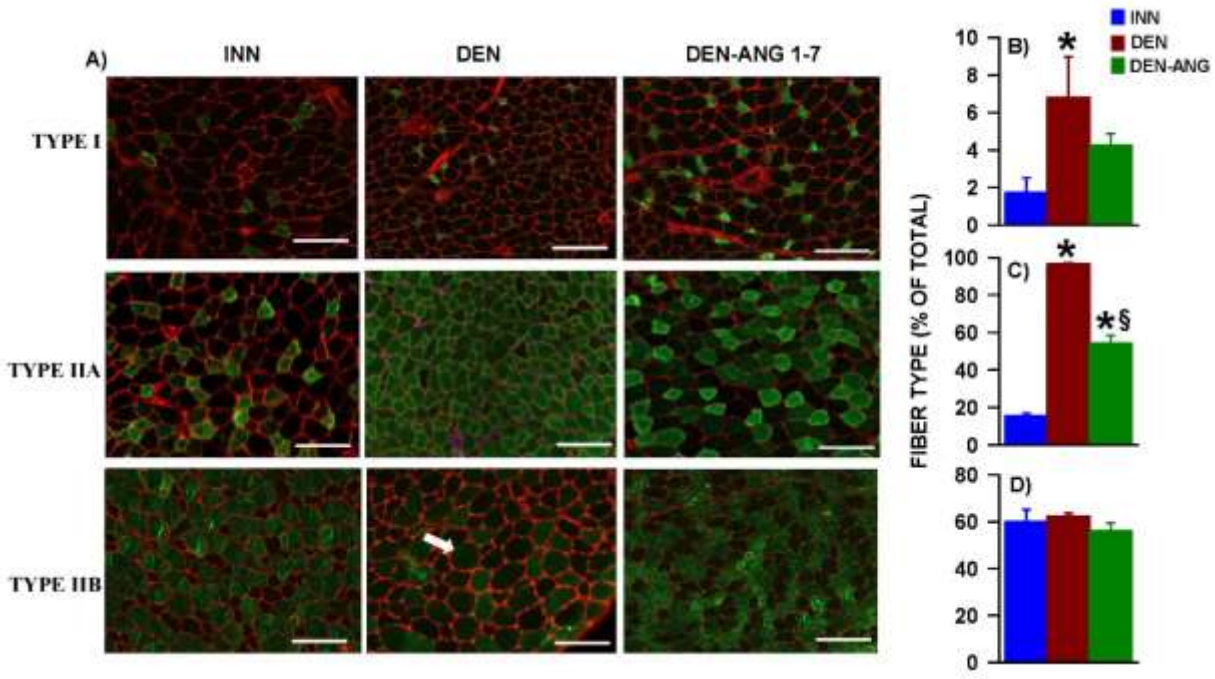


**Figure 4.12. Denervation significantly increased the expression of myosin I and IIA in CD-1 EDL while Ang 1-7 partially reduced that effect.** A) Images of type I, IIA and IIB fibers in innervated (INN), denervated (DEN) and denervated Ang 1-7 treated EDL (DEN-ANG 1-7). The numbers of fibers expressing B) myosin I, C) myosin IIA and D) myosin IIB fibers are expressed as a percent of the total number of fibers. Percent values were calculated for each muscle, then mean and S.E. (vertical bars) were calculated from 4-5 muscles. Horizontal white bars: 100 µm. The total number of fibers analyzed for INN, DEN and DEN-Ang 1-7 were respectively 3293, 4144 and 4321.

***** Mean value significantly different from that of INN muscle;

**§** Mean value significantly different from that of DEN muscle; ANOVA and L.S.D., $P < 0.05$.

# FIGURE 4.13

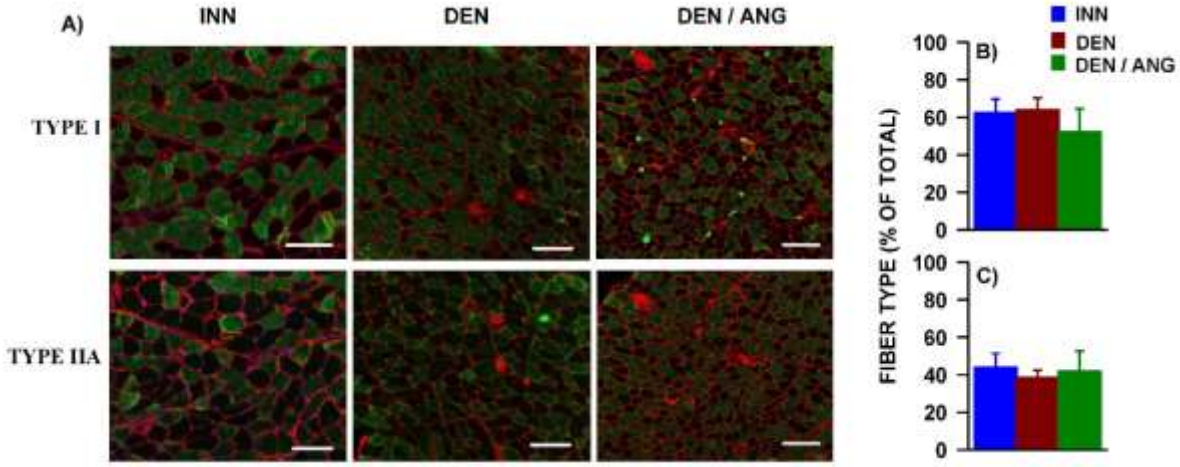


**Figure 4.13. Neither denervation nor Ang 1-7 affected the expression of myosin I and IIA in CD-1 soleus.** A) Images of type I and IIA and fibers in innervated (INN), denervated (DEN) and denervated Ang 1-7 treated EDL (DEN-ANG 1-7). The number of fibers expressing B) myosin I and C) myosin IIA expressed as a percent of the total number of fibers. Percent values were calculated for each muscle, then mean and S.E. (vertical bars) were calculated from 4-5 muscles. Horizontal white bars: 100 µm. The total number of fibers analyzed for INN, DEN and DEN-Ang 1-7 were respectively 2889, 2877 and 3826.

## HYPERTROPHIC AND ATROPHIC PATHWAY

Total Akt (T-Akt) and phosphorylated Akt (P-Akt) protein contents were significantly greater in 2 and 4 week of denervation, but not after three days, when compared to levels in innervated EDL (Fig. 4.14A, B). Neither Ang 1-7 nor DIZE affected T-Akt and P-Akt content. T-4EBP and P-4EBP slightly increased after 3 days and 2 week of denervation followed by a decrease at 4 week (Fig. 4.14C, D). Ang 1-7 had only one significant effect as it increased T-4EBP at 3 days. Significant increase in P-S6K content was observed only at 2 week denervation without any effect of Ang 1-7 or DIZE (Fig, 4.14E, F). In soleus, denervation significantly increased T-Akt content at 2 week; there were also increases in P-Akt content at 2 and 4 week, but the differences to innervated were not significant (Fig. 4.15A, B). There were no significant changes in T-4EPB and P-4EPB as well as for T-S6K and P-S6K (Fig. 4.15-C-F). Neither Ang 1-7 nor DIZE affected levels of Akt, 4EPB and S6K. Significant decreases in MuRF-1 protein content were observed in EDL at 4 week and in soleus at both 2 and 4 week (Fig. 4.16A, B), while decreases in atrogin-1 were observed at both 2 and 4 week, being especially significant at 4 week (Fig. 4.16, C, B). Neither Ang 1-7 nor DIZE affected MuRF-1 and atrogin-1 levels.

# FIGURE 4.14

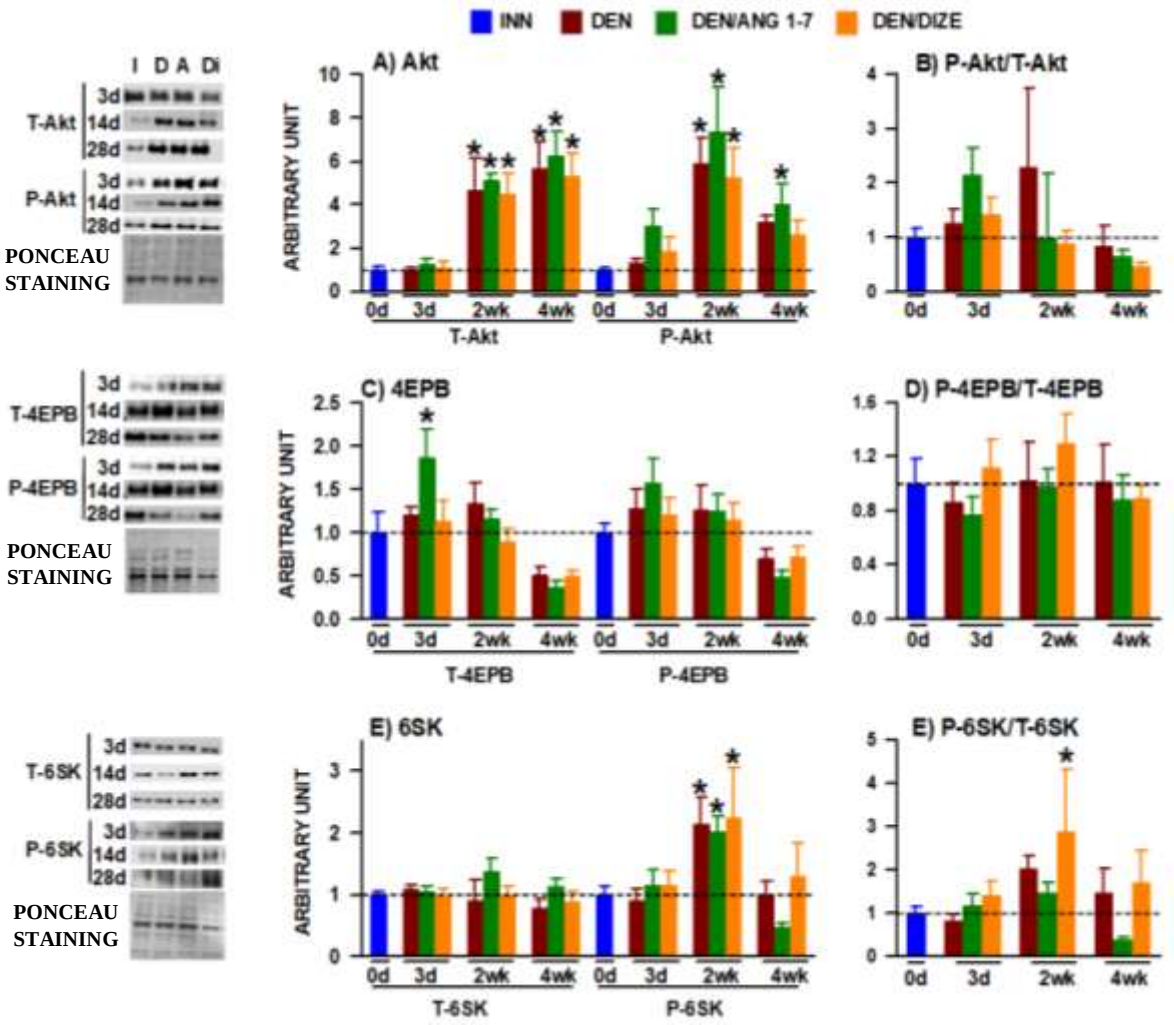


**Figure 4.14. In CD-1 EDL, Ang 1-7 did not significantly affect the changes in total (T) and phosphorylated (P) A-B) Akt, C-D) 4-EPB and E-F) S6K protein content associated with 3 days, 2 and 4 week denervation (DEN).** Protein contents were first normalized to the total protein content and then expressed relative to the content in innervated muscle. Ponceau staining is from the 3 day Western Blots to provide an example for total proteins. Abbreviations: I, INN and 0d: innervated; D and DEN; denervated; A: denervated-Ang 1-7 treated; Di: denervated-DIZE treated. Vertical bars represent the S.E of 6-8 muscles.

***** Mean protein content significantly different from that of INN muscles; ANOVA and L.S.D, $P < 0.05$.

# FIGURE 4.15

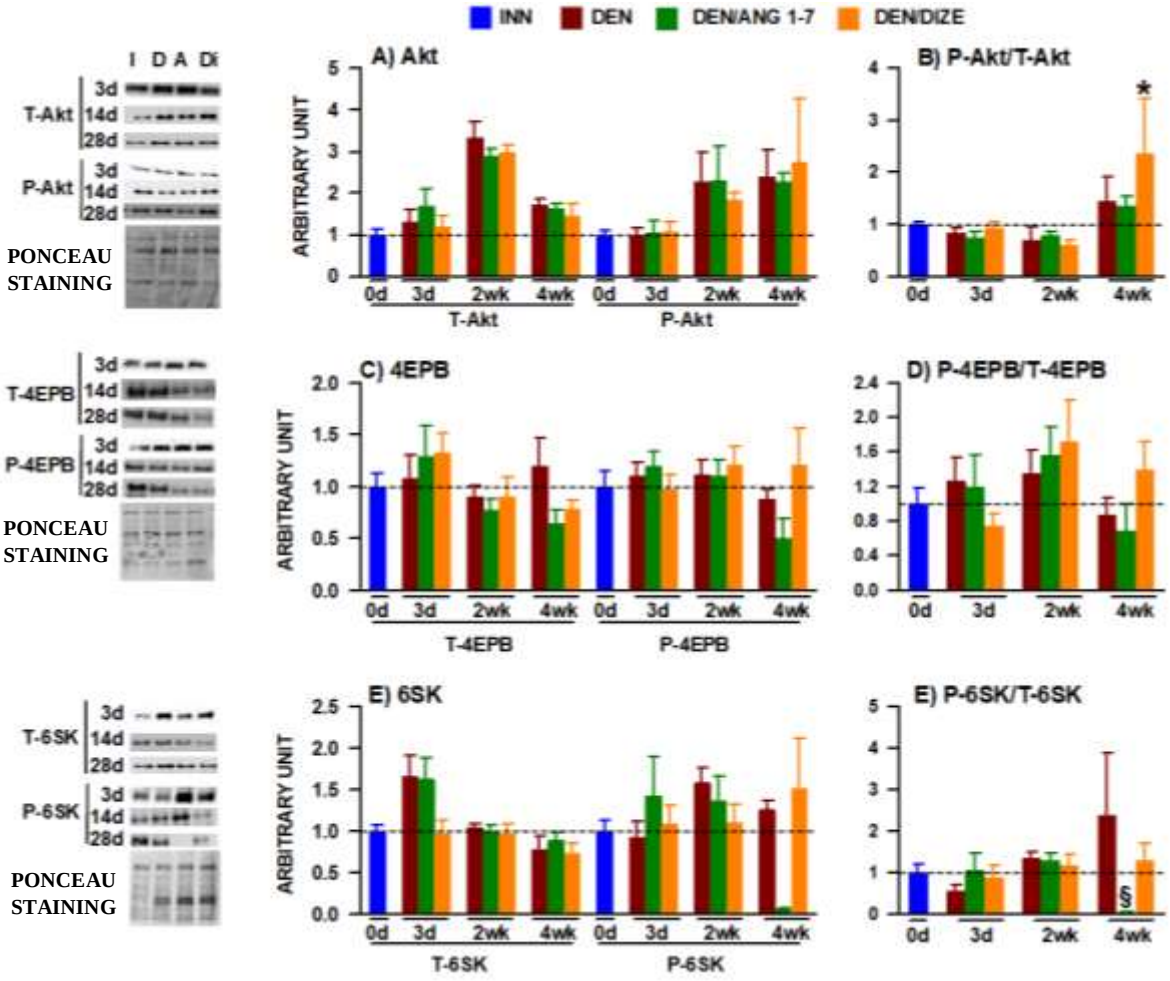


**Figure 4.15. In CD-1 soleus, Ang 1-7 mostly did not significantly affect the changes total and phosphorylated A-B) Akt, C-D) 4-EPB and E-F) S6K protein content associated with 3 day, 2 and 4 week denervation.** Protein contents were first normalized to the total protein content and then expressed relative to the content in innervated muscle. Ponceau staining is from the 3 day Western Blots to provide an example for total proteins. Abbreviations: I, INN and 0d: innervated; D and DEN; denervated; A: denervated-Ang 1-7 treated; Di: denervated-DIZE treated. Vertical bars represent the S.E of 6-8 muscles.

***** Mean protein content significantly different from that of INN muscles;

**§** Mean protein content significantly different from DEN muscles; ANOVA and L.S.D, $P < 0.05$.

# FIGURE 4.16

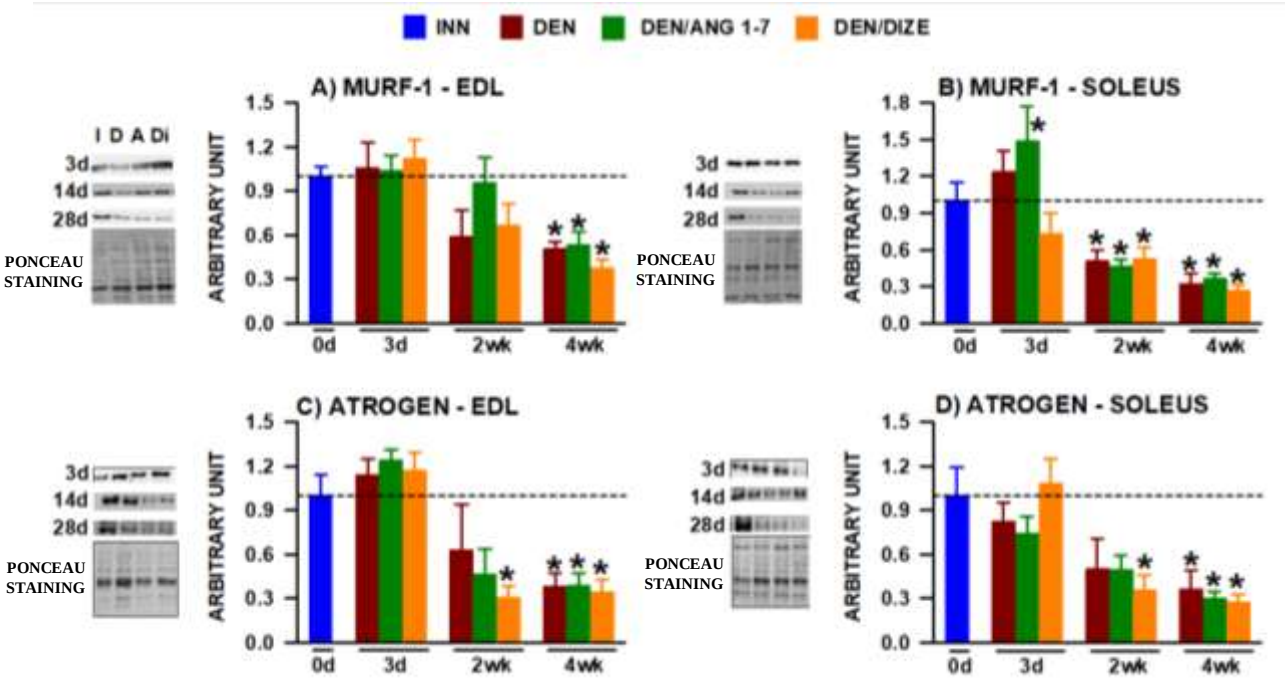


**Figure 4.16. In CD-1 EDL and soleus, Ang 1-7 had no significant effect on the changes MuRF-1 and atrogin-1 protein content associated with 3 day, 2 and 4 week denervation.** Protein contents were first normalized to the total protein content and then expressed relative to the content in innervated muscle. Ponceau staining is from the 3 day Western Blots to provide an example for total proteins: I, INN and 0d: innervated; D and DEN; denervated; A: denervated-Ang 1-7 treated; Di: denervated-DIZE treated. Vertical bars represent the S.E of 6-8 muscles.

***** Mean protein content significantly different from that of INN muscles; ANOVA and L.S.D, $P < 0.05$.

# CHAPTER 5

# RESULTS

# AIM 3

# "ANGIOTENSIN 1-7 PREVENT THE EXCESSIVE FORCE LOSS ASSOCIATED WITH 16 WEEK DENERVATION IN MOUSE EDL BUT NOT IN SOLEUS AND ENHANCING MUSCLE RECOVERY UPON REINNERVATION"

This Results section contains the text from a manuscript, which will be submitted to the Journal of Physiology: Cell Physiology. Text and title of this section are from the manuscript.

## VARIATIONS IN THE FORCE-FREQUENCY RELATIONSHIP

Sixteen weeks after the denervation surgery, the force- frequency relationship of EDL and soleus muscles could be divided into three groups (Fig. 5.1A, B). One group had force-frequency relationship significantly shifted toward lower stimulation frequencies when compared to innervated muscles as observed after 2 and 4 week denervation (Chapter 4). A second muscle group had force- frequency relationship either similar to that of innervated muscles in the case of EDL or slightly shifted toward greater stimulation frequency than innervated muscles in the case of soleus. For the third muscle group, force-frequency relationship was intermediate between the first two groups.

Next, we plotted the FF50, which is the stimulation frequency at which muscles generated 50% of maximum force, against muscle mass. EDL muscles with very low FF50 also had the lowest muscle/body weight ratio, while other EDL had FF50 above 80 Hz had muscle mass similar to that of innervated muscles (Fig. 5.1C). Similarly, soleus muscles with very low FF50 had very low muscle/body weight ratio. However, not all soleus with FF50 above 40 Hz, like innervated ones, had normal muscle/body weight ratio (Fig. 5.1D). To test whether some reinnervation had occurred, we repeated the experiments and observed the presence of a nerve entering muscles that had larger muscle mass and FF50 values while muscles without a nerve had low FF50 and muscle mass.

# FIGURE 5.1

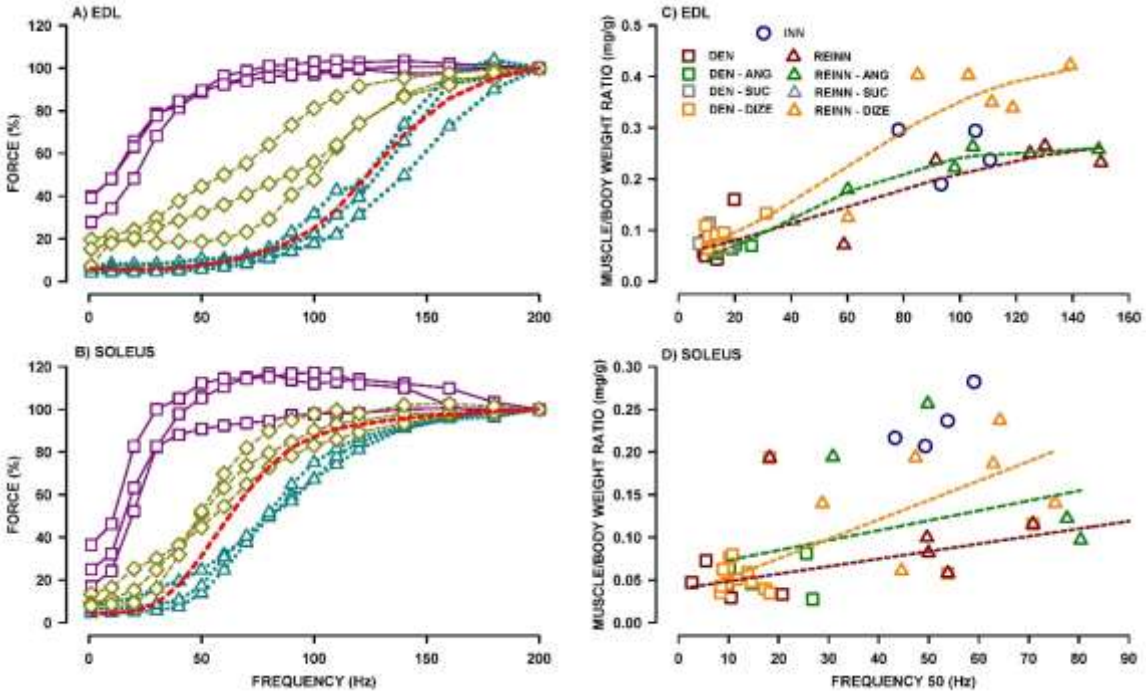


**Figure 5.1. Examples of force-stimulation frequency relationships and frequency 50-muscle/body weight ratios 16 week after the denervation surgery.** A-B) The force-stimulation frequency relationships could be divided into three groups: □, typical relationship of denervated muscles (see text for more details); Δ, relationship close to the mean relationship of innervated muscles (----); ◊, intermediate relationship. C-D) Frequency 50 is the stimulation frequency at which 50% of maximum force is generated (see Methods for calculations) and is plotted against the muscle/body weight ratios. The dashed lines were generated by non-linear regression to better visualize the difference in the increase in FF50 and muscle/body weight ratios.

Next, we determine if the increase in FF50 and muscle mass were associated with increases in fiber CSA. Using another group of denervated muscles stained for laminin, we observed three different situations: i) all fibers with low mass had very small CSA (Fig. 5.2B), while muscles with a large mass either had ii) a mixture of small and large fibers (Fig. 5.2C), or iii) all fibers had large CSA (data not shown). To determine that large fibers were not the results of some regeneration as reported in human muscles (Bacou et al., 1996; Maier and Bornemann, 1999), muscle sections were stained with embryonic myosin. As expected, there was no embryonic myosin in normal innervated soleus while every fibers of a denervated soleus expressed embryonic myosin (Fig. 5.3A, B). Notably, embryonic myosin expression was much less in large fibers with large muscle mass (Fig. 5.3C). Finally, other muscles cross-sections were stained with hematoxylin and eosin to determine if large fibers had central nuclei, which is a feature of regenerated fibers. As shown in Fig. 5.4, there were no central nuclei in normal innervated fibers and very few in large fibers of muscles that had been denervated (Fig. 5.4).

We therefore suggest that the large fibers observed in muscles that had been denervated was not the results of fiber regeneration, but to a reinnervation which is some cases was partial and in other complete (see Discussion for more details). The data were therefore separated into two groups: i) fully denervated muscles were those with FF50 lower than 40 Hz for EDL, and 30 Hz for soleus (Fig. 5.1), and ii) reinnervated muscles were those with FF50 >40 Hz and >30 Hz in EDL and soleus, respectively. As we did not control the reinnervation process, we often ended up with small number of reinnervated muscles, as small as either one or zero, for some conditions. The differences in muscle weight, FF50, twitch and tetanic force between untreated and sucrose treated mice, between Ang 1-7 and DIZE treated mice, and between Ang 1-7/A779 and DIZE/A779 treated mice were small. Data were therefore combined for each of denervated

and reinnervated muscles to represent: i) untreated mice, ii) Ang 1-7/DIZE treated and iii) Ang 1-7/DIZE/A779 treated muscles in order to properly do statistical analyses.

# FIGURE 5.2

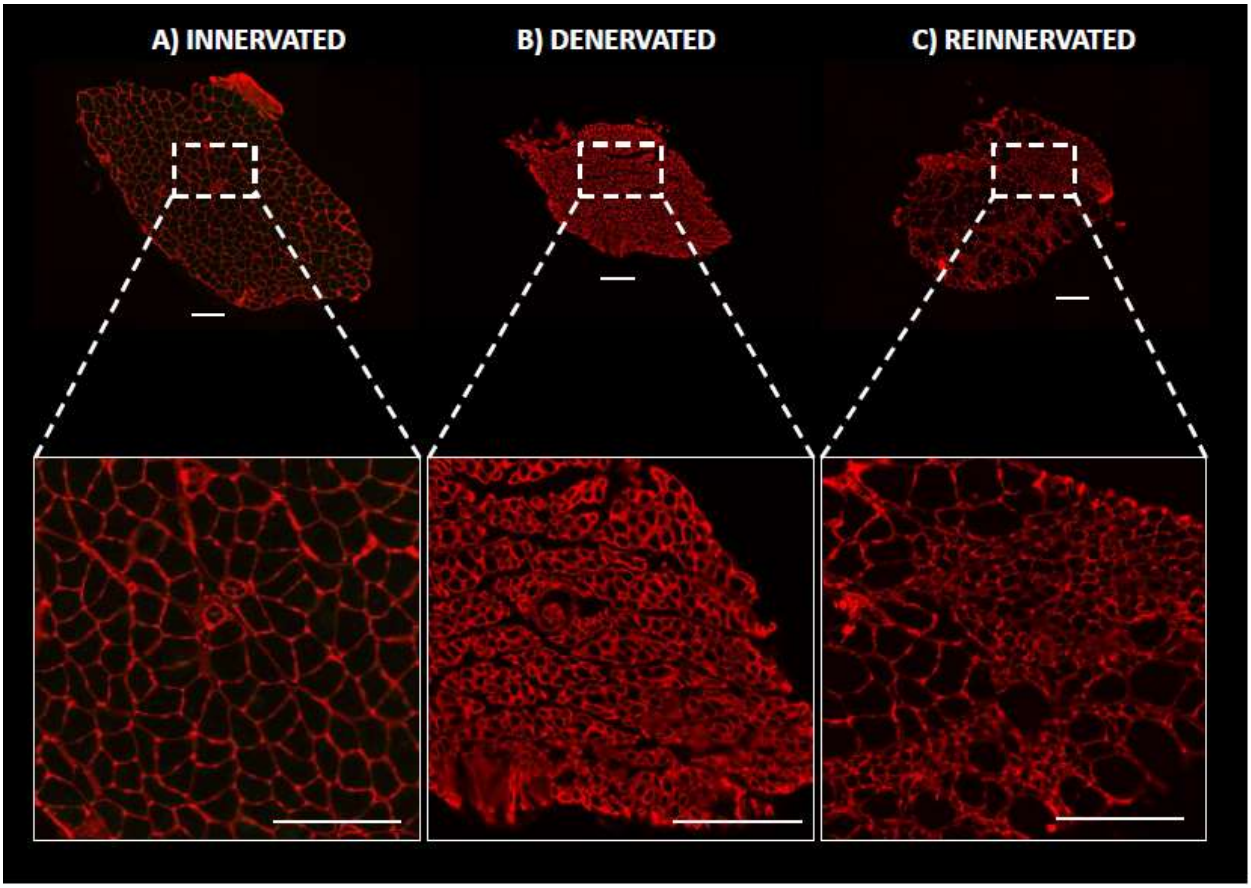


**Figure 5.2: Examples of differences in CSA between A) normal innervated soleus, and in soleus that had been denervated for which B) all fibers had small CSA and C) some but not all fibers had CSA similar to that of innervated muscle**. Red: laminin staining. Horizontal bar: 100 µm.

# FIGURE 5.3

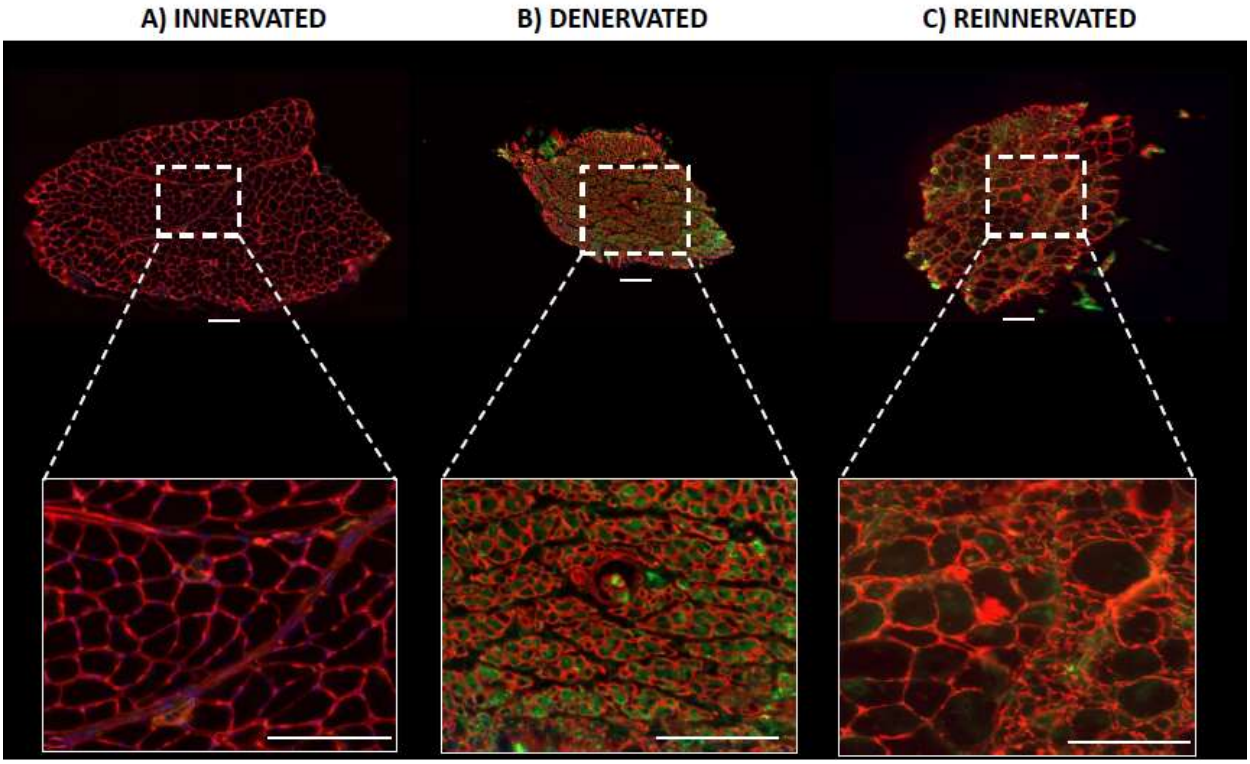


**Figure 5.3: Examples of embryonic myosin expression in A) normal innervated soleus, and in soleus that had been denervated for which B) all fibers had small CSA and C) some but not all fibers had CSA similar to that of innervated muscle**. Green: embryonic myosin; red: laminin staining. Horizontal bar: 100 µm.

# FIGURE 5.4

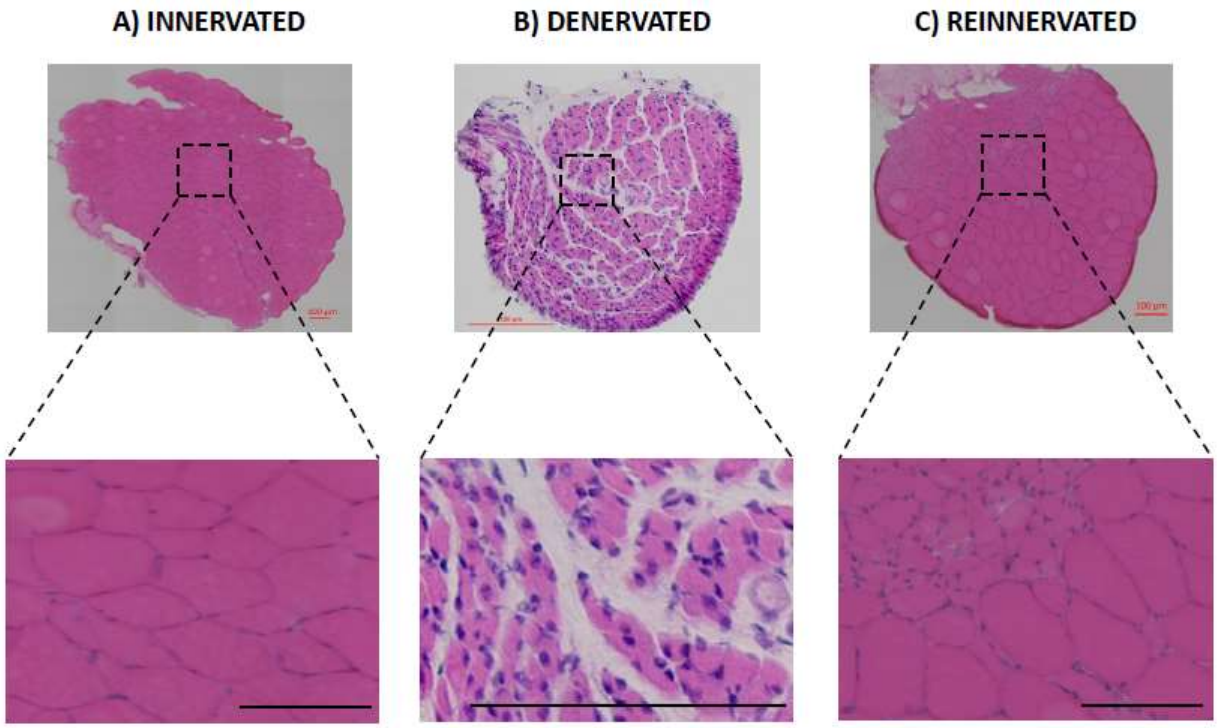


**Figure 5.4: Examples of hematoxylin and eosin staining in A) normal innervated soleus, and in soleus that had been denervated for which B) all fibers had small CSA and C) some but not all fibers had CSA similar to that of innervated muscle**. Horizontal bar: 100 µm.

## REINNERVATION INCIDENCE, MUSCLE WEIGHT AND FORCE GENERATION

Reinnervation incidence in EDL was 39% for both untreated (7 of 18 muscles) and Ang 1-7/DIZE (10 of 26 muscles) treated muscles. For soleus, reinnervation incidence was 33% (6 of 18 muscles) for untreated muscles and 39% (10 of 26 muscles) for Ang 1-7/DIZE treated muscles. Notably, reinnervation incidences were lower in Ang 1-7/DIZE/A779 treated muscles, being 30% (3 of 10 muscles) for EDL and 20% (2 of 10 muscles) for soleus muscles.

Mean muscle masses of EDL either expressed in mg or as a ratio to the body weight in mg/g were significantly lower in denervated muscles, but were not significantly different between untreated, Ang 1-7/DIZE or Ang 1-7/DIZE/A779 treated muscles (Fig. 5.5A, B). Reinnervated EDL had significantly greater mean muscle mass than denervated EDL. Furthermore, Ang 1-7/DIZE treatment further increased EDL muscle mass to the point where the muscle/body weight ratio of was no longer different from that of innervated EDL (Fig. 5.5B). A779 partially reduced the Ang 1-7/DIZE effects as mean muscle/body weight ratio of reinnervated EDL remained significantly lower than those of innervated EDL. The situation was the same in soleus (Fig. 5.5C, D), except for the Ang 1-7/DIZE/A779 treated muscles. However, there were only two muscles for this group with values of 0.087 and 0.323 mg/g.

# FIGURE 5.5

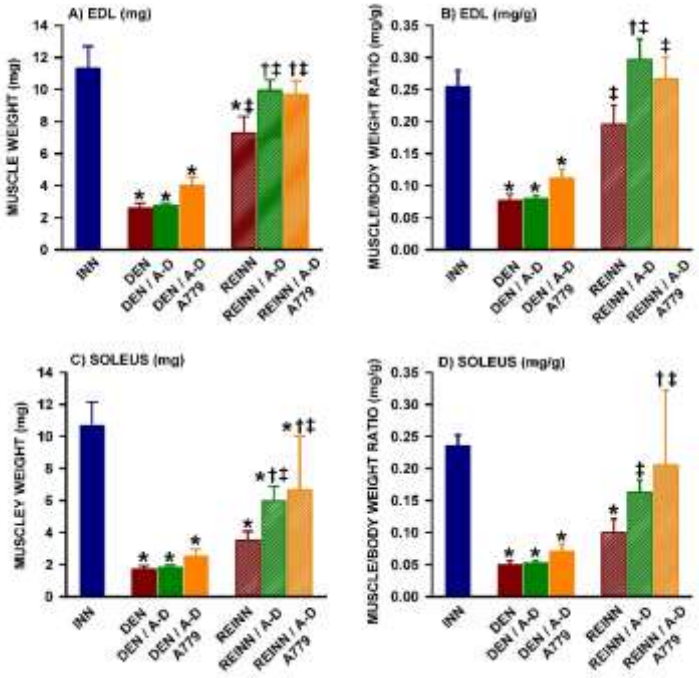


**Figure 5.5. Angiotensin 1-7 had no effect on muscle weight loss in 16 week denervated muscles while it significantly improved muscle weight of reinnervated muscles.** Muscle weight are presented A) & C) in mg and B) & D) as a ratio of muscle body/weight in mg/g. Abbreviations and as explained in the text: INN, innervated; DEN, data from denervated mice with and without sucrose treatment; REINN, data from mice with reinnervated muscles with and without sucrose treatment; A-D, mice treated with either Ang 1-7 or DIZE. Vertical bars represent the S.E of 3-16 muscles.

***** Mean value significantly different from that of innervated muscles.

**†** Mean value significantly different from that of reinnervated muscles;

**‡** Mean value significantly different from that of denervated muscles under similar conditions; ANOVA and L.S.D., $P < 0.05$.

Denervated EDL had force-frequency relationship shifted toward lower stimulation frequencies compared to innervated EDL; mean FF50 of innervated and denervated EDL being, respectively, 97 and 13 Hz (Fig. 5.6A, C). Ang 1-7/DIZE treatment had no significant effect on the relationship in denervated EDL. Reinnervated EDL, on the other hand, had force-stimulation relationship and mean FF50 similar to that of normal innervated EDL. Ang 1-7/DIZE treatment did not affect the relationship of reinnervated EDL, but when A779 was added to the treatment, there was a significant shift of the relationship toward higher stimulation frequency. The situation was basically the same for soleus, except that the relationship for untreated and treated soleus were slightly shifted to higher stimulation frequencies when compared to normal innervated soleus (Fig. 5.6B, D).

# FIGURE 5.6

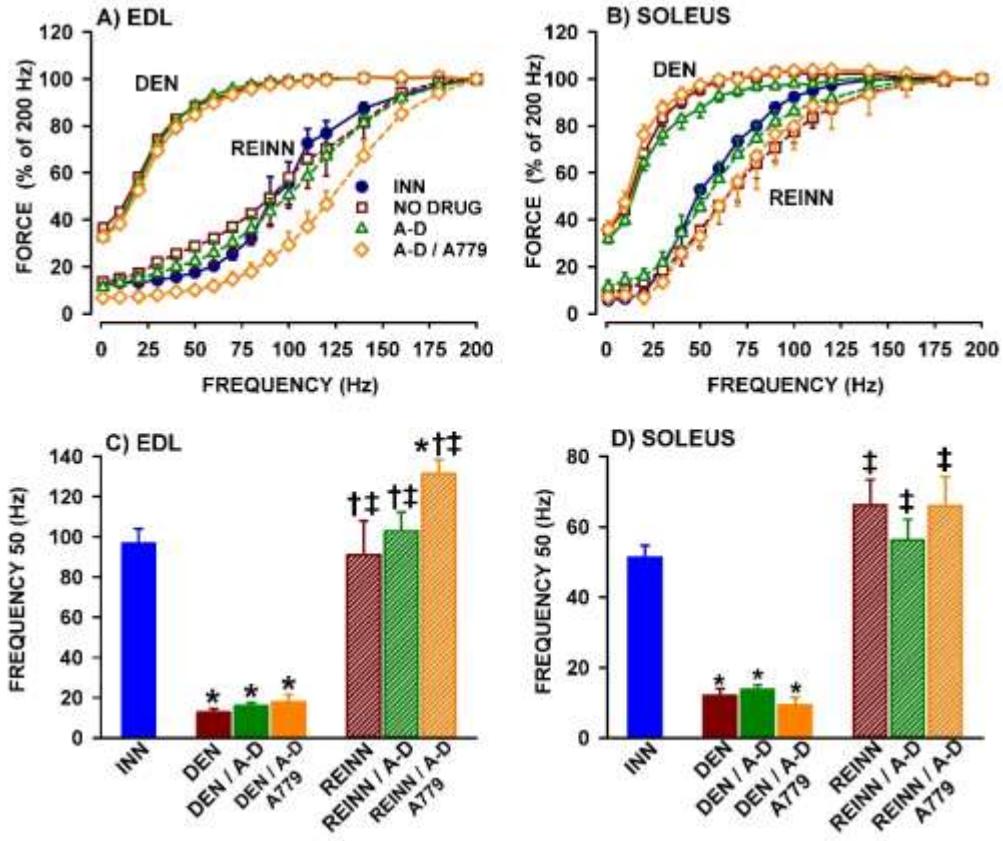


**Figure 5.6. Ang 1-7 did not affect the force-stimulation frequency relationships of denervated and reinnervated EDL and soleus**. Mean force-frequency relationship of A) EDL and B) soleus. Forces are expressed as a percent of the force measured at 200 Hz. Mean frequency 50 of C) EDL and D) soleus. Abbreviations and as explained in the text: INN, innervated; DEN, data from denervated mice with and without sucrose treatment; REINN, data from mice with reinnervated muscles with and without sucrose treatment; A-D, mice treated with either Ang 1-7 or DIZE. Vertical bars represent the S.E of 3-16 muscles.

* Mean value significantly different from that of innervated muscles.

† Mean value significantly different from that of reinnervated muscles;

‡ Mean value significantly different from that of denervated muscles under similar conditions; ANOVA and L.S.D., $P < 0.05$.

As a result of muscle mass loss, mean twitch and tetanic force in Newton (N) were significantly less in denervated than normal innervated EDL (Fig. 5.7A, B). Although mean normalized twitch force to CSA was 46% greater in denervated than in innervated EDL, the difference was not significant due to a large variability (Fig. 5.7A). Ang 1-7/DIZE treated denervated EDL mean twitch force was 78% greater than that of innervated EDL. A779 blocked the Ang 1-7-induced twitch force increase. The increased in twitch force of denervated EDL was associated with prolonged contraction and relaxation times for both denervated treated and untreated muscle (Table. 5.1).

Mean normalized tetanic force of denervated EDL was significantly lower by 55% compared to innervated muscle (Fig. 5.7D), while the loss was reduced to 40% in Ang 1-7/DIZE treated EDL; an effect completely blocked by A779. Ang 1-7 did not reverse the prolongation of tetanic time to peak and half-relaxation time in muscles that remained denervated for 16 weeks (Table. 5.2). Reinnervated EDL still generated less tetanic force than innervated ones while those treated with Ang 1-7/DIZE generated similar tetanic force compared to innervated EDL. Again, this effect was blocked by A779. The denervation and reinnervation effects as well as the Ang 1-7/DIZE and A779 effects were qualitatively similar in soleus compared to EDL (Fig. 5.7E-H). On a quantitative basis, however, denervation caused greater loss in normalized tetanic force and the Ang 1-7/DIZE treatment had smaller effects.

# FIGURE 5.7

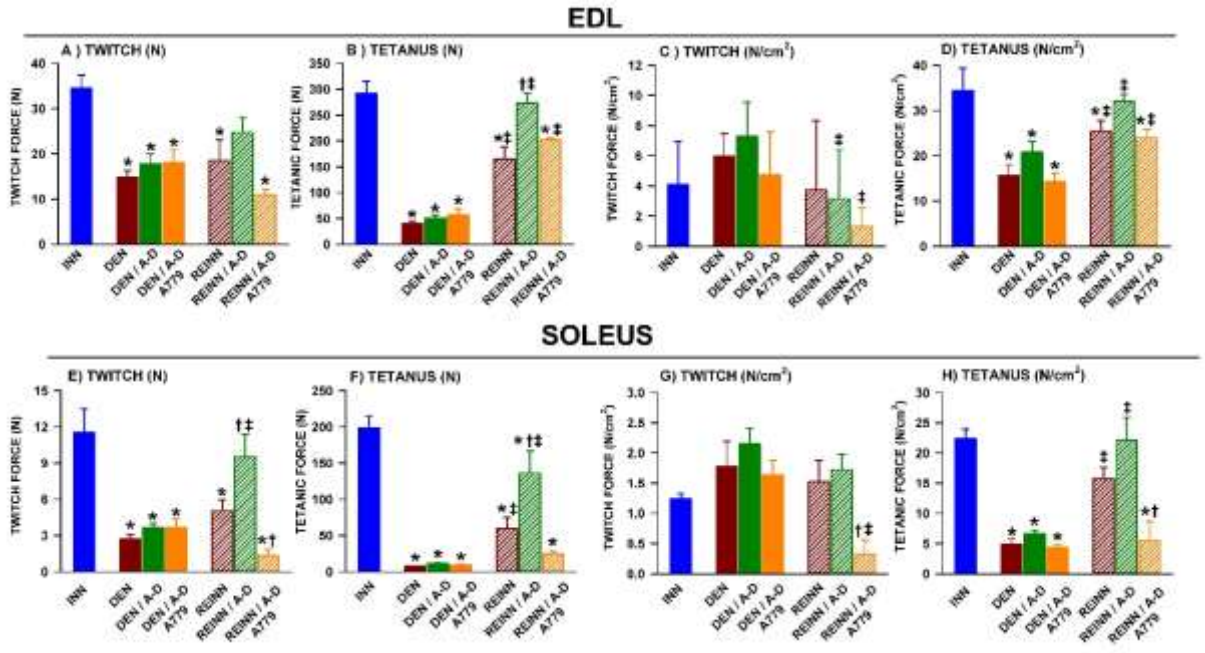


**Figure 5.7. Ang 1-7 increased tetanic force of both denervated and reinnervated EDL and soleus.** Twitch contraction were elicited with one stimulation while tetanic contractions were elicited with 400 msec train of pulses at 200 Hz. A-B and E-F) Forces are in Newton (N). C-D and G-H) Forces were normalized to the muscle CSA in $N/cm^2$. Abbreviations and as explained in the text: INN, innervated; DEN, data from denervated mice with and without sucrose treatment; REINN, data from mice with reinnervated muscles with and without sucrose treatment; A-D, mice treated with either Ang 1-7 or DIZE. Vertical bars represent the S.E of 3-16 muscles.

* Mean force significantly different from that of innervated muscles.

§ Mean force significantly different from that of denervated muscles.

† Mean force significantly different from that of reinnervated muscles.

‡ Mean force significantly different from that of denervated muscles under similar treatment conditions; ANOVA and L.S.D., $P < 0.05$.

# TABLE 5.1

| MUSCLES | PARAMETERS | CONDITIONS | DENERVATED | REINNERVATED |
|---|---|---|---|---|
| EDL | Time to Peak (msec) | INN | 7.2 ± 1.1 (5) | |
| | | DEN | 17.8 ± 0. 8 (9)* | 9.1 ± 3.8 (3) |
| | | Ang 1-7 & DIZE | 17.2 ± 1.1 (9)* | 7.0 ± 0.8 (7) |
| | | Ang 1-7 & DIZE / A779 | 19.7 ± 1.2 (7)* | 5.9 ± 0.4 (3) |
| | ½-Relaxation Time (msec) | INN | 5.8 ± 0.3 (5) | |
| | | DEN | 22.3 ± 1.3 (9)* | 12.6 ± 6.7 (3) |
| | | Ang 1-7 & DIZE | 21.9 ± 1.1 (9)* | 8.4 ± 1.6 (7) |
| | | Ang 1-7 & DIZE / A779 | 23.3 ± 1.7 (7)* | 7.7 ± 1.5 (3) |
| SOLEUS | Time to Peak (msec) | INN | 15.7 ± 0. 6 (6) | |
| | | DEN & DEN-SUC | 27.9 ± 1.9 (9)* | 13.9 ± 2.4 (4) |
| | | Ang 1-7 & DIZE | 26.3 ± 1.0 (7)* | 10.0 ± 0.7 (6)*† |
| | | Ang 1-7 & DIZE / A779 | 31.9 ± 1.1 (8)*§ | 10.8 (1)* |
| | ½-Relaxation Time (msec) | INN | 10.3 ± 1.1 (6) | |
| | | DEN | 33.0 ± 3.5 (9)* | 23.2 ± 7.0 (4)* |
| | | Ang 1-7 & DIZE | 37.1 ± 1.4 (7)* | 15.3 ± 1.1 (6)† |
| | | Ang 1-7 & DIZE / A779 | 42.4 ± 2.9 (8)*§ | 19.8 (1)* |

**Table 5.1. Ang 1-7 did not reverse the prolongation of twitch contraction for muscles that remained denervated for 16 weeks**. Delivery of Ang 1-7 or DIZE, sucrose and A779 was as described in Fig. 5.1. There was no significant difference ($P > 0.05$) between denervated and sucrose-

treated denervated mice, between Ang 1-7 or DIZE-treated mice, and between Ang 1-7/A779 and DIZE/A779-treated mice; so data were combined. Data are presented as MEAN ± S.E. (number of muscles).

* Mean value significantly different from that of innervated muscles.

§ Mean value significantly different from that of denervated muscles.

† Mean value significantly different from that of reinnervated muscles; ANOVA and L.S.D., $P < 0.05$.

# TABLE 5.2

| MUSCLES | PARAMETERS | CONDITIONS | DENERVATED | REINNERVATED |
|---|---|---|---|---|
| EDL | Time to Peak (msec) | INN | 118.8 ± 11.0 (5) | |
| | | DEN | 196.6 ± 3.9 (9)* | 153.4 ± 37.7 (3) |
| | | Ang 1-7 & DIZE | 206.6 ± 4.0 (9)* | 160.4 ± 23.1 (7)* |
| | | Ang 1-7 & DIZE / A779 | 200.7 ± 7.6 (7)* | 166.0 ± 19.8 (3)* |
| | ½-Relaxation Time (msec) | INN | 19.0 ± 2.9 (5) | |
| | | DEN | 62.8 ± 2.5 (9)* | 33.4 ± 0.3 (3) |
| | | Ang 1-7 & DIZE | 69.3 ± 9.3 (9)* | 33.6 ± 1.4 (7) |
| | | Ang 1-7 & DIZE / A779 | 68.4 ± 3.7 (7)* | 29.5 ± 1.5 (3) |
| SOLEUS | Time to Peak (msec) | INN | 204.6 ± 0.7 (6) | |
| | | DEN & DEN-SUC | 215.8 ± 6.4 (9) | 210.8 ± 3.5 (4) |
| | | Ang 1-7 & DIZE | 212.0 ± 9.2 (7) | 209.9 ± 6.1 (6) |
| | | Ang 1-7 & DIZE / A779 | 213.4 ± 7.3 (6) | 204.3 ± 3.7 (2) |
| | ½-Relaxation Time (msec) | INN | 43.3 ± 1.7 (6) | |
| | | DEN | 82.2 ± 6.7 (9)* | 56.7 ± 3.9 (4) |
| | | Ang 1-7 & DIZE | 80.2 ± 6.2 (6)* | 53.9 ± 4.2 (6) |
| | | Ang 1-7 & DIZE / A779 | 95.7 ± 6.9 (8)* | 62.9 ± 6.1 (2)* |

**Table 5.2. Ang 1-7 did not reverse the prolongation of tetanic time to peak and half-relaxation time in muscles that remained denervated for 16 weeks**. Delivery of Ang 1-7 or DIZE, sucrose and A779 was as described in Fig. 5.1. There was no significant difference ($P > 0.05$)

between denervated and sucrose-treated denervated mice, between Ang 1-7 or DIZE-treated mice, and between Ang 1-7/A779 and DIZE/A779-treated mice; so data were combined. Data are presented as MEAN ± S.E. (number of muscles).

* Mean value significantly different from that of innervated muscles.

§ Mean value significantly different from that of denervated muscles; ANOVA and L.S.D., $P < 0.05$.

## REINNERVATION INCIDENCE, MUSCLE WEIGHT AND FORCE GENERATION IN MASR$^{-/-}$ MUSCLES

Sixteen weeks after the denervation surgery, 11% (1 of 9 muscles) of EDL had been reinnervated in MasR$^{-/-}$muscles, and this percent increased to 33% (2 of 6 EDL) after 19 weeks. For soleus, the incidence of reinnervated was 12% (1 of 8 muscles) and 67% (4 of 6 muscles) after 16 and 19 weeks, respectively. Although the reinnervation incidence was greater after 19 than after 16 weeks, means values of muscle weight, tetanic force, twitch force and force-frequency relationship for 16 and 19 weeks were similar, so all data were combined.

In EDL muscle, the force frequency relationship shifted toward lower frequencies while reinnervated muscle partially shifted toward innervated muscle (Fig. 5.8A). Again, denervation significantly decreased the FF50, muscle weight, muscle/body ratio and tetanic force, while it increased twitch force (Fig. 5.8B-H). Contrary to wild type reinnervated EDL, for which some parameters fully returned back to the values in innervated muscles, all parameters of MasR$^{-/-}$ reinnervated EDL only partially returned back toward values in innervated EDL. The situation was basically the same for soleus, except that the recovery of reinnervated soleus was much better than that of EDL (Fig. 5.9).

# FIGURE 5.8

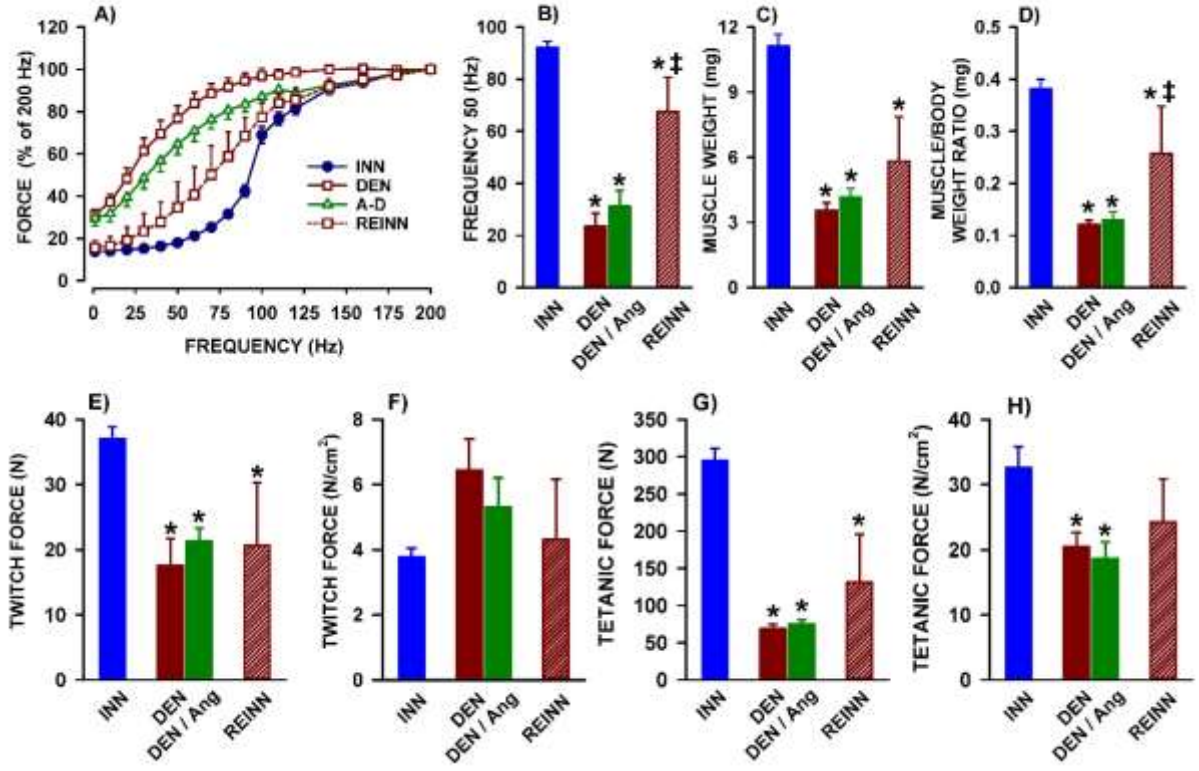


**Figure 5.8. In denervated MasR$^{-/-}$ EDL Ang 1-7 did not affect A) force-frequency relationship, B) frequency 50, C) muscle mass in mg, D) muscle/body weight ratio, E) twitch force in N; F) normalized twitch force in N/cm$^2$, G) tetanic force in N and H) normalized tetanic force in N/cm$^2$ 16 week after a denervation surgery**. Abbreviation: INN, innervated; DEN, denervated; Ang, Ang 1-7. Vertical bars represent the S.E. of 3-8 muscles.

***** Mean value significantly different from that of innervated muscles.

**‡** Mean value significantly different from that of denervated muscles; ANOVA and L.S.D., $P < 0.05$.

# FIGURE 5.9

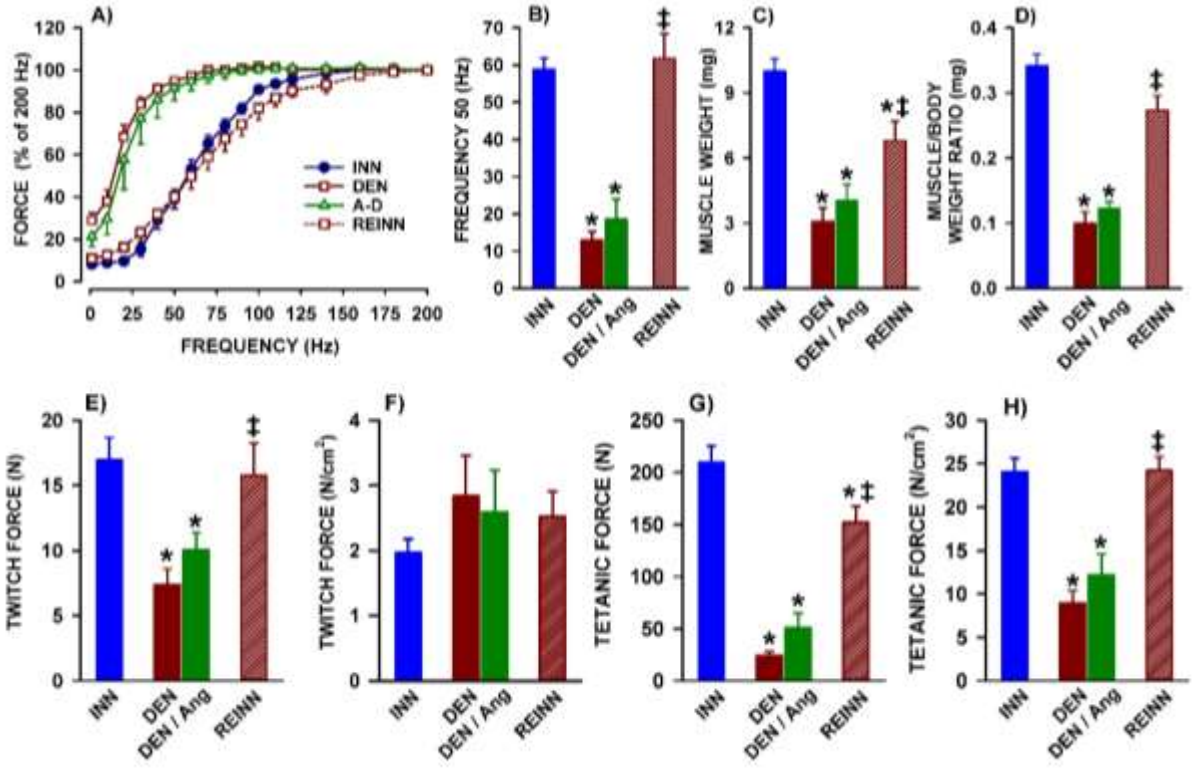


**Figure 5.9. In denervated MasR$^{-/-}$ soleus Ang 1-7 did not affect A) force-frequency relationship, B) frequency 50, C) muscle mass in mg, D) muscle/body weight ratio, E) twitch force in N; F) normalized twitch force in N/cm$^2$, G) tetanic force in N and H) normalized tetanic force in N/cm$^2$ 16 week after a denervation surgery**. Abbreviation: INN, innervated; DEN, denervated; Ang, Ang 1-7. Vertical bars represent the S.E. of 3-8 muscles.

***** Mean value significantly different from that of innervated muscles.

**‡** Mean value significantly different from that of denervated muscles; ANOVA and L.S.D., $P < 0.05$.

## MEMBRANES EXCITABLITITY AND RESTING MEMBRANE DEPOLARIZATION

Ang 1-7 and DIZE treatments fully prevented the loss of normalized tetanic force in EDL and soleus during a 4 week denervation period by partially preventing the membrane depolarization, which then allows for a recovery of normal excitability and action potential overshoot (Chapter 4). We therefore measured action potential to determine the extent of which the improvement in tetanic force in Ang 1-7/DIZE treated denervated and reinnervated muscles is related to an improvement of membrane excitability. For innervated EDL muscle, 100% of fibers were excitable (Fig. 5.10A) and the mean resting Em was -76 mV (Fig. 5.10B). Following 16 week denervation, fiber excitability had significantly declined by 45% (Fig. 5.10A) while mean resting Em became -65 mV (Fig. 5.10B). The decline in resting Em in denervated muscle also lead to significant decrease in mean action potential overshoot to -1 mV as well as lower maximum rate of depolarization (Fig. 5.10C-D). Ang 1-7/DIZE fully prevented membrane excitability loss, increased resting $E_M$ to -74 mV, action potential overshot to 15mV and maximum rate of depolarization to 670 V/sec. Reinnervation fully improved all membrane parameters to normal, i.e., to the values observed in normal innervated muscles. The same was observed with soleus muscle with one exception; that is. membrane excitability of reinnervated muscle did not improved whereas it fully recovered with the Ang 1-7/DIZE treatment (Fig. 5.10E-H).

In terms of resting $E_M$ distribution, all innervated fibers had resting $E_M$ more negative than -60 mV (Fig. 5.11A). The resting $E_M$ distribution of denervated EDL was significantly shifted toward less negative values. More importantly, 21% of fibers in denervated EDL had resting $E_M$ less negative than -60 mV, a range of resting $E_M$ for which fibers become unexcitable (Ammar et al., 2015a). Ang 1-7 shifted the $E_M$ distribution curve back toward that of innervated

fibers and less than 2% of fibers had resting $E_M$ less negative than -60 mV. Reinnervated untreated and Ang 1-7/DIZE treated EDL had resting $E_M$ distribution that was not significantly different from that of innervated EDL. Denervated soleus had a much greater number of resting $E_M$ less negative than -60 mV, the value being 58% (Fig. 5.11C). Furthermore, untreated reinnervated soleus still had 20% of fibers with resting $E_M$ less negative than -60 mV (Fig. 5.11D). Finally, for both denervated and reinnervated soleus, the number of fibers with resting $E_M$ less negative than -60 mV was reduced to less than 2% when treated with Ang 1-7 or DIZE.

# FIGURE 5.10

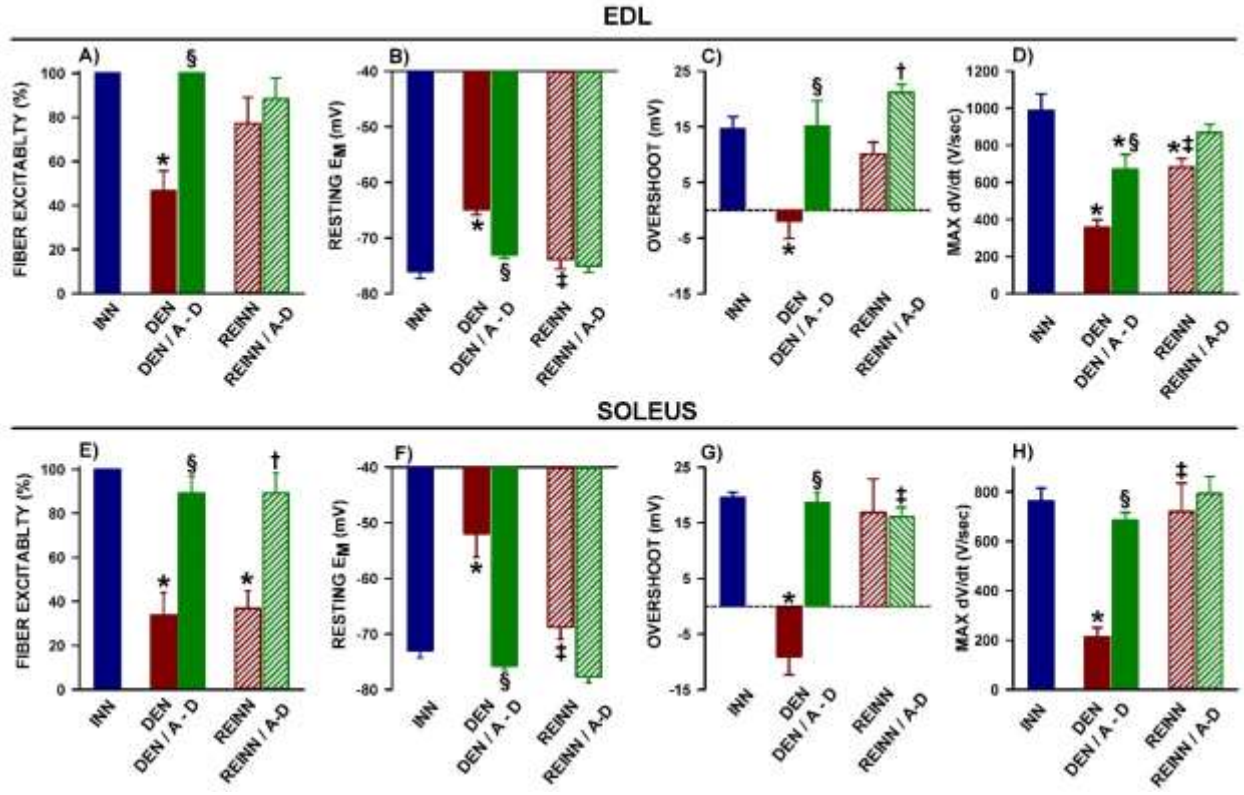


**Figure 5.10: Ang 1-7/DIZE significantly improved membrane excitability in denervated and reinnervated EDL and soleus.** Action potentials were elicited with one stimulation. Excitability was calculated as the number of fibers that generated an action potential and is expressed as a percent of the total number of tested fibers. Abbreviations: INN: innervated; DEN: denervated; REINN; reinnervated; A-D: mice treated with either Ang 1-7 or DIZE. Vertical bars represent S.E. of 4-9 denervated muscles (76-175 fibers) and 3 reinnervated muscles (39-53 fibers).

* Mean value significantly different from that of innervated muscles.

§ Mean value significantly different from that of denervated muscles.

† Mean value significantly different from that of reinnervated muscles.

‡ Mean value significantly different from that of denervated muscles; ANOVA and L.S.D., $P < 0.05$.

# FIGURE 5.11

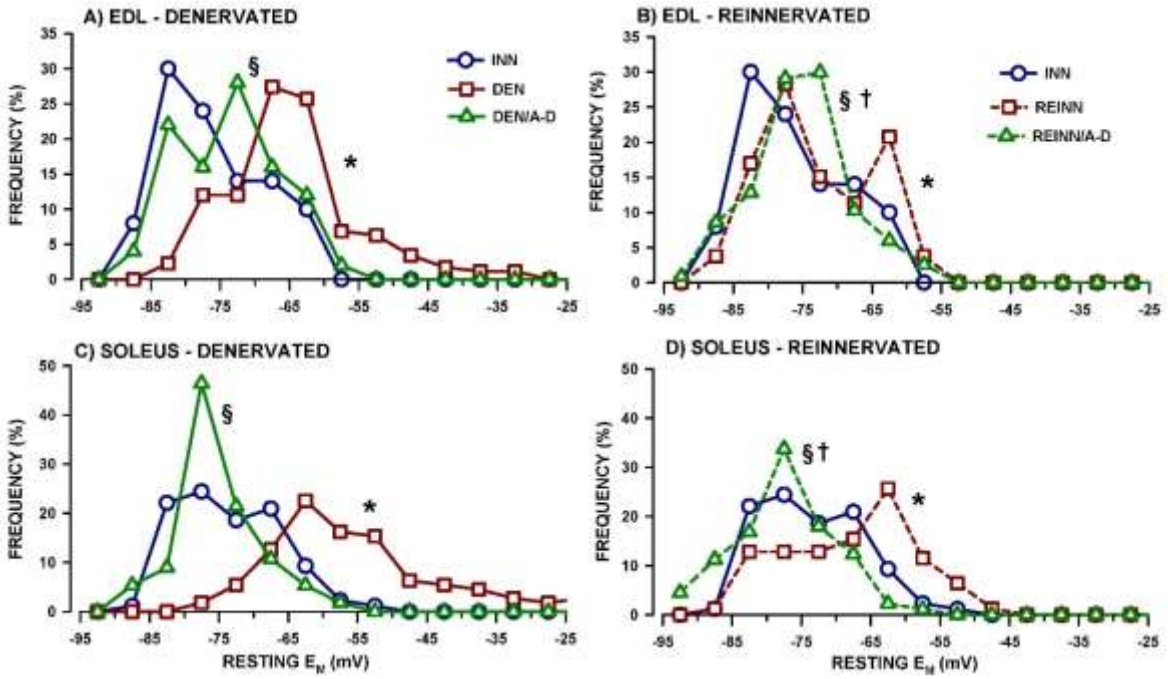


**Figure 5.11. Ang 1-7 shifted the resting $E_M$ distribution of denervated and reinnervated CD-1 EDL and soleus toward that of normal innervated muscles.** Resting $E_M$ were divided in bin of 5 mV; the number of fibers from all muscles was counted for each bin and is expressed as a percent of the total number of fibers tested. Abbreviations**:** INN: innervated; DEN: denervated; REINN: reinnervated; A-D: Ang 1-7 or DIZE treated muscles. The number of fibers/muscles are as provided in Fig. 5.10.

***** Resting $E_M$ distribution significantly different to that of innervated muscles;

**§** Resting $E_M$ distribution significantly different from that of denervated muscles.

**†** Resting $E_M$ distribution significantly different from that of reinnervated muscles; Fisher test, $P < 0.05$.

# CHAPTER 6

# DISCUSSION

NOTE: This chapter contained the integrated discussion of the three manuscripts mentioned in Chapters 3-5. No quotation mark will appear in the Discussion.

The overall objective of this study was to test the hypothesis that "**Angiotensin 1-7 (Ang 1-7) prevents muscle atrophy and force loss following denervation**". To test this hypothesis, three aims were proposed in the Introduction. The aims and the major findings for each of them were as follows:

**Aim 1** was to "document the hypertrophy effect of Ang 1-7 in normal mouse skeletal muscle". The major findings were: 1) Ang 1-7 increased skeletal muscle weight in a muscle dependent manner; 2) it significantly increased both twitch and tetanic force; 3) Ang 1-7 shifted the force-frequency relationship toward lower stimulation frequencies, an effect associated with longer relaxation period; 4) Ang 1-7 had no effect on fiber type composition but significantly increased fiber CSA, especially in type I and IIA fibers; 5) Ang 1-7 caused an initial increase in P-Akt and P-4EBP protein contents within 3 days of treatment before it returns to normal by 2 weeks; 7) Ang 1-7 did not affect the S6K protein expression; 8) $MasR^{-/-}$ EDL and soleus had greater muscle/body weight ratios, generated greater twitch force, but similar tetanic force, had a force-frequency relationship shifted toward lower stimulation frequency, and in some cases had smaller fiber CSA when compared to wild type EDL and soleus; 9) the Ang 1-7 effects on muscle weight, force and CSA observed in wild type EDL and soleus did not occur in $MasR^{-/-}$ skeletal muscle.

**Aim 2** was "to test the hypothesis that Ang 1-7 prevents muscle atrophy and force loss following a short 2 and 4 weeks denervation period". The major findings were: 1) neither Ang 1-7 nor DIZE prevented the loss of muscle mass and fiber CSA; 2) twitch force increased and was further potentiated by Ang 1-7 and DIZE; 3) Ang 1-7 and DIZE were fully effective at maintaining normalized maximal tetanic force; 4) A779, a MasR antagonist, fully blocked the effect of Ang 1-7 and DIZE on twitch and tetanic force; 5) normalized tetanic force of $MasR^{-/-}$

EDL and soleus were less affected when compared to their wild type counterpart and Ang 1-7 did not potentiate twitch force; 6) neither Ang 1-7 nor DIZE prevented the shift in force-frequency relationship in denervated EDL while causing a further shift in denervated soleus; 7) Ang 1-7 prevented the loss in membrane excitability, membrane depolarization and decreases in action potential overshoot; 8) Na-K pump protein content increased in EDL, an effect potentiated by Ang 1-7 whereas in soleus denervation reduced pump content while Ang 1-7 had no effect; 9) Ang 1-7 did not allow for an increase in actin and myosin content; 10) there was a shift in fiber type toward type I and IIA in denervated EDL muscle, an effect partially reversed by Ang 1-7, whereas fiber type composition of soleus was unaffected by denervation and Ang 1-7; 11) Ang 1-7 and DIZE had little effect on the protein content of total and phosphorylated Akt, 4EPB and S6K, three important hypertrophic factors, as well as little effects on MuRF-1 and atrogin-1 content.

**Aim 3** was "to test the hypothesis that Ang 1-7 prevents muscle atrophy and force loss following a long 16 week denervation period". The major findings were: 1) sixteen weeks after denervation, many EDL and soleus muscles remained denervated while about a third became reinnervated; 2) compared to innervated muscles, denervated muscles had force-frequency relationship shifted toward lower stimulation frequencies as observed for the 2 and 4 week denervation period; 3) reinnervation was associated with increases in muscle weight, tetanic force, and a shift in the force-frequency relationship closer to that of innervated muscle; 4) Ang 1-7 and DIZE did not increase the incidence of reinnervation, but A779, a MasR antagonist, reduced the incidence of reinnervation while reinnervation was delayed by a few week in $MasR^{-/-}$ muscles; 4) Ang 1-7 and DIZE did not prevent muscle weight loss in denervated EDL and soleus but significantly improved weight recovery in reinnervated muscles; 5) Ang 1-7 and DIZE had a

small effect on normalized tetanic force of denervated muscles, whereas it significantly improved tetanic force recovery in both reinnervated EDL and soleus; 6) Ang 1-7 and DIZE significantly increased twitch force further in denervated muscle; 7) neither Ang 1-7 nor DIZE prevented the shift in force-frequency relationship in denervated EDL and soleus; 8) Ang 1-7 prevented the loss in membrane excitability, membrane depolarization and decreases in action potential overshoot in denervated muscles.

## 6.1 ANG 1-7 HYPERTROPHIC EFFECTS ON MUSCLE MASS IN INNERVATED MUSCLE IS LOST FOLLOWING DENERVATION

Ang 1-7, over a 4 or 16 week treatment, only caused small increases in muscle mass of normal innervated muscles, an effect that varied between muscles. That is, significant increases were observed in soleus and gastrocnemius muscles, but there was no effect in EDL. It is therefore not surprising that Ang 1-7 had little effect on body weight. When expressed in mg, $MasR^{-/-}$ EDL, tibialis and gastrocnemius muscle mass were smaller than their age match wild type counterpart, which is in agreement with the finding that Ang 1-7 is important at increasing muscle mass in wild type mice. Considering that skeletal muscle constitutes a large portion of the body mass, it is therefore not surprising that $MasR^{-/-}$ mice also have smaller body weight than wild type mice.

Ang 1-7 increased mean fiber CSA of innervated fibers. The largest effect was observed for type I fibers for both EDL and soleus. The effect was smaller for EDL and soleus type IIA fibers and very small for EDL type IIB. It thus appears that the Ang 1-7 effectiveness at increasing fiber CSA is in the order of type I > IIA > IIB fibers. Considering the smaller amount of type I and IIA fibers in EDL, this also explain why Ang 1-7 has a smaller effect on muscle mass in EDL compared to soleus.

For the short denervation period, only DIZE reduced the extent of muscle mass loss during a 4 week denervation period. DIZE, at 15 mg/kg•day as in this study, increases plasma Ang 1-7 levels by almost 4-fold (Zhang et al., 2015). At 350-390 ng/kg•min using an osmotic pump, Ang 1-7 plasma and kidney level increases by ~2-fold (Oh et al., 2012; Mori et al., 2014); so, at a dose of 100 ng/kg•day as in this study, the increase in Ang 1-7 level is expected to be less than with DIZE. Although one can then suggest that at a high concentration Ang 1-7 has the capacity to reduce the extent of muscle mass loss during denervation, such conclusion is not supported by the results on fiber CSA as neither Ang 1-7 nor the DIZE treatment prevented the reduction in fiber CSA. Notably, A779 worsened the reduction in fiber CSA in soleus but not in EDL. This suggest that the endogenous Ang 1-7, but not an increase in plasma level, helps at preventing muscle atrophy in terms of mass, at least in soleus. The lack of a similar effect in EDL may be related to the fact that denervation had greater effects on the extent of muscle mass and force loss in soleus than EDL. Being more sensitive to the denervation effect, soleus may also be more sensitive to a MasR inhibition. Finally, for a longer denervation period, i.e., 16 week, neither Ang 1-7 nor DIZE prevented the mass loss.

Taken together, the results suggest that Ang 1-7 at the dosages used in this study is effective at inducing hypertrophy in normal innervated muscle in regard to muscle mass and fiber CSA; an effect that is basically loss in denervated muscles, except for the soleus over a short denervation period.

## 6.2 ANG 1-7 EFFECT ON CONTRACTILITY IN INNERVATED MUSCLES IS MAINTAINED IN DENERVATED MUSCLES

Maximum tetanic force

Ang 1-7 increased the normalized maximum tetanic force to CSA in innervated muscle. One possible mechanism is an increased density/number of actin and myosin protein; the two proteins responsible to generate force. However, Ang 1-7 did not affect the myosin protein content while a statistically non-significant increase in actin was observed only in soleus. It is therefore unlikely that increases in actin and myosin protein content are a mechanism for the Ang 1-7 induced increase in force. Further studies will be necessary to elucidate this mechanism.

Considering the Ang 1-7 effects on innervated wild type skeletal muscle, one would expect that $MasR^{-/-}$ EDL and soleus would generate less force. However, no difference was observed in maximum tetanic force between wild type and $MasR^{-/-}$ EDL and soleus. This may not be that surprising because the Ang 1-7 induced increase in tetanic force in wild type muscles was small so that other factors regulating force generation could easily compensate for the lack of Ang 1-7 stimulation.

Contrary to the situation with muscle mass and fiber CSA, the capacity of Ang 1-7 to increase tetanic force is maintained in denervated muscles. As a consequence of muscle mass loss, the capacity of denervated muscles to generate force is drastically reduced whether it is expressed in N or normalized to CSA in $N/cm^2$ as previously reported (Finol et al., 1981). The decrease in normalized tetanic force suggests that the extent of the decrease exceeds the expected decrease from just a reduction in muscle mass. This study now demonstrates for the first time that Ang 1-7 completely prevents the loss of normalized tetanic force in both EDL and soleus during 4 week denervation. Ang 1-7 still had a small effect after 16 week denervation. The increases in mean normalized tetanic force in Ang 1-7 treated muscles were small and non-

significant, but they were completely blocked by A779, a MasR antagonist, and completely absent in $MasR^{-/-}$, suggesting that Ang 1-7 still have an effect on tetanic force in 16 week denervated muscles.

Ang 1-7 had little and no consistent effects on α-actin or myosin content in 4 week denervated muscles, so the preservation of the contractile proteins cannot be a mechanism for the maintenance of normalized force. Considering the smaller Ang 1-7 effect after 16 week denervation, it is also unlikely that Ang 1-7 reduces the decrease in α-actin and myosin content during prolonged denervation period. Another potential mechanism is a change in fiber type. In EDL, 4 week denervation leads to decreases in myosin IIB expression and increases in type IIA; an effect reversed by Ang 1-7. However, single type IIA and IIB fibers develop similar maximum force (Bottinelli et al., 1991). Furthermore, neither denervation nor Ang 1-7 affected fiber type composition in soleus. It is therefore unlikely that changes in fiber type composition is involved in the preservation of normalized tetanic force in Ang 1-7 treated denervated muscles.

**Recovery of membrane excitability as a major mechanism for the Ang 1-7 effect on tetanic force**

Mean resting $E_M$ was much less negative in 4 and 16 week denervated than in innervated muscle fibers as previously reported (Albuquerque et al., 1971b; Albuquerque and Thesleff, 1968a; Wareham, 1978; CLAUSEN et al., 1981). Furthermore, a large proportion of denervated muscle fibers had resting $E_M$ less negative than -60 mV, resting $E_M$ at which muscle no longer generate action potential and thus force (Cairns et al., 1995; Ammar et al., 2015b). The loss of membrane excitability was completely prevented by Ang 1-7 and almost completely by DIZE for both denervation periods. Although mean resting $E_M$ of Ang 1-7/DIZE treated denervated muscle

fibers was still less negative compared to those of innervated fibers, almost none of the Ang 1-7/DIZE treated fibers had resting $E_M$ less negative than -60 mV, again for both denervation periods. Finally, action potential overshoot and maximum rate of depolarization, which has been used as an index of $Na^+$ current during the depolarization phase (Hodgkin and Katz, 1949), were both depressed in denervated muscle fibers. Ang 1-7/DIZE allowed for normal action potential overshoot in 4 and 16 week denervated muscle fibers and significant increases in maximum rate of depolarization in 16 week denervated muscles. It is therefore suggested that the primary mechanism by which Ang 1-7 completely prevents the loss of normalized tetanic force during the 4 week denervation period is by reducing the extent of the membrane depolarization associated with denervation allowing fibers to remain fully excitable with normal action potential amplitude.

The situation is, however, different after 16 week denervation. That is, while Ang 1-7 still fully prevents the loss of membrane excitability, it does not fully prevent the loss of normalized tetanic force. This suggest that over a 16 week denervation period the loss of tetanic force is not solely due to a loss of membrane excitability, but to other factors for which Ang 1-7 has no effect. Future studies will be necessary to determine the nature of those factors. Finally, it is important to note that such mechanism cannot explain the increase in tetanic force observed in normal innervated muscles. This is because all fibers from normal innervated muscles are fully excitable, so even if Ang 1-7 improves resting $E_M$ in innervated fibers, it will not result in any increase in tetanic force.

It is interesting to note that changes in resting $E_M$ during the 4 week denervation period with and without Ang 1-7 treatment occurs to the same extent in denervated EDL and soleus despite the fact that the $Na^+$ $K^+$ pump content increases in the former muscle and decreases in the

latter. Using the $^{3}$H-ouabain binding technique, fifteen and 31 day denervation periods result in pump content that decreases by about 35% in rat soleus and only 15% in rat EDL (Clausen et al., 1982; Ward et al., 1987). So, the decrease in soleus α1 and α2 pump content observed in this study is in agreement with previous studies whereas the increase in EDL is not. The increase in pump content in mouse EDL may reflect a difference in species and may also be related to the large increase in the number of fibers expressing type IIA fibers. Soleus muscle has fibers that primarily express type I (63%) and type IIA (51%) myosin compared to only 25 and 16% respectively in EDL (this study) while the pump content is 2-times greater in soleus that in EDL(Clausen et al., 2011b; Ammar et al., 2015b). Also, the number of Hyperkalemic Periodic Paralysis EDL fibers that expresses type IIA fibers is about ~60% (Khogali et al., 2015) compared to 16% in normal EDL muscle while the pump content is 2-times greater in the former than the latter muscle (Ammar et al., 2015b). Together these facts suggest that fibers expressing type IIA myosin contains more $Na^{+}$ $K^{+}$ pump than fibers expressing type IIB myosin and as the number of fibers expressing type IIA myosin increases to 95% in denervated EDL, there is a concomitant increase in pump content.

The next question is how come the depolarization in denervated EDL and soleus muscles be the same with opposite changes in pump content as well as similar effects of Ang 1-7 on membrane excitability despite the fact that Ang 1-7 increases the pump content only in EDL. Compared to normal muscles, Hyperkalemic Periodic Paralysis EDL muscle fibers i) are largely depolarized, ii) contain 2-times more $Na^{+}$ $K^{+}$ pump than wild type muscles with iii) no increase in the pump electrogenic contribution. Hyperkalemic Periodic Paralysis diaphragm, on the other hand, has similar resting $E_M$ compared to normal diaphragm because the pump electrogenic contribution is twice that in normal diaphragm despite the fact that the pump content is not

elevated (Ammar et al., 2015b). It therefore appears that changes or the lack of pump content in both HyperKPP and denervated muscles cannot be an indication of the pump electrogenic contribution to the resting $E_M$. Thus, future studies will be necessary to fully understand how Ang 1-7 prevents the membrane depolarization in denervated muscles; by determining not only the pump electrogenic contribution, but also whether Ang 1-7 reverses the increase in $Na^+$ permeability and decrease in $K^+$ permeability (Kotsias and Venosa, 1987b) as well as changes in $K^+$ and $Cl^-$ conductance as all these components are known to affect resting $E_M$.

In denervated muscle, all Ang 1-7 effects on force were blocked by A779, a MasR antagonist, or absent in $MasR^{-/-}$ muscles that is in agreement with the fact that Ang 1-7 acts via its Mas receptor. A779 treatment also exacerbated the decrease in soleus fiber CSA during denervation. These results are in agreement with the fact that Ang 1-7 acts via its MasR in skeletal muscle. Interestingly, while the normalized tetanic force of wild type denervated EDL and soleus were respectively 35% and 56% less than their innervated counterpart, denervated $MasR^{-/-}$ soleus muscle develop similar normalized tetanic force as innervated soleus whereas a 17% decrease was observed in $MasR^{-/-}$ EDL. The resting $E_M$ depolarization in denervated $MasR^{-/-}$ was smaller than in denervated wild type muscles resulting in smaller but still significant decrease in membrane excitability. Furthermore, the overshoot was completely abolished in denervated $MasR^{-/-}$ muscles as the action potential peak remained negative. Together these results suggest that the normalized tetanic force should be less in denervated than innervated $MasR^{-/-}$ muscles. There is therefore another mechanism that prevented the decrease in normalized force, but this mechanism cannot be documented from this study.

Twitch force and force-frequency relationship

In innervated EDL and soleus muscle, Ang 1-7 also increased twitch force by 100%, which is in agreement with the increase in tetanic force, but the latter cannot explain all of the twitch force increase because the increases in tetanic force were only 21-24% in EDL and 22-37% in soleus; i.e., there were much smaller than those for twitch force. So, an increased capacity to generate force can only be a small component contributing to the increase in twitch force. The twitch force increase was associated with longer relaxation phase, which is likely due to slower $Ca^{2+}$ reuptake by the sarcoplasmic reticulum. This then should allow longer time for the force to increase. However, the twitch force increase was not associated with longer time to peak. Therefore, Ang 1-7 may also be affecting the amount of $Ca^{2+}$ release allowing for activation of the contractile proteins and greater force.

The situation is more complex in denervated muscles. Despite a decrease in action potential overshoot and a 60% loss in excitability, the normalized twitch force to CSA became greater in 4 week denervated EDL and soleus as previously reported (Dufresne et al., 2016; Finol et al., 1981). Although of smaller magnitude, a twitch force increase was also observed in 16 week denervated muscles. The decrease in mean overshoot to 1-5 mV in 4 week denervated fibers is not expected to cause large decrease in twitch force because twitch force decreases by about 10% as overshoot decreases from 30 to 1-5 mV (Yensen et al., 2002; Cairns et al., 2003). However, the complete loss of action potential overshoot is likely one mechanism responsible for the smaller increase in twitch force in 16 week denervated muscles. One factor that may counteract the expected decrease in twitch force from the excitability loss is a prolongation of the twitch contraction (this study, (Finol et al., 1981). Contrary to innervated muscles, denervated muscles had both time to peak and relaxation phase prolonged. The longer time periods then

allows for more time to develop force during a twitch; whether other factors can also contribute to the increase in twitch force cannot be determined from this study. The further increases in twitch force by Ang 1-7 in 4 week denervated muscles can then be explained in part by the maintenance of membrane excitability as explained above and perhaps by a direct increase in the capacity to generate force as discussed for innervated muscles. Similarly, the increases in twitch force in 16 week denervated muscles are most likely due to the longer time to peak and relaxation phase, but the increases are smaller than in 4 week denervated muscles because of the same other factors that cause large decreases in tetanic force. The prolongation of the twitch contraction is also responsible for the major shift in the force-frequency relationship toward lower frequencies in both innervated and denervated muscle because twitch contractions start to fuse at lower frequencies.

For denervated muscles, the cause for the twitch prolongation and shift in force-frequency relationship is most likely related to a decreased capacity of the $Ca^{2+}$ ATPase pump to transport $Ca^{2+}$ back in the sarcoplasmic reticulum. In denervated EDL, protein content of the fast $Ca^{2+}$ ATPase pump SERCA1 and the slow SERCA2 decreases in EDL and soleus, respectively (Schulte et al., 1994). More importantly, there is a net decrease in the maximal rate ($V_{MAX}$) of the total $Ca^{2+}$ ATPase activity; decrease in $V_{MAX}$ also occurred in soleus, but to a smaller extent when compared to EDL (Dufresne et al., 2016). Such decreases in $Ca^{2+}$ ATPase pump activity then slowdown $Ca^{2+}$ reuptake by the sarcoplasmic reticulum resulting in prolonged increase in $[Ca^{2+}]_i$ allowing more time to generate greater force during twitches. Finally the lack of Ang 1-7 effect on those two contractile parameters suggest that Ang 1-7 does not modify the denervation effect on the expression and activity of either SERCA 1 and 2.

Considering the Ang 1-7 effects on innervated wild type skeletal muscle, the mean twitch force, was much greater in both $MasR^{-/-}$ EDL and soleus than their wild type counterpart. Again the greater twitch force was associated with longer relaxation period and a shifted force-frequency relationship toward lower stimulation. Surprisingly, the prolongation of the relaxation phase in $MasR^{-/-}$ compared to wild type muscles was much greater than the Ang 1-7 effect in innervated wild type muscles. As discussed above, the most likely mechanism for the longer relaxation phase is slower $Ca^{2+}$ reuptake. Considering the well-known fact that the knockout of one gene affects the expression/activity of several other proteins, it is clear that the modulation of $Ca^{2+}$ reuptake by Ang 1-7 is complex and will require future studies to fully understand it.

## 6.3 ANG 1-7 HAS LITTLE EFFECT ON THE ATROPHY AND HYPERTROPHY PATHWAYS

Activation of the MasR by Ang 1-7 is known to activate the hypertrophic Akt/mTOR pathway (Cisternas et al., 2015). In innervated muscle, the elevation of P-Akt and P-4EPB, a mTOR downstream target, was only observed at day 3 of the Ang 1-7 treatment as the P-Akt and P-4EPB levels had returned to normal by the second week of treatment. It can be argued that the increases were not statistically significant. However, the increases ranged between 41% and 79% after 3 days of Ang 1-7 treatment. Furthermore, the Ang 1-7 effects over time on those two proteins were basically the same. Finally, the Ang 1-7 effects on twitch and tetanic force, force-frequency curve and fiber CSA did not increase from 4 to 16 weeks, suggesting that the effect on those parameters reached its maximum prior to the 4 week measurements. That therefore suggest the changes are in P-Akt and P-4EPB at 3 days and its return to normal thereafter are physiologically relevant and are involved in the physiological changes reported in this study.

Akt is known to phosphorylate FoxO proteins, which then decreases the expression of MuRF-1 and Atrogin-1 protein content (Morales et al., 2015b; Cisternas et al., 2015). However, in this case, the decreases were very small and not substantial, suggesting that the hypertrophic effect observed in innervated muscle is mainly via an increase activity of the Akt pathways.

Denervation has a strong impact on the content and phosphorylation of the Akt/mTOR pathway. In regard to Akt, we observed no change in protein content after a 3 day denervation period, but very large increases in both total and phosphorylated Akt after 2 and 4 week of denervation in EDL and after 2 week in soleus. Large increases in phosphorylated S6K, a mTOR downstream target, was also observed after 2 week in EDL while no change was observed for 4-EPB. It is surprising that the Akt/mTOR pathway and especially Akt is activated after 2 and 4 week in EDL, a time when atrophy is expected to be high. However, the effect of denervation on total and phosphorylated Akt, S6K and 4-EPB are in agreement with results recently published for the tibialis anterior muscle (Castets et al., 2019). The authors of the study actually suggested that a tight regulation of the Akt/mTOR pathway is required to maintain muscle homeostasis; a reduced activation promotes more atrophy while a large and sustained activation of mTOR results in muscle myopathy including formation of vacuoles, aggregates and abnormal nuclei. A 3 day denervation resulted in small increases in MuRF-1 and Atrogin-1 protein content while very large decreases were observed by 2 and 4 week. Considering i) the activation of the Akt pathway, which is known to inhibit the expression of both MuRF-1 and atrogin-1, and ii) the conclusion of Castets et al., (2019) then our results are not surprising; i.e., the large decreases at 2 and 4 week are most likely because of an inhibition from the Akt pathway.

However, we observed little or no consistent effect of Ang 1-7 and DIZE on Akt, S6K and 4EPB as well as for MuRF-1 and atrogin-1 content in denervated muscle. That therefore

suggest the lack of Ang 1-7 effects on those proteins is the reason why Ang 1-7 has no effect on actin and myosin protein content, muscle mass and fiber CSA in denervated muscle. What remains to be determined is how Ang 1-7 improves membrane excitability and resting $E_M$ in denervated muscles. However, as discussed above, future studies are first necessary to determine how Ang 1-7 modifies the activity of membrane components involved in the resting $E_M$ regulation and then determine whether the Akt or another pathway is involved.

## 6.4 ANG 1-7 IMPROVES MUSCLE MASS AND FORCE RECOVERY FOLLOWING REINNERVATION

On interesting finding of this study was 16 week after the denervation surgery the presence of fibers with large CSA and force-frequency relationship similar to that of normal innervated muscles. The presence of large muscle fibers has been reported following long period of spinal cord injury or denervation (Biral et al., 2008; Carraro et al., 2005; Ashley et al., 2006; Bacou et al., 1996; Maier and Bornemann, 1999). Biral et al. (2008) suggested that the large CSA fibers were atrophy resistance fibers. If this was the case in mouse muscle, then it would imply that following denervation there is an initial atrophy process because of the net atrophy observed after a 4 week denervation followed by a hypertrophy process by the 3$^{rd}$ week. This is quite unlikely because i) such event would be expected to occur in all muscles, not just one thrid of them as reproted in this study, ii) all fibers of some muscles, 16 week after the denervation surgery had large fibers as those of normal innervated muscles and it is more than unlikely that such a complete reversal hypertrophy of all fibers really had occurred. Ashley et al. (2006) suggested that the large fibers after a prolong period of denervation was due to incomplete fusion of small fibers or myoblasts during regeration of muscle fibers. Again this explanation is unlikely for mouse muscles as central nuclei were not present in the large fibers. The authors of

other studies, in which similar large fibers are observed after a prolonged denervation explained the phenomenon as selective reinnervation of muscle fibers that undergo compensatory hypertrophy as they become active (Bacou et al., 1996; Carraro et al., 2005). In this study no attempt was made to prevent reinnervation and the idea of the reinnervation is further supported by our observation that muscles with large muscle mass and FF50 closed to that of normal innervated muscles had a nerve entering them.

As a consequence of the reinnervation, there were large increases in muscle mass, fiber CSA, tetanic force and a shift of the force-frequency relationship toward that of innervated muscles. Interestingly, reinnervation did not necessarily involve all fibers within a muscle as some fibers still had CSA similar to those that had remained denervated, while another proportion of fibers had large CSA; i.e., reinnervation was incomplete (Fig. 5.2-4). This can then explain why some reinnervated muscles had a force-frequency relationship that was partially shifted toward that of normal innervated muscles. However, for most muscles the relationship of reinnervated muscles was similar to that of normal innervated muscles. The force generated by fully denervated muscles were very small and thus it is quite possible that a complete recovery of the force-frequency relationship occurred in partially reinnervated muscles because the large force generated by reinnervated fibers largely overcome the small force generated by the remaining denervated fibers.

Ang 1-7 did not increase the incidence of reinnervation, which suggests that an increase in Ang 1-7 levels does not enhance the reinnervation process. However, inhibiting MasR with A779 reduced the incidence of reinnervation while the extent of reinnervation in $MasR^{-/-}$ mice was greater 19 weeks after the denervation surgery compared to after 16 weeks in wild type; i.e.,

reinnervation was delayed. This suggests that the endogenous Ang 1-7 contributes to the reinnervation process and future studies will be necessary to understand that role.

Another aspect regarding Ang 1-7 and reinnervation is that muscle mass and contractility recovery is accelerated by Ang 1-7. Compared to untreated reinnervated muscles, muscle weight and tetanic force of reinnervated EDL and soleus were greater in Ang 1-7 treated muscles, while membrane excitability and action potential overshoot were the same in untreated and Ang 1-7 treated reinnervated muscles. Twitch force of Ang 1-7 treated reinnervated muscles remained greater than innervated muscle possibly due to a mechanism similar to that discussed for the increase in twitch force in Ang 1-7 treated innervated muscle. Therefore, these results suggest that the hypertrophic effect of Ang 1-7 that was observed in innervated muscles and lost in denervated muscles is regained upon reinnervation enhancing the recovery from denervation.

## 6.5 PERSPECTIVES

As discussed in the introduction nerve could take several months to regenerate such as in cases of nerve injury level II and III. Also, any delay in nerve repair negatively affects muscle mass and functional recovery following reinnervation. Therefore, the development of an efficient treatment to prevent atrophy associated with denervation and to preserve muscle function is extremely important. This study shows that treating denervated muscle with Ang 1-7 does not prevent mass loss, but it efficiently reduces the extent of muscle function loss over a 4 week denervation period in term of membrane excitability and force; the preservation of force, but not of membrane excitability, diminishes as denervation is prolonged to 16 week. Furthermore, once muscle gets reinnervated, Ang 1-7 enhances the restoration of muscle mass and force. This study provides a potential therapeutic Ang 1-7 treatment for denervated muscle to maintain at least

muscle function during the denervation period as well as to enhance muscle recovery upon reinnervation.

## 6.6 OVERALL CONCLUSION

Ang 1-7 is a hypertrophic factor in innervated muscles. It increases muscle weight and CSA as well as tetanic force. This effect is abolished in $Mas^{-/-}$ mice, which provides evidence that Ang 1-7 involves an activation of Ang 1-7-MasR. The transient increases in the Akt/mTOR signaling pathway activity occurs within a week.

Ang 1-7, however, loses its hypertrophic effects following denervation as it did not prevent muscle mass loss and decreases in fiber CSA following a 4 week denervation possibly because there was no evidence for an activation of the Akt/mTOR signaling pathway as well as an inhibition of MuRF-1 and atrogin-1 activity. On the other hand, Ang 1-7 is very effective at maintaining muscle function, i.e., maximum tetanic force, by preventing large membrane depolarization resulting in no loss of membrane excitability as observed in untreated denervated muscles at least up to 4 week denervation (Fig. 6.1). The denervation-induced membrane depolarization is mainly due to increases in $P_{Na}$ and decreases in $P_K$ and $P_{Cl}$. It will therefore be interesting to determine in future studies i) how Ang 1-7 treatment affects theses permeability and as well as which intracellular signaling pathways is involved in the Ang 1-7/MasR (Fig. 6.1).

The protective effect of Ang 1-7 on the maximum tetanic force was also observed after 16 weeks of denervation but to a small extent. Another new effect observed for Ang 1-7 was enhancing muscle mass and function upon reinnervation to improve recovery from denervation.

# FIGURE 6.1

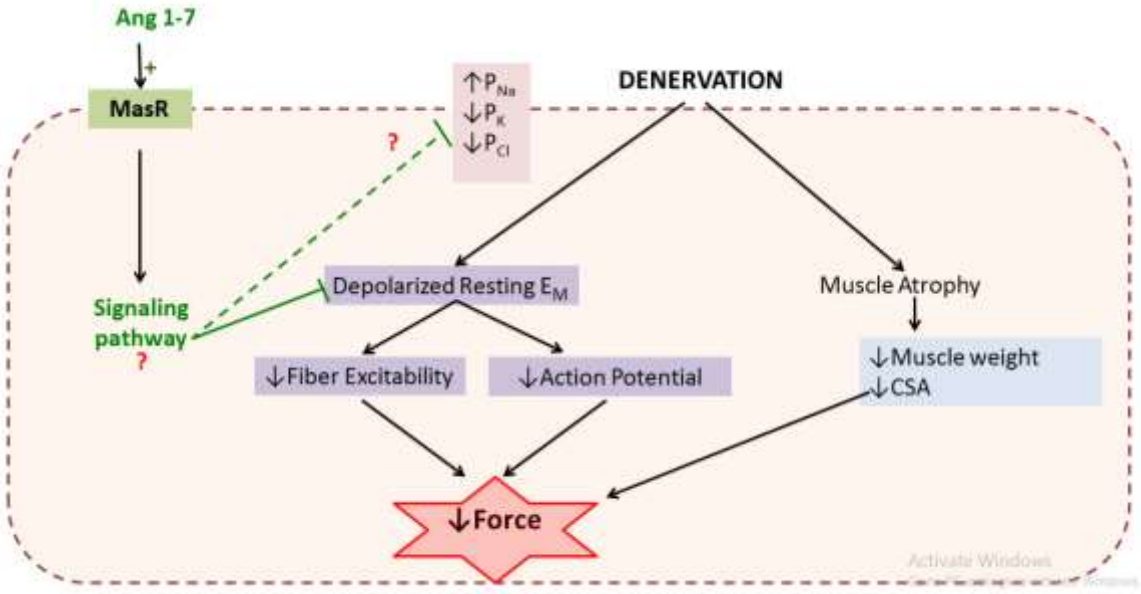


**Figure 6.1: Summary for major effect of Ang 1-7 on denervated muscles.** The major mechanism for the maintenance of normalized tetanic force by Ang 1-7 is reducing the extent of the membrane depolarization associated with denervation allowing for the maintenance of membrane excitability and normal action potential overshoot. Ang 1-7 possibly prevents the change in membrane permeability of Na, K and Cl associated with denervation. Ang 1-7 does not prevent weight and CSA loss following denervation.

# REFERENCES

A, C., C. K, L. MP, P. A, T. LA, S. AM, and L. SA. 2010. The Translation Regulatory Subunit eIF3f Controls the Kinase-Dependent mTOR Signaling Required for Muscle Differentiation and Hypertrophy in Mouse. *PLoS One*. 5. doi:10.1371/JOURNAL.PONE.0008994.

Acuña, M.J., P. Pessina, H. Olguin, D. Cabrera, C.P. Vio, M. Bader, P. Muñoz-Canoves, R.A. Santos, C. Cabello-Verrugio, and E. Brandan. 2014. Restoration of muscle strength in dystrophic muscle by angiotensin-1-7 through inhibition of TGF-β signalling. *Hum. Mol. Genet.* 23:1237–1249. doi:10.1093/hmg/ddt514.

Adams, L., B.M. Carlson, L. Henderson, and D. Goldman. 1995a. Adaptation of nicotinic acetylcholine receptor, myogenin, and MRF4 gene expression to long-term muscle denervation. *J. Cell Biol.* 131:1341–1349. doi:10.1083/jcb.131.5.1341.

Adams, L., B.M. Carlson, L. Henderson, and D. Goldman. 1995b. Adaptation of nicotinic acetylcholine receptor, myogenin, and MRF4 gene expression to long-term muscle denervation. *J. Cell Biol.* 131:1341–1349. doi:10.1083/jcb.131.5.1341.

Adhihetty, P.J., M.F.N. O'Leary, B. Chabi, K.L. Wicks, and D.A. Hood. 2007. Effect of denervation on mitochondrially mediated apoptosis in skeletal muscle. *J. Appl. Physiol.* 102:1143–1151. doi:10.1152/japplphysiol.00768.2006.

Adhihetty, P.J., M.F.N. O'Leary, and D.A. Hood. 2008. Mitochondria in skeletal muscle: adaptable rheostats of apoptotic susceptibility. *Exerc. Sport Sci. Rev.* 36:116–21. doi:10.1097/JES.0b013e31817be7b7.

al-Amood, W.S., D.M. Lewis, and H. Schmalbruch. 1991. Effects of chronic electrical stimulation on contractile properties of long-term denervated rat skeletal muscle. *J. Physiol.* 441:243–56.

al-Amood, W.S., D.M. Lewis, and H. Schmalbruch. 1991. Effects of chronic electrical stimulation on contractile properties of long-term denervated rat skeletal muscle. *J. Physiol.* 441:243–256. doi:10.1113/jphysiol.1991.sp018749.

Albuquerque, E.X., F.T. Schuh, and F.C. Kauffman. 1971a. Early membrane depolarization of the fast mammalian muscle after denervation. *Pfl*[illegible]*gers Arch. Eur. J. Physiol.* 328:36–50. doi:10.1007/BF00587359.

Albuquerque, E.X., F.T. Schuh, and F.C. Kauffman. 1971b. Early membrane depolarization of the fast mammalian muscle after denervation. *Pflügers Arch. Eur. J. Physiol.* 328:36–50. doi:10.1007/BF00587359.

Albuquerque, E.X., and S. Thesleff. 1968a. A Comparative Study of Membrane Properties of Innervated and Chronically Denervated Fast and Slow Skeletal Muscles of the Rat. *Acta Physiol. Scand.* 73:471–480. doi:10.1111/j.1365-201X.1968.tb10886.x.

Albuquerque, E.X., and S. Thesleff. 1968b. A Comparative Study of Membrane Properties of Innervated and Chronically Denervated Fast and Slow Skeletal Muscles of the Rat. *Acta Physiol. Scand.* 73:471–480. doi:10.1111/j.1365-201X.1968.tb10886.x.

Ammar, T., W. Lin, A. Higgins, L.J. Hayward, and J.-M. Renaud. 2015a. Understanding the physiology of the asymptomatic diaphragm of the M1592V hyperkalemic periodic paralysis mouse. *J. Gen. Physiol.* 146:509–25. doi:10.1085/jgp.201511476.

Ammar, T., W. Lin, A. Higgins, L.J. Hayward, and J.M. Renaud. 2015b. Understanding the physiology of the asymptomatic diaphragm of the M1592V hyperkalemic periodic paralysis mouse. *J. Gen. Physiol.* 146:509–525. doi:10.1085/jgp.201511476.

Apel, P.J., T. Alton, C. Northam, J. Ma, M. Callahan, W.E. Sonntag, and Z. Li. 2009. How age impairs the response of the neuromuscular junction to nerve transection and repair: An experimental study in

rats. *J. Orthop. Res.* 27:385–93. doi:10.1002/jor.20773.

Arancio, O., A. Cangiano, and D. De Grandis. 1989. Fibrillatory activity and other membrane changes in partially denervated muscles. *Muscle Nerve.* 12:149–153. doi:10.1002/mus.880120210.

Aravamudan, B., C.B. Mantilla, W.Z. Zhan, and G.C. Sieck. 2006. Denervation effects on myonuclear domain size of rat diaphragm fibers. *J. Appl. Physiol.* 100:1617–1622. doi:10.1152/japplphysiol.01277.2005.

Ashley, Z., Æ, S. Salmons, S. Boncompagni, F. Protasi, M. Russold, H. Lanmuller, W. Mayr, H. Sutherland, and J.C. Jarvis. 2007a. Effects of chronic electrical stimulation on long-term denervated muscles of the rabbit hind limb.

Ashley, Z., S. Salmons, S. Boncompagni, F. Protasi, M. Russold, H. Lanmuller, W. Mayr, H. Sutherland, and J.C. Jarvis. 2007b. Effects of chronic electrical stimulation on long-term denervated muscles of the rabbit hind limb. *J. Muscle Res. Cell Motil.* 28:203–17. doi:10.1007/s10974-007-9119-4.

Ashley, Z., H. Sutherland, H. Lanmuller, M.F. Russold, E. Unger, M. Bijak, W. Mayr, S. Boncompagni, F. Protasi, S. Salmons, and J.C. Jarvis. 2006. Atrophy, but not necrosis, in rabbit skeletal muscle denervated for periods up to one year. *AJP Cell Physiol.* 292:C440–C451. doi:10.1152/ajpcell.00085.2006.

Awad, S.S., R.N. Lightowlers, C. Young, Z.M. Chrzanowska-Lightowlers, T. Lomo, and C.R. Slater. 2001. Sodium channel mRNAs at the neuromuscular junction: distinct patterns of accumulation and effects of muscle activity. *J. Neurosci.* 21:8456–63.

Aydin, M.A., S.E. Mackinnon, X.M. Gu, J. Kobayashi, and W.M. Kuzon. 2004. Force deficits in skeletal muscle after delayed reinnervation. *Plast. Reconstr. Surg.* 113:1712–1718. doi:10.1097/01.PRS.0000118049.93654.CA.

Bacou, F., P. Rouanet, C. Barjot, C. Janmot, P. Vigneron, and A. D'Albis. 1996. Expression of myosin

isoforms in denervated, cross-reinnervated, and electrically stimulated rabbit muscles. *Eur. J. Biochem.* 236:539–547. doi:10.1111/j.1432-1033.1996.00539.x.

Baehr, L.M., J.D. Furlow, and S.C. Bodine. 2011. Muscle sparing in muscle RING finger 1 null mice: response to synthetic glucocorticoids. *J. Physiol.* 589:4759–76. doi:10.1113/jphysiol.2011.212845.

Baehr, L.M., D.S. Waddell, H.Y. Yang, J.D. Furlow, and S.C. Bodine. 2007. Upregulation of FOXO1 and FOXO3a Following Denervation and Dexamethasone Treatment. *FASEB J.* 21:A1308-b-.

Bain, J.R., K.L. Veltri, D. Chamberlain, and M. Fahnestock. 2001. Improved functional recovery of denervated skeletal muscle after temporary sensory nerve innervation. *Neuroscience.* 103:503–510. doi:10.1016/S0306-4522(00)00577-7.

Baumann, A.P., C. Ibebunjo, W.A. Grasser, and V.M. Paralkar. 2003. Myostatin expression in age and denervation-induced skeletal muscle atrophy. *J. Musculoskelet. Neuronal Interact.* 3:8–16.

Baumann, C.W., H.M. Liu, and L. V. Thompson. 2016a. Denervation-Induced Activation of the Ubiquitin-Proteasome System Reduces Skeletal Muscle Quantity Not Quality. *PLoS One.* 11:e0160839. doi:10.1371/journal.pone.0160839.

Baumann, C.W., H.M. Liu, and L. V. Thompson. 2016b. Denervation-Induced Activation of the Ubiquitin-Proteasome System Reduces Skeletal Muscle Quantity Not Quality. *PLoS One.* 11:e0160839. doi:10.1371/journal.pone.0160839.

Beehler, B.C., P.G. Sleph, L. Benmassaoud, and G.J. Grover. 2006. Reduction of skeletal muscle atrophy by a proteasome inhibitor in a rat model of denervation. *Exp. Biol. Med.* 231:335–341. doi:10.1177/153537020623100315.

Bekoff, A., and W.J. Betz. 1977. Physiological properties of dissociated muscle fibres obtained from innervated and denervated adult rat muscle. *J. Physiol.* 271:25–40.

Bennion, D.M., C.A. Rosado, E.A. Haltigan, R.W. Regenhardt, C. Sumners, and M.F. Waters. 2016.

Serum activity of angiotensin converting enzyme 2 is decreased in patients with acute ischemic stroke. *J. Renin. Angiotensin. Aldosterone. Syst.* 17. doi:10.1177/1470320316661060.

Berry, H., and V. Bril. 1982. Axillary nerve palsy following blunt trauma to the shoulder region: a clinical and electrophysiological review. *J. Neurol. Neurosurg. Psychiatry*. 45:1027–32.

Bezakova, G., I. Rabben, I. Sefland, G. Fumagalli, and T. Lømo. 2001. Neural agrin controls acetylcholine receptor stability in skeletal muscle fibers. *Proc. Natl. Acad. Sci. U. S. A.* 98:9924–9929. doi:10.1073/pnas.171539698.

Bhaskar, P.T., and N. Hay. 2007. The two TORCs and Akt. *Dev. Cell.* 12:487–502. doi:10.1016/j.devcel.2007.03.020.

Biral, D., H. Kern, N. Adami, and S. Boncompagni. 2008. Atrophy-resistant fibers in permanent peripheral denervation of human skeletal muscle. doi:10.1179/174313208X281145.

Blaauw, B., C. Marta, L. Agatea, L. Toniolo, C. Mammucari, E. Masiero, R. Abraham, M. Sandri, S. Schiaffino, and C. Reggiani. 2010. Inducible Activation of Akt Increases Skeletal Muscle Mass and Force Without Satellite Cell Activation. *Biophys. J.* 98:153a. doi:10.1016/j.bpj.2009.12.823.

Blom, S., and L.O. Dahlbäck. 1970. Nerve injuries in dislocations of the shoulder joint and fractures of the neck of the humerus. A clinical and electromyographical study. *Acta Chir. Scand.* 136:461–6.

Bodine, S.C., T.N. Stitt, M. Gonzalez, W.O. Kline, G.L. Stover, R. Bauerlein, E. Zlotchenko, A. Scrimgeour, J.C. Lawrence, D.J. Glass, and G.D. Yancopoulos. 2001a. Akt/mTOR pathway is a crucial regulator of skeletal muscle hypertrophy and can prevent muscle atrophy in vivo. *Nat. Cell Biol.* 3:1014–9. doi:10.1038/ncb1101-1014.

Bodine, S.C., T.N. Stitt, M. Gonzalez, W.O. Kline, G.L. Stover, R. Bauerlein, E. Zlotchenko, A. Scrimgeour, J.C. Lawrence, D.J. Glass, and G.D. Yancopoulos. 2001b. Akt/mTOR pathway is a crucial regulator of skeletal muscle hypertrophy and can prevent muscle atrophy in vivo. *Nat. Cell*

*Biol.* 3:1014–1019. doi:10.1038/ncb1101-1014.

Bonaldo, P., and M. Sandri. 2013. Cellular and molecular mechanisms of muscle atrophy. *Dis. Model. Mech.* 6:25–39. doi:10.1242/dmm.010389.

Borisov, A., E. Dedkov, and B. Carlson. 2001a. Interrelations of myogenic response, progressive atrophy of muscle fibers, and cell death in denervated skeletal muscle. *Anat. Rec.* 218:203–218. doi:10.1002/ar.1155.

Borisov, A.B., and B.M. Carlson. 2000a. Cell Death in Denervated Skeletal Muscle Is Distinct From. 318:305–318.

Borisov, A.B., and B.M. Carlson. 2000b. Cell death in denervated skeletal muscle is distinct from classical apoptosis. *Anat. Rec.* 258:305–18.

Borisov, A.B., E.I. Dedkov, and B.M. Carlson. 2001b. Interrelations of Myogenic Response , Progressive Atrophy of Muscle Fibers , and Cell Death in Denervated Skeletal Muscle. 218:203–218. doi:10.1002/ar.1155.

Borisov, A.B., E.I. Dedkov, and B.M. Carlson. 2001c. Interrelations of myogenic response, progressive atrophy of muscle fibers, and cell death in denervated skeletal muscle. *Anat. Rec.* 264:203–218. doi:10.1002/ar.1155.

Borisov, A.B., S.-K. Huang, and B.M. Carlson. 2000. Remodeling of the Vascular Bed and Progressive Loss of Capillaries in Denervated Skeletal Muscle.

Bottinelli, R., S. Schiaffino, and C. Reggiani. 1991. Force-velocity relations and myosin heavy chain isoform compositions of skinned fibres from rat skeletal muscle. *J. Physiol.* 437:655–672. doi:10.1113/jphysiol.1991.sp018617.

Boulware, S.D., W. V. Tamborlane, N.J. Rennert, N. Gesundheit, and R.S. Sherwin. 1994. Comparison of the metabolic effects of recombinant human insulin-like growth factor-I and insulin. Dose-response

relationships in healthy young and middle-aged adults. *J. Clin. Invest.* 93:1131–1139. doi:10.1172/JCI117065.

Bray, J.J., M.J. Hawken, J.I. Hubbard, S. Pockett, and L. Wilson. 1976. The membrane potential of rat diaphragm muscle fibres and the effect of denervation. *J. Physiol.* 255:651–67.

Brookes, P.S., Y. Yoon, J.L. Robotham, M.W. Anders, and S.-S. Sheu. 2004. Calcium, ATP, and ROS: a mitochondrial love-hate triangle. *Am. J. Physiol. Physiol.* 287:C817–C833. doi:10.1152/ajpcell.00139.2004.

Brown, D.L., T.M. Bennett, B.J. Dowsing, A. Hayes, M. Abate, and W.A. Morrison. 2002. Immediate and delayed nerve repair: Improved muscle mass and function with leukemia inhibitory factor. *J. Hand Surg. Am.* 27:1048–1055. doi:10.1053/jhsu.2002.36518.

Brunetti, A., and I.D. Goldfine. 1990. Role of Myogenin in Myoblast Differentiation and Its Regulation by Fibroblast Growth Factor*. 265. 5960–5963 pp.

Burns, A.S., V.S. Boyce, A. Tessler, and M.A. Lemay. 2007. Fibrillation potentials following spinal cord injury: Improvement with neurotrophins and exercise. *Muscle and Nerve*. 35:607–613. doi:10.1002/mus.20738.

Cabello-Verrugio, C., M.G. Morales, J.C. Rivera, D. Cabrera, and F. Simon. 2015. Renin-angiotensin system: an old player with novel functions in skeletal muscle. *Med. Res. Rev.* 35:437–63. doi:10.1002/med.21343.

Cairns, S.P., S.J. Buller, D.S. Loiselle, and J.M. Renaud. 2003. Changes of action potentials and force at lowered [Na+] o in mouse skeletal muscle: Implications for fatigue. *Am. J. Physiol. - Cell Physiol.* 285. doi:10.1152/ajpcell.00401.2002.

Cairns, S.P., J.A. Flatman, and T. Clausen. 1995. Relation between extracellular [K+], membrane potential and contraction in rat soleus muscle: modulation by the Na+-K+ pump. *Pflügers Arch.*

*Eur. J. Physiol.* 430:909–915. doi:10.1007/BF01837404.

Carlson, B.M., L. Billington, and J. Faulkner. 1996. Studies on the regenerative recovery of long-term denervated muscle in rats. *Restor. Neurol. Neurosci.* 10:77–84. doi:10.3233/rnn-1996-10203.

Caron, A.Z., S. Haroun, É. Leblanc, F. Trensz, C. Guindi, A. Amrani, and G. Grenier. 2011. The proteasome inhibitor MG132 reduces immobilization-induced skeletal muscle atrophy in mice. *BMC Musculoskelet. Disord.* 12:185. doi:10.1186/1471-2474-12-185.

Carraro, U., K. Rossini, W. Mayr, and H. Kern. 2005. Muscle fiber regeneration in human permanent lower motoneuron denervation: Relevance to safety and effectiveness of FES-training, which induces muscle recovery in SCI subjects. *Artif. Organs*. 29:187–191. doi:10.1111/j.1525-1594.2005.29032.x.

Castets, P., N. Rion, M. Théodore, D. Falcetta, S. Lin, M. Reischl, F. Wild, L. Guérard, C. Eickhorst, M. Brockhoff, M. Guridi, C. Ibebunjo, J. Cruz, M. Sinnreich, R. Rudolf, D.J. Glass, and M.A. Rüegg. 2019. mTORC1 and PKB/Akt control the muscle response to denervation by regulating autophagy and HDAC4. *Nat. Commun.* 10:1–16. doi:10.1038/s41467-019-11227-4.

Ceccacci, E., and S. Minucci. 2016. Inhibition of histone deacetylases in cancer therapy: Lessons from leukaemia. *Br. J. Cancer*. 114:605–611. doi:10.1038/bjc.2016.36.

Cederna, P.S., M.K.H. Youssef, H. Asato, M.G. Urbanchek, W.M. Kuzon, and J.R. Bain. 2000. Skeletal muscle reinnervation by reduced axonal numbers results in whole muscle force deficits: Discussion. *Plast. Reconstr. Surg.* 105:2010–2011. doi:10.1097/00006534-200005000-00015.

Chahine, M., I. Deschene, L.Q. Chen, and R.G. Kallen. 1996. Electrophysiological characteristics of cloned skeletal and cardiac muscle sodium channels. *Am. J. Physiol. - Hear. Circ. Physiol.* 271. doi:10.1152/ajpheart.1996.271.2.h498.

Chen, D., S. Chen, W. Wang, F. Liu, J. Jing, G. Chen, and H. Zheng. 2010. Functional modulation of

satellite cells in long-term denervated human laryngeal muscle. *Laryngoscope*. 120:353–358. doi:10.1002/lary.20796.

Chen, H., and D.C. Chan. 2005. Emerging functions of mammalian mitochondrial fusion and fission. *Hum. Mol. Genet.* 14 Spec No. 2:R283-9. doi:10.1093/hmg/ddi270.

Chen, M.-F., and H. Jockusch. 1999. Role of Phosphorylation and Physiological State in the Regulation of the Muscular Chloride Channel ClC-1: A Voltage-Clamp Study on Isolated M. interosseus Fibers. *Biochem. Biophys. Res. Commun.* 261:528–533. doi:10.1006/BBRC.1999.1061.

Chibalin, A. V., J.A. Heiny, B. Benziane, A. V. Prokofiev, A. V. Vasiliev, V. V. Kravtsova, and I.I. Krivoi. 2012. Chronic nicotine modifies skeletal muscle Na,K-ATPase activity through its interaction with the nicotinic acetylcholine receptor and phospholemman. *PLoS One*. 7. doi:10.1371/journal.pone.0033719.

Cisternas, F., M.G. Morales, C. Meneses, F. Simon, E. Brandan, J. Abrigo, Y. Vazquez, and C. Cabello-Verrugio. 2015. Angiotensin-(1-7) decreases skeletal muscle atrophy induced by angiotensin II through a Mas receptor-dependent mechanism. *Clin. Sci. (Lond).* 128:307–19. doi:10.1042/CS20140215.

Clarke, B.A., D. Drujan, M.S. Willis, L.O. Murphy, R.A. Corpina, E. Burova, S. V. Rakhilin, T.N. Stitt, C. Patterson, E. Latres, and D.J. Glass. 2007. The E3 Ligase MuRF1 Degrades Myosin Heavy Chain Protein in Dexamethasone-Treated Skeletal Muscle. *Cell Metab.* 6:376–385. doi:10.1016/J.CMET.2007.09.009.

Clausen, T., O. Hansen, K. Kjeldsen, and A. Nørgaard. 1982. Effect of age, potassium depletion and denervation on specific displaceable [3H]ouabain binding in rat skeletal muscle in vivo. *J. Physiol.* 333:367–381. doi:10.1113/jphysiol.1982.sp014458.

Clausen, T., O.B. Nielsen, J.D. Clausen, T.H. Pedersen, and L.J. Hayward. 2011a. Na+,K+-pump

stimulation improves contractility in isolated muscles of mice with hyperkalemic periodic paralysis. *J. Gen. Physiol.* 138:117–30. doi:10.1085/jgp.201010586.

Clausen, T., O.B. Nielsen, J.D. Clausen, T.H. Pedersen, and L.J. Hayward. 2011b. Na+,K+-pump stimulation improves contractility in isolated muscles of mice with hyperkalemic periodic paralysis. *J. Gen. Physiol.* 138:117–130. doi:10.1085/jgp.201010586.

CLAUSEN, T., L.C. SELLIN, and S. THESLEFF. 1981. Quantitative changes in ouabain binding after denervation and during reinnervation of mouse skeletal muscle. *Acta Physiol. Scand.* 111:373–375. doi:10.1111/j.1748-1716.1981.tb06750.x.

Cohen, S., J.J. Brault, S.P. Gygi, D.J. Glass, D.M. Valenzuela, C. Gartner, E. Latres, and A.L. Goldberg. 2009. During muscle atrophy, thick, but not thin, filament components are degraded by MuRF1-dependent ubiquitylation. *J. Cell Biol.* 185:1083–1095. doi:10.1083/jcb.200901052.

Cong, H., L. Sun, C. Liu, and P. Tien. 2011. Inhibition of atrogin-1/MAFbx expression by adenovirus-delivered small hairpin RNAs attenuates muscle atrophy in fasting mice. *Hum. Gene Ther.* 22:313–324. doi:10.1089/hum.2010.057.

Crompton, M. 1999. The mitochondrial permeabitity transition pore and its role in cell death. *Biochem. J.* 341:233–249. doi:10.1042/0264-6021:3410233.

Davis, H.L., and J.A. Kiernan. 1980. Neurotrophic effects of sciatic nerve extract on denervated extensor digitorum longus muscle in the rat. *Exp. Neurol.* 69:124–134. doi:10.1016/0014-4886(80)90148-X.

Dejean, L.M., S. Martinez-Caballero, and K.W. Kinnally. 2006. Is MAC the knife that cuts cytochrome c from mitochondria during apoptosis? *Cell Death Differ.* 13:1387–95. doi:10.1038/sj.cdd.4401949.

Diness, J.G., B.H. Bentzen, U.S. Sørensen, and M. Grunnet. 2015. Role of calcium-activated potassium channels in atrial fibrillation pathophysiology and therapy. *J. Cardiovasc. Pharmacol.* 66:441–448. doi:10.1097/FJC.0000000000000249.

Dow, D.E., P.S. Cederna, C.A. Hassett, T.Y. Kostrominova, J.A. Faulkner, and R.G. Dennis. 2004. Number of contractions to maintain mass and force of a denervated rat muscle. *Muscle and Nerve*. 30:77–86. doi:10.1002/mus.20054.

Dragović, T., R. Minshall, H.L. Jackman, L.X. Wang, and E.G. Erdös. 1996. Kininase II-type enzymes. Their putative role in muscle energy metabolism. *Diabetes*. 45 Suppl 1:S34-7. doi:10.2337/diab.45.1.s34.

Dufresne, S.S., N.A. Dumont, A. Boulanger-Piette, V.A. Fajardo, D. Gamu, S.A. Kake-Guena, R.O. David, P. Bouchard, É. Lavergne, J.M. Penninger, P.C. Pape, A. Russell Tupling, and J. Frenette. 2016. Muscle RANK is a key regulator of Ca2+ storage, SERCA activity, and function of fast-twitch skeletal muscles. *Am. J. Physiol. - Cell Physiol.* 310:C663–C672. doi:10.1152/ajpcell.00285.2015.

Dulhunty, A.F. 1978. The dependence of membrane potential on extracellular chloride concentration in mammalian skeletal muscle fibres. *J. Physiol.* 276:67–82. doi:10.1113/jphysiol.1978.sp012220.

Edwards, J.N., W.A. Macdonald, C. Van Der Poel, and D.G. Stephenson. 2007. O2.- production at 37°C plays a critical role in depressing tetanic force of isolated rat and mouse skeletal muscle. *Am. J. Physiol. - Cell Physiol.* 293. doi:10.1152/ajpcell.00037.2007.

Eftimie, R., H.R. Brenner, and A. Buonanno. 1991. Myogenin and MyoD join a family of skeletal muscle genes regulated by electrical activity. *Proc. Natl. Acad. Sci. U. S. A.* 88:1349–1353. doi:10.1073/pnas.88.4.1349.

El-Hashim, A.Z., W.M. Renno, R. Raghupathy, H.T. Abduo, S. Akhtar, and I.F. Benter. 2012. Angiotensin-(1-7) inhibits allergic inflammation, via the MAS1 receptor, through suppression of ERK1/2- and NF-κB-dependent pathways. *Br. J. Pharmacol.* 166:1964–76. doi:10.1111/j.1476-5381.2012.01905.x.

Favero, M., D.-J. Jiang, C. Chiamulera, A. Cangiano, and G.F. Fumagalli. 2008. Expression of small-conductance calcium-activated potassium channels (SK3) in skeletal muscle: regulation by muscle activity. *J. Physiol.* 586:4763–4774. doi:10.1113/jphysiol.2008.156588.

Fernandes, T., N.Y. Hashimoto, and E.M. Oliveira. 2010. Characterization of angiotensin-converting enzymes 1 and 2 in the soleus and plantaris muscles of rats. *Brazilian J. Med. Biol. Res. = Rev. Bras. Pesqui. médicas e biológicas / Soc. Bras. Biofísica ... [et al.]*. 43:837–42.

Fielitz, J., M.S. Kim, J.M. Shelton, S. Latif, J.A. Spencer, D.J. Glass, J.A. Richardson, R. Bassel-Duby, and E.N. Olson. 2007. Myosin accumulation and striated muscle myopathy result from the loss of muscle RING finger 1 and 3. *J. Clin. Invest.* 117:2486–2495. doi:10.1172/JCI32827.

Finol, H.J., D.M. Lewis, and R. Owens. 1981. The effects of denervation on contractile properties or rat skeletal muscle. *J. Physiol.* 319:81–92. doi:10.1113/jphysiol.1981.sp013893.

G. E. KirschM. F. Anderson. 1986. Sodium channel kinetics in normal. 738–747.

Galvin, J.W., and J.K. Eichinger. 2016. Outcomes Following Closed Axillary Nerve Injury: A Case Report and Review of the Literature. *Mil. Med.* 181:e291–e297. doi:10.7205/MILMED-D-15-00205.

Glass, D.J. 2005. Skeletal muscle hypertrophy and atrophy signaling pathways. *Int. J. Biochem. Cell Biol.* 37:1974–84. doi:10.1016/j.biocel.2005.04.018.

Gonoi, T., and S. Hasegawa. 1991. Postnatal induction and neural regulation of inward rectifiers in mouse skeletal muscle. *Pflügers Arch. Eur. J. Physiol.* 418:601–7.

Gosker, H.R., E.F. Wouters, G.J. van der Vusse, and A.M. Schols. 2000. Skeletal muscle dysfunction in chronic obstructive pulmonary disease and chronic heart failure: underlying mechanisms and therapy perspectives. *Am J Clin Nutr*. 71:1033–1047.

Greer, E.L., and A. Brunet. 2008. FOXO transcription factors in ageing and cancer. *In* Acta Physiologica.

Acta Physiol (Oxf). 19–28.

Guertin, D.A., D.M. Stevens, C.C. Thoreen, A.A. Burds, N.Y. Kalaany, J. Moffat, M. Brown, K.J. Fitzgerald, and D.M. Sabatini. 2006. Ablation in mice of the mTORC components raptor, rictor, or mLST8 reveals that mTORC2 is required for signaling to Akt-FOXO and PKCalpha, but not S6K1. *Dev. Cell*. 11:859–71. doi:10.1016/j.devcel.2006.10.007.

Gutmann, E., and J. Zelená. 1962. Morphological Changes in the Denervated Muscle. *In* The Denervated Muscle. Springer US, Boston, MA. 57–102.

H, W., G. Y, X. J, S. L, and L. J. 2001. Comparative Study of Different Surgical Procedures Using Sensory Nerves or Neurons for Delaying Atrophy of Denervated Skeletal Muscle. *J. Hand Surg. Am.* 26. doi:10.1053/JHSU.2001.22522.

Hacihanefioglu, A., A. Pinar, T. Ae, and E. Gonullu. Acute severe cardiac failure in a myeloma patient due to proteasome inhibitor bortezomib. doi:10.1007/s12185-008-0139-7.

Hakuno, F., and S.I. Takahashi. 2018. 40 years of IGF1: IGF1 receptor signaling pathways. *J. Mol. Endocrinol.* 61:T69–T86. doi:10.1530/JME-17-0311.

Hall, J.E., A.C. Guyton, and H.L. Mizelle. 1990. Role of the renin-angiotensin system in control of sodium excretion and arterial pressure. *In* Acta Physiologica Scandinavica, Supplement. Acta Physiol Scand Suppl. 48–62.

Hämäläinen, N., and D. Pette. 2001. Myosin and SERCA isoform expression in denervated slow-twitch muscle of euthyroid and hyperthyroid rabbits. *J. Muscle Res. Cell Motil.* 22:453–7.

Hartzell, H.C., and D.M. Fambrough. 1972. Acetylcholine receptors. Distribution and extrajunctional density in rat diaphragm after denervation correlated with acetylcholine sensitivity. *J. Gen. Physiol.* 60:248–62.

Hayward, L.J., R.H. Brown, and S.C. Cannon. 1997. Slow inactivation differs among mutant Na channels

associated with myotonia and periodic paralysis. *Biophys. J.* 72:1204–1219. doi:10.1016/S0006-3495(97)78768-X.

Heaton, J.T., and J.B. Kobler. 2005. Use of muscle fibrillation for tracking nerve regeneration. *Muscle and Nerve*. 31:235–241. doi:10.1002/mus.20257.

Higashino, K., T. Matsuura, K. Suganuma, K. Yukata, T. Nishisho, and N. Yasui. 2013. Early changes in muscle atrophy and muscle fiber type conversion after spinal cord transection and peripheral nerve transection in rats. *J. Neuroeng. Rehabil.* 10:46. doi:10.1186/1743-0003-10-46.

Hikida, R.S., S. Van Nostran, J.D. Murray, R.S. Staron, S.E. Gordon, and W.J. Kraemer. 1997. Myonuclear Loss in Atrophied Soleus Muscle Fibers. 247. Wiley-Liss, Inc. 350–354 pp.

Hines, H.M., and G.C. Knowlton. 1933. CHANGES IN THE SKELETAL MUSCLE OF THE RAT FOLLOWING DENERVATION. *Am. J. Physiol. Content*. 104:379–391. doi:10.1152/ajplegacy.1933.104.2.379.

Hinkle, R.T., K.M.B. Hodge, D.B. Cody, R.J. Sheldon, B.K. Kobilka, and R.J. Isfort. 2002. Skeletal muscle hypertrophy and anti-atrophy effects of clenbuterol are mediated by the beta2-adrenergic receptor. *Muscle Nerve*. 25:729–34. doi:10.1002/mus.10092.

Hník, P. 1962. Rate of Denervation Muscle Atrophy. *In* The Denervated Muscle. Springer US, Boston, MA. 341–375.

Hodgkin, A.L., and B. Katz. 1949. The effect of sodium ions on the electrical activity of the giant axon of the squid. *J. Physiol.* 108:37–77. doi:10.1113/jphysiol.1949.sp004310.

Ingalls, C.P., G.L. Warren, and R.B. Armstrong. 1999. Intracellular Ca2+ transients in mouse soleus muscle after hindlimb unloading and reloading. *J. Appl. Physiol.* 87:386–390. doi:10.1152/jappl.1999.87.1.386.

Irintchev, A., A. Draguhn, and A. Wernig. 1990. Reinnervation and recovery of mouse soleus muscle

after long-term denervation. *Neuroscience*. 39:231–243. doi:10.1016/0306-4522(90)90236-W.

Izumiya, Y., T. Hopkins, C. Morris, K. Sato, L. Zeng, J. Viereck, J.A. Hamilton, N. Ouchi, N.K. LeBrasseur, and K. Walsh. 2008. Fast/Glycolytic muscle fiber growth reduces fat mass and improves metabolic parameters in obese mice. *Cell Metab.* 7:159–72. doi:10.1016/j.cmet.2007.11.003.

J, M., S. J, G. JP, L. CA, L. Z, E. GA, R. A, H. J, T. KH, S. TL, S. BP, and K. LA. 2007. Gene Expression of Myogenic Regulatory Factors, Nicotinic Acetylcholine Receptor Subunits, and GAP-43 in Skeletal Muscle Following Denervation in a Rat Model. *J. Orthop. Res.* 25. doi:10.1002/JOR.20414.

Jakubiec-Puka, A. 1992. Changes in myosin and actin filaments in fast skeletal muscle after denervation and self-reinnervation. *Comp. Biochem. Physiol. Part A Physiol.* 102:93–98. doi:10.1016/0300-9629(92)90017-K.

Jamart, C., J.-M. Raymackers, G. Li An, L. Deldicque, and M. Francaux. 2011. Prevention of muscle disuse atrophy by MG132 proteasome inhibitor. *Muscle Nerve*. 43:708–715. doi:10.1002/mus.21949.

Jefferies, H.B.J., S. Fumagalli, P.B. Dennis, C. Reinhard, R.B. Pearson, and G. Thomas. 1997. Rapamycin suppresses 5'TOP mRNA translation through inhibition of p70(s6k). *EMBO J.* 16:3693–3704. doi:10.1093/emboj/16.12.3693.

Jg, X., and G. Yd. 1999. Experimental study of morphology and electrophysiology on denervated skeletal muscle. *undefined*.

Kadoguchi, T., S. Kinugawa, S. Takada, A. Fukushima, T. Furihata, T. Homma, Y. Masaki, W. Mizushima, M. Nishikawa, M. Takahashi, T. Yokota, S. Matsushima, K. Okita, and H. Tsutsui. 2015. Angiotensin II can directly induce mitochondrial dysfunction, decrease oxidative fibre number

and induce atrophy in mouse hindlimb skeletal muscle. *Exp. Physiol.* 100:312–22. doi:10.1113/expphysiol.2014.084095.

Kadoguchi, T., S. Takada, T. Yokota, T. Furihata, J. Matsumoto, M. Tsuda, W. Mizushima, A. Fukushima, K. Okita, and S. Kinugawa. 2018. Deletion of NAD(P)H Oxidase 2 Prevents Angiotensin II-Induced Skeletal Muscle Atrophy. *Biomed Res. Int.* 2018:3194917. doi:10.1155/2018/3194917.

Kallen, R.G., Z.H. Sheng, J. Yang, L. Chen, R.B. Rogart, and R.L. Barchi. 1990. Primary structure and expression of a sodium channel characteristic of denervated and immature rat skeletal muscle. *Neuron*. 4:233–242. doi:10.1016/0896-6273(90)90098-Z.

Kalliainen, L.K., S.S. Jejurikar, L.W. Liang, M.G. Urbanchek, and W.M. Kuzon. 2002. A specific force deficit exists in skeletal muscle after partial denervation. *Muscle and Nerve*. 25:31–38. doi:10.1002/mus.1216.

Kang, C., C.A. Goodman, T.A. Hornberger, and L.L. Ji. 2015. PGC-1α overexpression by in vivo transfection attenuates mitochondrial deterioration of skeletal muscle caused by immobilization. *FASEB J.* 29:4092–106. doi:10.1096/fj.14-266619.

Kang, C., and L.L. Ji. 2016. PGC-1α overexpression via local transfection attenuates mitophagy pathway in muscle disuse atrophy. *Free Radic. Biol. Med.* 93:32–40. doi:10.1016/j.freeradbiomed.2015.12.032.

Karpati, G., and W.K. Engel. 1968. Correlative histochemical study of skeletal muscle after suprasegmental denervation, peripheral nerve section, and skeletal fixation. *Neurology*. 18:681–692. doi:10.1212/wnl.18.7.681.

Khogali, S., B. Lucas, T. Ammar, D. Dejong, M. Barbalinardo, L.J. Hayward, and J.M. Renaud. 2015. Physiological basis for muscle stiffness and weakness in a knock-in M1592V mouse model of

hyperkalemic periodic paralysis. *Physiol. Rep.* 3. doi:10.14814/phy2.12656.

Klocke, R., K. Steinmeyer, T.J. Jentsch, and H. Jockusch. 1994. Role of innervation, excitability, and myogenic factors in the expression of the muscular chloride channel ClC-1. A study on normal and myotonic muscle. *J. Biol. Chem.* 269:27635–9.

Kobayashi, J., S.E. Mackinnon, O. Watanabe, D.J. Ball, X.M. Gu, D.A. Hunter, and W.M. Kuzon. 1997. The effect of duration of muscle denervation on functional recovery in the rat model. *Muscle and Nerve*. 20:858–866. doi:10.1002/(SICI)1097-4598(199707)20:7<858::AID-MUS10>3.0.CO;2-O.

Kotsias, B.A., and R.A. Venosa. 1987a. Role of sodium and potassium permeabilities in the depolarization of denervated rat muscle fibres. *J. Physiol.* 392:301–13.

Kotsias, B.A., and R.A. Venosa. 1987b. Role of sodium and potassium permeabilities in the depolarization of denervated rat muscle fibres. *J. Physiol.* 392:301–313. doi:10.1113/jphysiol.1987.sp016781.

Kotsias, B.A., and R.A. Venosa. 2001. Sodium influx during action potential in innervated and denervated rat skeletal muscles. *Muscle and Nerve*. 24:1026–1033. doi:10.1002/mus.1106.

Krawiec, B.J., R.A. Frost, T.C. Vary, L.S. Jefferson, and C.H. Lang. 2005. Hindlimb casting decreases muscle mass in part by proteasome-dependent proteolysis but independent of protein synthesis. *Am. J. Physiol. - Endocrinol. Metab.* 289. doi:10.1152/ajpendo.00126.2005.

Lecker, S.H., R.T. Jagoe, A. Gilbert, M. Gomes, V. Baracos, J. Bailey, S.R. Price, W.E. Mitch, and A.L. Goldberg. 2004. Multiple types of skeletal muscle atrophy involve a common program of changes in gene expression. *FASEB J.* 18:39–51. doi:10.1096/fj.03-0610com.

Lee, S., H.-S. Yang, T. Sasakawa, M.A.S. Khan, A. Khatri, M. Kaneki, and J.A.J. Martyn. 2014. Immobilization with atrophy induces de novo expression of neuronal nicotinic α7 acetylcholine receptors in muscle contributing to neurotransmission. *Anesthesiology*. 120:76–85.

doi:10.1097/ALN.0000000000000025.

Leech, C.A., and P.R. Stanfield. 1981. Inward rectification in frog skeletal muscle fibres and its dependence on membrane potential and external potassium. *J. Physiol.* 319:295–309. doi:10.1113/jphysiol.1981.sp013909.

Leivseth, G., T. Clausen, M.E. Everts, and E. Bjordal. 1992. Effects of reduced joint mobility and training on Na,K-ATPase and Ca-ATPase in skeletal muscle. *Muscle Nerve.* 15:843–9. doi:10.1002/mus.880150714.

Li, H., X. Liu, Z. Ren, J. Gu, Y. Lu, X. Wang, and L. Zhang. 2016. Effects of Diabetic Hyperglycemia on Central Ang-(1-7)-Mas-R-nNOS Pathways in Spontaneously Hypertensive Rats. *Cell. Physiol. Biochem.* 40:1186–1197. doi:10.1159/000453172.

Liu, Z., H. Fan, Y. Li, and S.G. Zheng. 2008. Experimental studies on the differentiation of fibroblasts into myoblasts induced by MyoD genes in vitro. *Int. J. Biomed. Sci.* 4:14–19.

Lu, D.-X., S.-K. Huang, and B.M. Carlson. 1997. Electron Microscopic Study of Long-Term Denervated Rat Skeletal Muscle. 248. Wiley-Liss, Inc. 355–365 pp.

Ma, J., J. Shen, J.P. Garrett, C.A. Lee, Z. Li, G.A. Elsaidi, A. Ritting, J. Hick, K.H. Tan, T.L. Smith, B.P. Smith, and L.A. Koman. 2007a. Gene expression of myogenic regulatory factors, nicotinic acetylcholine receptor subunits, and GAP-43 in skeletal muscle following denervation in a rat model. *J. Orthop. Res.* 25:1498–1505. doi:10.1002/jor.20414.

Ma, J., J. Shen, J.P. Garrett, C.A. Lee, Z. Li, G.A. Elsaidi, A. Ritting, J. Hick, K.H. Tan, T.L. Smith, B.P. Smith, and L.A. Koman. 2007b. Gene expression of myogenic regulatory factors, nicotinic acetylcholine receptor subunits, and GAP-43 in skeletal muscle following denervation in a rat model. *J. Orthop. Res.* 25:1498–1505. doi:10.1002/jor.20414.

MacDonald, E.M., E. Andres-Mateos, R. Mejias, J.L. Simmers, R. Mi, J.-S. Park, S. Ying, A. Hoke, S.-J.

Lee, and R.D. Cohn. 2014a. Denervation atrophy is independent from Akt and mTOR activation and is not rescued by myostatin inhibition. *Dis. Model. Mech.* 7.

MacDonald, E.M., E. Andres-Mateos, R. Mejias, J.L. Simmers, R. Mi, J.-S. Park, S. Ying, A. Hoke, S.-J. Lee, and R.D. Cohn. 2014b. Denervation atrophy is independent from Akt and mTOR activation and is not rescued by myostatin inhibition. *Dis. Model. Mech.* 7.

Macintosh, B.R., R.J. Holash, and J.M. Renaud. 2012. Skeletal muscle fatigue-regulation of excitation-contraction coupling to avoid metabolic catastrophe. *J. Cell Sci.* 125:2105–2114. doi:10.1242/jcs.093674.

Maier, F., and A. Bornemann. 1999. COMPARISON OF THE MUSCLE FIBER DIAMETER AND SATELLITE CELL FREQUENCY IN HUMAN MUSCLE BIOPSIES.

Martinez, P.F., K. Okoshi, L.A.M. Zornoff, R.F. Carvalho, S.A. Oliveira Junior, A.R.R. Lima, D.H.S. Campos, R.L. Damatto, C.R. Padovani, C.R. Nogueira, M. Dal Pai-Silva, and M.P. Okoshi. 2010. Chronic heart failure-induced skeletal muscle atrophy, necrosis, and changes in myogenic regulatory factors. *Med. Sci. Monit.* 16:BR374-83.

Marzetti, E., G. Privitera, V. Simili, S.E. Wohlgemuth, L. Aulisa, M. Pahor, and C. Leeuwenburgh. 2010. Multiple Pathways to the Same End: Mechanisms of Myonuclear Apoptosis in Sarcopenia of Aging. *Sci. World J.* 10:340–349. doi:10.1100/tsw.2010.27.

McArdle, J.J., L. Michelson, and A.J. D'Alonzo. 1980. Action potentials in fast- and slow-twitch mammalian muscles during reinnervation and development. *J. Gen. Physiol.* 75:655–672. doi:10.1085/jgp.75.6.655.

McGraw. 1999. HUMAN PHYSIOLOGY : SIXTH EDITION by Fox , Stuart: McGraw-Hill Book Co (UK) Ltd Hardcover - GREENSLEEVES BOOKS.

Mendias, C.L., J.E. Marcin, D.R. Calerdon, and J.A. Faulkner. 2006. Contractile properties of EDL and

soleus muscles of myostatin-deficient mice. *J. Appl. Physiol.* 101:898–905. doi:10.1152/japplphysiol.00126.2006.

Meneses, C., M.G. Morales, J. Abrigo, F. Simon, E. Brandan, and C. Cabello-Verrugio. 2015. The angiotensin-(1-7)/Mas axis reduces myonuclear apoptosis during recovery from angiotensin II-induced skeletal muscle atrophy in mice. *Pflügers Arch. Eur. J. Physiol.* 467:1975–84. doi:10.1007/s00424-014-1617-9.

Menorca, R.M.G., T.S. Fussell, and J.C. Elfar. 2013. Nerve physiology: mechanisms of injury and recovery. *Hand Clin.* 29:317–30. doi:10.1016/j.hcl.2013.04.002.

Merlie, J.P., K.E. Isenberg, S.D. Russell, and J.R. Sanes. 1984. Denervation supersensitivity in skeletal muscle: analysis with a cloned cDNA probe. *J. Cell Biol.* 99:332–5. doi:10.1083/jcb.99.1.332.

Milan, G., V. Romanello, F. Pescatore, A. Armani, J.-H. Paik, L. Frasson, A. Seydel, J. Zhao, R. Abraham, A.L. Goldberg, B. Blaauw, R.A. DePinho, and M. Sandri. 2015a. Regulation of autophagy and the ubiquitin-proteasome system by the FoxO transcriptional network during muscle atrophy. *Nat. Commun.* 6:6670. doi:10.1038/ncomms7670.

Milan, G., V. Romanello, F. Pescatore, A. Armani, J.-H. Paik, L. Frasson, A. Seydel, J. Zhao, R. Abraham, A.L. Goldberg, B. Blaauw, R.A. DePinho, and M. Sandri. 2015b. Regulation of autophagy and the ubiquitin–proteasome system by the FoxO transcriptional network during muscle atrophy. *Nat. Commun.* 6:6670. doi:10.1038/ncomms7670.

Mödlin, M., C. Forstner, C. Hofer, W. Mayr, W. Richter, U. Carraro, F. Protasi, and H. Kern. 2005. Electrical Stimulation of Denervated Muscles : First Results of a Clinical Study. 29:203–206.

Morales, M.G., J. Abrigo, M.J. Acuña, R.A. Santos, M. Bader, E. Brandan, F. Simon, H. Olguin, D. Cabrera, and C. Cabello-Verrugio. 2016. Angiotensin-(1-7) attenuates disuse skeletal muscle atrophy in mice via its receptor, Mas. *Dis. Model. Mech.* 9:441–9. doi:10.1242/dmm.023390.

Morales, M.G., J. Abrigo, C. Meneses, F. Cisternas, F. Simon, and C. Cabello-Verrugio. 2015a. Expression of the Mas receptor is upregulated in skeletal muscle wasting. *Histochem. Cell Biol.* 143:131–41. doi:10.1007/s00418-014-1275-1.

Morales, M.G., J. Abrigo, C. Meneses, F. Simon, F. Cisternas, J.C. Rivera, Y. Vazquez, and C. Cabello-Verrugio. 2014. The Ang-(1-7)/Mas-1 axis attenuates the expression and signalling of TGF-β1 induced by AngII in mouse skeletal muscle. *Clin. Sci. (Lond).* 127:251–64. doi:10.1042/CS20130585.

Morales, M.G., H. Olguín, G. Di Capua, E. Brandan, F. Simon, and C. Cabello-Verrugio. 2015b. Endotoxin-induced skeletal muscle wasting is prevented by angiotensin-(1-7) through a p38 MAPK-dependent mechanism. *Clin. Sci. (Lond).* 129:461–76. doi:10.1042/CS20140840.

Morales, M.G., Y. Vazquez, M.J. Acuña, J.C. Rivera, F. Simon, J.D. Salas, J. Alvarez Ruf, E. Brandan, and C. Cabello-Verrugio. 2012. Angiotensin II-induced pro-fibrotic effects require p38MAPK activity and transforming growth factor beta 1 expression in skeletal muscle cells. *Int. J. Biochem. Cell Biol.* 44:1993–2002. doi:10.1016/j.biocel.2012.07.028.

Morel, J., F. Rannou, H. Talarmin, M. a Giroux-Metges, J.P. Pennec, G. Dorange, and G. Gueret. 2010. Sodium channel Na(V)1.5 expression is enhanced in cultured adult rat skeletal muscle fibers. *J. Membr. Biol.* 235:109–19. doi:10.1007/s00232-010-9262-5.

Moresi, V., M. Carrer, C.E. Grueter, O.F. Rifki, J.M. Shelton, J.A. Richardson, R. Bassel-Duby, and E.N. Olson. 2012. Histone deacetylases 1 and 2 regulate autophagy flux and skeletal muscle homeostasis in mice. *Proc. Natl. Acad. Sci.* 109:1649–1654. doi:10.1073/pnas.1121159109.

Moresi, V., A.H. Williams, E. Meadows, J.M. Flynn, M.J. Potthoff, J. McAnally, J.M. Shelton, J. Backs, W.H. Klein, J.A. Richardson, R. Bassel-Duby, and E.N. Olson. 2010a. Myogenin and Class II HDACs Control Neurogenic Muscle Atrophy by Inducing E3 Ubiquitin Ligases. *Cell.* 143:35. doi:10.1016/J.CELL.2010.09.004.

Moresi, V., A.H. Williams, E. Meadows, J.M. Flynn, M.J. Potthoff, J. McAnally, J.M. Shelton, J. Backs, W.H. Klein, J.A. Richardson, R. Bassel-Duby, and E.N. Olson. 2010b. Myogenin and class II HDACs control neurogenic muscle atrophy by inducing E3 ubiquitin ligases. *Cell.* 143:35–45. doi:10.1016/j.cell.2010.09.004.

Mori, J., V.B. Patel, T. Ramprasath, O.A. Alrob, J. Desaulniers, J.W. Scholey, G.D. Lopaschuk, and G.Y. Oudit. 2014. Angiotensin 1-7 mediates renoprotection against diabetic nephropathy by reducing oxidative stress, inflammation, and lipotoxicity. *Am. J. Physiol. - Ren. Physiol.* 306. doi:10.1152/ajprenal.00655.2013.

Mori, S., and K. Tokuyama. 2007. Variation in ACE activity affects myogenic differentiation in C2C12 cells. *Biochem. Biophys. Res. Commun.* 353:369–75. doi:10.1016/j.bbrc.2006.12.056.

Mounier, R., H. Cavalié, G. Lac, and E. Clottes. 2007. Molecular impact of clenbuterol and isometric strength training on rat EDL muscles. *Pflugers Arch.* 453:497–507. doi:10.1007/s00424-006-0122-1.

Mu, L., S. Sobotka, J. Chen, and T. Nyirenda. 2017. Reinnervation of denervated muscle by implantation of nerve-muscle-endplate band graft to the native motor zone of the target muscle. *Brain Behav.* 7. doi:10.1002/brb3.668.

Murton, A.J., D. Constantin, and P.L. Greenhaff. 2008. The involvement of the ubiquitin proteasome system in human skeletal muscle remodelling and atrophy. *Biochim. Biophys. Acta - Mol. Basis Dis.* 1782:730–743. doi:10.1016/j.bbadis.2008.10.011.

Neelands, T.R., P.S. Herson, D. Jacobson, J.P. Adelman, and J. Maylie. 2001a. Small-conductance calcium-activated potassium currents in mouse hyperexcitable denervated skeletal muscle. *J. Physiol.* 536:397–407.

Neelands, T.R., P.S. Herson, D. Jacobson, J.P. Adelman, and J. Maylie. 2001b. Small-conductance

calcium-activated potassium currents in mouse hyperexcitable denervated skeletal muscle. *J. Physiol.* 536:397–407. doi:10.1111/j.1469-7793.2001.0397c.xd.

Neff, N.T., D. Prevette, L.J. Houenou, M.E. Lewis, M.A. Glicksman, Q.W. Yin, and R.W. Oppenheim. 1993. Insulin-like growth factors: putative muscle-derived trophic agents that promote motoneuron survival. *J. Neurobiol.* 24:1578–88. doi:10.1002/neu.480241203.

Niederle, B., and R. Mayr. 1978. Course of denervation atrophy in type I and type II fibres of rat extensor digitorum longus muscle. *Anat. Embryol. (Berl).* 153:9–21. doi:10.1007/BF00569846.

O'Leary, M.F.N., and D.A. Hood. 2008. Effect of prior chronic contractile activity on mitochondrial function and apoptotic protein expression in denervated muscle. *J. Appl. Physiol.* 105:114–120. doi:10.1152/japplphysiol.00724.2007.

O'Leary, M.F.N., A. Vainshtein, H.N. Carter, Y. Zhang, and D.A. Hood. 2012. Denervation-induced mitochondrial dysfunction and autophagy in skeletal muscle of apoptosis-deficient animals. *Am. J. Physiol. - Cell Physiol.* 303. doi:10.1152/ajpcell.00451.2011.

Oh, Y. Bin, J.H. Kim, B.M. Park, B.H. Park, and S.H. Kim. 2012. Captopril intake decreases body weight gain via angiotensin-(1-7). *Peptides*. 37:79–85. doi:10.1016/j.peptides.2012.06.005.

Ono, T., S. Takada, S. Kinugawa, and H. Tsutsui. 2015. Curcumin ameliorates skeletal muscle atrophy in type 1 diabetic mice by inhibiting protein ubiquitination. *Exp. Physiol.* 100:1052–1063. doi:10.1113/EP085049.

Patterson, M.F., G.M.M. Stephenson, and D.G. Stephenson. 2006. Denervation produces different single fiber phenotypes in fast- and slow-twitch hindlimb muscles of the rat. *Am. J. Physiol. - Cell Physiol.* 291:518–528. doi:10.1152/ajpcell.00013.2006.

Pedersen, T.H., W.A. Macdonald, F.V. de Paoli, I.S. Gurung, and O.B. Nielsen. 2009a. Comparison of regulated passive membrane conductance in action potential–firing fast- and slow-twitch muscle. *J.*

*Gen. Physiol.* 134:323–337. doi:10.1085/jgp.200910291.

Pedersen, T.H., F.V. De Paoli, J.A. Flatman, and O.B. Nielsen. 2009b. Regulation of ClC-1 and KATP channels in action potential-firing fast-twitch muscle fibers. *J. Gen. Physiol.* 134:309–322. doi:10.1085/jgp.200910290.

Pellegrino, C., and C. Franzini. 1963. AN ELECTRON MICROSCOPE STUDY OF DENERVATION ATROPHY IN RED AND WHITE SKELETAL MUSCLE FIBERS. *J. Cell Biol.* 17:327. doi:10.1083/JCB.17.2.327.

Péréon, Y., V. Sorrentino, C. Dettbarn, J. Noireaud, and P. Palade. 1997. Dihydropyridine Receptor and Ryanodine Receptor Gene Expression in Long-Term Denervated Rat Muscles. *Biochem. Biophys. Res. Commun.* 240:612–617. doi:10.1006/bbrc.1997.7712.

Pinsky, M.R. 2004. Dysregulation of the immune response in severe sepsis. *Am. J. Med. Sci.* 328:220–9. doi:10.1097/00000441-200410000-00005.

Plant, P.J., J.R. Bain, J.E. Correa, M. Woo, and J. Batt. 2009. Absence of caspase-3 protects against denervation-induced skeletal muscle atrophy. *J. Appl. Physiol.* 107:224–234. doi:10.1152/japplphysiol.90932.2008.

Powers, S.K., J. Duarte, A.N. Kavazis, and E.E. Talbert. 2010. Reactive oxygen species are signalling molecules for skeletal muscle adaptation. *Exp. Physiol.* 95:1–9. doi:10.1113/expphysiol.2009.050526.

Powers, S.K., M.P. Wiggs, J.A. Duarte, A.M. Zergeroglu, and H.A. Demirel. 2012. Mitochondrial signaling contributes to disuse muscle atrophy. *Am. J. Physiol. Endocrinol. Metab.* 303:E31-9. doi:10.1152/ajpendo.00609.2011.

Pribnow, D., T. Johnson-Pais, C.T. Bond, J. Keen, R.A. Johnson, A. Janowsky, C. Silvia, M. Thayer, J. Maylie, and J.P. Adelman. 1999. Skeletal muscle and small-conductance calcium-activated

potassium channels. *Muscle Nerve*. 22:742–50.

Protasi, F. 2002. Structural interaction between RYRs and DHPRs in calcium release units of cardiac and skeletal muscle cells. *Front. Biosci.* 7:d650-8.

Purves, D., and B. Sakmann. 1974. Membrane properties underlying spontaneous activity of denervated muscle fibres. *J. Physiol.* 239:125–53.

Ramahi, A.A., and R.L. Ruff. 2014. Membrane Potential. *In* Encyclopedia of the Neurological Sciences. Elsevier Inc. 1034–1035.

Robinson, A., N. Tufft, and D.M. Lewis. 1991. A comparison of fibrillation in denervated skeletal muscle of the anaesthetized rat and guinea-pig. *J. Muscle Res. Cell Motil.* 12:271–80.

Rogart, R.B., and L.J. Regan. 1985. Two subtypes of sodium channel with tetrodotoxin sensitivity and insensitivity detected in denervated mammalian skeletal muscle. *Brain Res.* 329:314–8.

Romanello, V., and M. Sandri. 2016. Mitochondrial quality control and muscle mass maintenance. *Front. Physiol.* 6:422. doi:10.3389/fphys.2015.00422.

Rommel, C., S.C. Bodine, B.A. Clarke, R. Rossman, L. Nunez, T.N. Stitt, G.D. Yancopoulos, and D.J. Glass. 2001. Mediation of IGF-1-induced skeletal myotube hypertrophy by PI(3)K/Akt/mTOR and PI(3)K/Akt/GSK3 pathways. *Nat. Cell Biol.* 3:1009–13. doi:10.1038/ncb1101-1009.

Rossini, K., M.E. Zanin, M. Podhorska-Okołów, and U. Carraro. 2002. Stage and quantify regenerative myogenesis in FES-induced functional recovery of human long-term permanent denervated muscle.

Salafsky, B., J. Bell, and M.A. Prewitt. 1968. Development of fibrillation potentials in denervated fast and slow skeletal muscle. *Am. J. Physiol.* 215:637–643. doi:10.1152/ajplegacy.1968.215.3.637.

Salvotri, S., E. Damiani, F. Zorzato, P. Volpe, S. Pierobon, D. Quaglino, G. Salviati, and A. Margreth. 1988. Denervation-induced proliferative changes of triads in rabbit skeletal muscle. *Muscle Nerve*.

11:1246–1259. doi:10.1002/mus.880111209.

Santos, S.H.S., J.F. Giani, V. Burghi, J.G. Miquet, F. Qadri, J.F. Braga, M. Todiras, K. Kotnik, N. Alenina, F.P. Dominici, R.A.S. Santos, and M. Bader. 2014. Oral administration of angiotensin-(1-7) ameliorates type 2 diabetes in rats. *J. Mol. Med. (Berl).* 92:255–65. doi:10.1007/s00109-013-1087-0.

Sartori, R., G. Milan, M. Patron, C. Mammucari, B. Blaauw, R. Abraham, and M. Sandri. 2009. Smad2 and 3 transcription factors control muscle mass in adulthood. *Am. J. Physiol. - Cell Physiol.* 296.

Sartori, R., E. Schirwis, B. Blaauw, S. Bortolanza, J. Zhao, E. Enzo, A. Stantzou, E. Mouisel, L. Toniolo, A. Ferry, S. Stricker, A.L. Goldberg, S. Dupont, S. Piccolo, H. Amthor, and M. Sandri. 2013a. BMP signaling controls muscle mass. *Nat. Genet.* 45:1309–1321. doi:10.1038/ng.2772.

Sartori, R., E. Schirwis, B. Blaauw, S. Bortolanza, J. Zhao, E. Enzo, A. Stantzou, E. Mouisel, L. Toniolo, A. Ferry, S. Stricker, A.L. Goldberg, S. Dupont, S. Piccolo, H. Amthor, and M. Sandri. 2013b. BMP signaling controls muscle mass. *Nat. Genet.* 45:1309–1321. doi:10.1038/ng.2772.

Scelsi, R. 2001. Skelatal muscle pathalogy after spinal cord injery:our 20 year experience and results on skeletal muscle changes in paraplegics, related to functional rehabililtation .

Scheffner, M., U. Nuber, and J.M. Huibregtse. 1995. Protein ubiquitination involving an E1–E2–E3 enzyme ubiquitin thioester cascade. *Nature*. 373:81–83. doi:10.1038/373081a0.

Schiaffino, S., K.A. Dyar, S. Ciciliot, B. Blaauw, and M. Sandri. 2013. Mechanisms regulating skeletal muscle growth and atrophy. *FEBS J.* 280:4294–314. doi:10.1111/febs.12253.

Schiaffino, S., and C. Mammucari. 2011. Regulation of skeletal muscle growth by the IGF1-Akt/PKB pathway: insights from genetic models. *Skelet. Muscle*. 1:4. doi:10.1186/2044-5040-1-4.

Schiaffino, S., and C. Reggiani. 2011. Fiber Types in Mammalian Skeletal Muscles. *Physiol. Rev.* 91:1447–1531. doi:10.1152/physrev.00031.2010.

Schmalbruch, H., W.S. al-Amood, and D.M. Lewis. 1991. Morphology of long-term denervated rat soleus muscle and the effect of chronic electrical stimulation. *J. Physiol.* 441:233–41.

Schulte, L., D. Peters, J. Taylor, J. Navarro, and S. Kandarian. 1994. Sarcoplasmic reticulum Ca2+ pump expression in denervated skeletal muscle. *Am. J. Physiol.* 267:C617-22.

Schulz, R.A., and K.E. Yutzey. 2004. Calcineurin signaling and NFAT activation in cardiovascular and skeletal muscle development. *Dev. Biol.* 266:1–16. doi:10.1016/j.ydbio.2003.10.008.

Seabrooke, S.R., M.R. Ward, and N.K. White. 1988. The effect of sodium pump blockade and denervation on the steady-state sodium permeability of mouse skeletal muscle fibres. *Q. J. Exp. Physiol.* 73:561–72.

Sekiguchi, K., F. Kanda, S. Mitsui, N. Kohara, and K. Chihara. 2012a. Fibrillation potentials of denervated rat skeletal muscle are associated with expression of cardiac-type voltage-gated sodium channel isoform Nav1.5. *Clin. Neurophysiol.* 123:1650–1655. doi:10.1016/j.clinph.2012.01.002.

Sekiguchi, K., F. Kanda, S. Mitsui, N. Kohara, and K. Chihara. 2012b. Fibrillation potentials of denervated rat skeletal muscle are associated with expression of cardiac-type voltage-gated sodium channel isoform Nav1.5. *Clin. Neurophysiol.* 123:1650–5. doi:10.1016/j.clinph.2012.01.002.

Semprun-Prieto, L.C., S. Sukhanov, T. Yoshida, B.M. Rezk, R.A. Gonzalez-Villalobos, C. Vaughn, A. Michael Tabony, and P. Delafontaine. 2011. Angiotensin II induced catabolic effect and muscle atrophy are redox dependent. *Biochem. Biophys. Res. Commun.* 409:217–21. doi:10.1016/j.bbrc.2011.04.122.

Siegl, P.K.S., S.D. Kivlighn, and T.P. Broten. 1995. Pharmacology of losartan, an angiotensin II receptor antagonist, in animal models of hypertension. *In* Journal of Hypertension, Supplement. Lippincott Williams and Wilkins.

Singh, K., and D. Hood. 2011a. Effect of denervation-induced muscle disuse on mitochondrial protein

import. *Am. J. Physiol. …*. 3:138–145. doi:10.1152/ajpcell.00181.2010.

Singh, K., and D.A. Hood. 2011b. Effect of denervation-induced muscle disuse on mitochondrial protein import. *Am. J. Physiol. Physiol.* 300:C138–C145. doi:10.1152/ajpcell.00181.2010.

Siu, P.M., and S.E. Alway. 2005. Mitochondria-associated apoptotic signalling in denervated rat skeletal muscle. *J. Physiol.* 565:309–23. doi:10.1113/jphysiol.2004.081083.

Spector, S.A. 1985. Trophic effects on the contractile and histochemical properties of rat soleus muscle. *J. Neurosci.* 5:2189–2196. doi:10.1523/jneurosci.05-08-02189.1985.

Squecco, R., U. Carraro, H. Kern, A. Pond, N. Adami, D. Biral, V. Vindigni, S. Boncompagni, T. Pietrangelo, G. Bosco, G. Fanò, M. Marini, P.M. Abruzzo, E. Germinario, D. Danieli-Betto, F. Protasi, F. Francini, and S. Zampieri. 2009. A subpopulation of rat muscle fibers maintains an assessable excitation-contraction coupling mechanism after long-standing denervation despite lost contractility. *J. Neuropathol. Exp. Neurol.* 68:1256–1268. doi:10.1097/NEN.0b013e3181c18416.

Supinski, G.S., J. Vanags, and L.A. Callahan. 2009. Effect of proteasome inhibitors on endotoxin-induced diaphragm dysfunction. *Am. J. Physiol. Lung Cell. Mol. Physiol.* 296:L994–L1001. doi:10.1152/ajplung.90404.2008.

Takekura, H., N. Kasuga, K. Kitada, and T. Yoshioka. 1996. Morphological changes in the triads and sarcoplasmic reticulum of rat slow and fast muscle fibres following denervation and immobilization. *J. Muscle Res. Cell Motil.* 17:391–400. doi:10.1007/BF00123356.

Tando, T., A. Hirayama, M. Furukawa, Y. Sato, T. Kobayashi, A. Funayama, A. Kanaji, W. Hao, R. Watanabe, M. Morita, T. Oike, K. Miyamoto, T. Soga, M. Nomura, A. Yoshimura, M. Tomita, M. Matsumoto, M. Nakamura, Y. Toyama, and T. Miyamoto. 2016. Smad2/3 Proteins Are Required for Immobilization-induced Skeletal Muscle Atrophy. *J. Biol. Chem.* 291:12184–94. doi:10.1074/jbc.M115.680579.

Tyapkina, O., E. Volkov, L. Nurullin, B. Shenkman, I. Kozlovskaya, E. Nikolsky, and F. Vyskočil. 2009. Resting membrane potential and Na+,K+-ATPase of rat fast and slow muscles during modeling of hypogravity. *Physiol. Res.* 58:599–603.

Vaghy, P.L., J.S. Russell, L.E. Lantry, R.E. Stephens, and P.E. Ward. 1995. Angiotensin and bradykinin metabolism by peptidases identified in cultured human skeletal muscle myocytes and fibroblasts. *Peptides*. 16:1367–73. doi:10.1016/0196-9781(95)02034-9.

Vandenburgh, H.H., P. Karlisch, and J. Shansky. 1990. Insulin and insulin-like growth factor-1 induce pronounced hypertrophy of skeletal myofibers in tissue culture.

Vandenburgh, H.H., P. Karlisch, J. Shansky, and R. Feldstein. 1991. Insulin and IGF-I induce pronounced hypertrophy of skeletal myofibers in tissue culture. *Am. J. Physiol.* 260:C475-84.

Vergara, C., and B.U. Ramirez. 1997. Age-Dependent Expression of the Apamin-Sensitive Calcium-Activated K+Channel in Fast and Slow Rat Skeletal Muscle. *Exp. Neurol.* 146:282–285. doi:10.1006/exnr.1997.6486.

Viguie, C.A., D.-X. Lu, S.-K. Huang, H. Rengen, and B.M. Carlson. 1997. Quantitative Study of the Effects of Long-Term Denervation on the Extensor Digitorum Longus Muscle of the Rat. 248. Wiley-Liss, Inc. Cell Biology. 346–354 pp.

Vyskočil, F., B. Carlson, and E. Gutmann. 1973. Changes in resting membrane potential and contractility of innervated and denervated skeletal muscle free grafts in the rat. *Pflügers Arch. Eur. J. Physiol.* 344:181–186. doi:10.1007/BF00586551.

Wada, K.I., H. Takahashi, S. Katsuta, and H. Soya. 2002. No decrease in myonuclear number after long-term denervation in mature mice. *Am. J. Physiol. - Cell Physiol.* 283:484–488. doi:10.1152/ajpcell.00025.2002.

Walsh, K., and H. Perlman. 1997. Cell cycle exit upon myogenic differentiation. *Curr. Opin. Genet. Dev.*

7:597–602. doi:10.1016/S0959-437X(97)80005-6.

Walther, T., D. Balschun, J.P. Voigt, H. Fink, W. Zuschratter, C. Birchmeier, D. Ganten, and M. Bader. 1998. Sustained long term potentiation and anxiety in mice lacking the Mas protooncogene. *J. Biol. Chem.* 273:11867–73.

Wang, H., Y. Gu, J. Xu, L. Shen, and J. Li. 2001. Comparative study of different surgical procedures using sensory nerves or neurons for delaying atrophy of denervated skeletal muscle. *J. Hand Surg. Am.* 26:326–331. doi:10.1053/jhsu.2001.22522.

Wang, L., S. Copray, N. Brouwer, M.F. Meek, and D. Kernell. 2002. Regional distribution of slow-twitch muscle fibers after reinnervation in adult rat hindlimb muscles. *Muscle and Nerve*. 25:805–815. doi:10.1002/mus.10114.

Wang, R.N., J. Green, Z. Wang, Y. Deng, M. Qiao, M. Peabody, Q. Zhang, J. Ye, Z. Yan, S. Denduluri, O. Idowu, M. Li, C. Shen, A. Hu, R.C. Haydon, R. Kang, J. Mok, M.J. Lee, H.L. Luu, and L.L. Shi. 2014. Bone Morphogenetic Protein (BMP) signaling in development and human diseases. *Genes Dis.* 1:87–105. doi:10.1016/j.gendis.2014.07.005.

Wang, X.H., and W.E. Mitch. 2014. Mechanisms of muscle wasting in chronic kidney disease. *Nat. Rev. Nephrol.* 10:504–516. doi:10.1038/nrneph.2014.112.

Ward, K.M., W. Manning, and A.C. Wareham. 1987. Effects of denervation and immobilisation during development upon [3H]ouabain binding by slow- and fast-twitch muscle of the rat. *J. Neurol. Sci.* 78:213–224. doi:10.1016/0022-510X(87)90062-1.

Ward, P.E., J.S. Russell, and P.L. Vaghy. 1995. Angiotensin and bradykinin metabolism by peptidases identified in skeletal muscle. *Peptides*. 16:1073–8. doi:10.1016/0196-9781(95)00082-u.

Wareham, A.C. 1978. Effect of denervation and ouabain on the response of the resting membrane potential of rat skeletal muscle to potassium. *Pflügers Arch. Eur. J. Physiol.* 373:225–228.

doi:10.1007/BF00580828.

Werner, H., D. Weinstein, and I. Bentov. 2008. Similarities and differences between insulin and IGF-I: Structures, receptors, and signalling pathways. *Arch. Physiol. Biochem.* 114:17–22. doi:10.1080/13813450801900694.

Wessig, C., M. Koltzenburg, K. Reiners, L. Solymosi, and M. Bendszus. 2004. Muscle magnetic resonance imaging of denervation and reinnervation: correlation with electrophysiology and histology. *Exp. Neurol.* 185:254–61.

Winbanks, C.E., J.L. Chen, H. Qian, Y. Liu, B.C. Bernardo, C. Beyer, K.I. Watt, R.E. Thomson, T. Connor, B.J. Turner, J.R. McMullen, L. Larsson, S.L. McGee, C.A. Harrison, and P. Gregorevic. 2013. The bone morphogenetic protein axis is a positive regulator of skeletal muscle mass. *J. Cell Biol.* 203:345. doi:10.1083/JCB.201211134.

Winters, B.D., M. Eberlein, J. Leung, D.M. Needham, P.J. Pronovost, and J.E. Sevransky. 2010. Long-term mortality and quality of life in sepsis: a systematic review. *Crit. Care Med.* 38:1276–83. doi:10.1097/CCM.0b013e3181d8cc1d.

Xu, J., and Y.D. Gu. 1999. [Experimental study of morphology and electrophysiology on denervated skeletal muscle]. *undefined*.

Yang, J.S., J.T. Sladky, R.G. Kallen, and R.L. Barchi. 1991. TTX-sensitive and TTX-insensitive sodium channel mRNA transcripts are independently regulated in adult skeletal muscle after denervation. *Neuron*. 7:421–7.

Yang, X., P. Xue, H. Chen, M. Yuan, Y. Kang, D. Duscher, H.G. Machens, and Z. Chen. 2020. Denervation drives skeletal muscle atrophy and induces mitochondrial dysfunction, mitophagy and apoptosis via miR-142a-5p/MFN1 axis. *Theranostics*. 10:1415–1432. doi:10.7150/thno.40857.

Yensen, C., W. Matar, and J.M. Renaud. 2002. K+-induced twitch potentiation is not due to longer action

potential. *Am. J. Physiol. - Cell Physiol.* 283. doi:10.1152/ajpcell.00549.2001.

Zammit, P.S., T. a Partridge, and Z. Yablonka-Reuveni. 2006. The skeletal muscle satellite cell: the stem cell that came in from the cold. *J. Histochem. Cytochem.* 54:1177–91. doi:10.1369/jhc.6R6995.2006.

Zeman, R.J., R. Ludemann, and J.D. Etlinger. 1987. Clenbuterol, a beta 2-agonist, retards atrophy in denervated muscles. *Am. J. Physiol.* 252:E152-5.

Zemková, H., J. Teisinger, R.R. Almon, R. Vejsada, P. Hník, and F. Vyskočil. 1990. Immobilization atrophy and membrane properties in rat skeletal muscle fibres. *Pflügers Arch. Eur. J. Physiol.* 416:126–129. doi:10.1007/BF00370233.

Zhang, Y., J. Liu, J.-Y. Luo, X.Y. Tian, W.S. Cheang, J. Xu, C.W. Lau, L. Wang, W.T. Wong, C.M. Wong, H.Y. Lan, X. Yao, M.K. Raizada, and Y. Huang. 2015. Upregulation of Angiotensin (1-7)-Mediated Signaling Preserves Endothelial Function Through Reducing Oxidative Stress in Diabetes. *Antioxid. Redox Signal.* 23:880–892. doi:10.1089/ars.2014.6070.

Zhao, W., S.A. Swanson, J. Ye, X. Li, J.M. Shelton, W. Zhang, and G.D. Thomas. 2006. Reactive oxygen species impair sympathetic vasoregulation in skeletal muscle in angiotensin II-dependent hypertension. *Hypertens. (Dallas, Tex. 1979)*. 48:637–43. doi:10.1161/01.HYP.0000240347.51386.ea.

Zhong, H., R.R. Roy, B. Siengthai, and V.R. Edgerton. 2005. Effects of inactivity on fiber size and myonuclear number in rat soleus muscle. *J. Appl. Physiol.* 99:1494–1499. doi:10.1152/japplphysiol.00394.2005.

Zhu, Z., A. Sierra, C.M.L. Burnett, B. Chen, E. Subbotina, S.R.K. Koganti, Z. Gao, Y. Wu, M.E. Anderson, L.S. Song, D.J. Goldhamer, W.A. Coetzee, D.M. Hodgson-Zingman, and L. V. Zingman. 2014. Sarcolemmal ATP-sensitive potassium channels modulate skeletal muscle function under low-

intensity workloads. *J. Gen. Physiol.* 143:119–134. doi:10.1085/jgp.201311063.

# APPENDIX 1

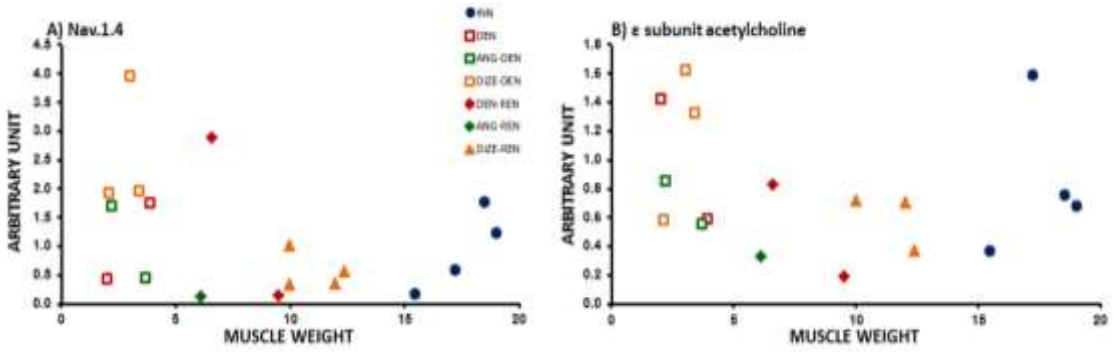


**Appendix 1: A) Nav 1.4 and B) ε subunit acetylcholine protein content of 16 week denervated EDL**. The same sample used in Fig.5.1 for force-frequency curve: □, typical relationship of denervated muscles; Δ, relationship close to the mean relationship of innervated muscles; ◊, intermediate relationship. Protein content of A) Nav 1.4 and B) ε Ach is plotted against the muscle weight.